EXPERIMENTAL EVIDENCE FOR THE PEPTIDE COMPETITION BETWEEN TYPE 1 DIABETES ASSOCIATED HLA-DQ8 AND DR4 MOLECULES

by

Xinhui Ge

BS, Fudan University, Shanghai, PR. China, 1998

Submitted to the Graduate Faculty of

Graduate School of Public Health in partial fulfillment

of the requirements for the degree of

Doctor of Philosophy

University of Pittsburgh

2006

UNIVERSITY OF PITTSBURGH

Graduate School of Public Health

This dissertation was presented

by

Xinhui Ge

It was defended on

March 16, 2006

and approved by

Dissertation Advisor:
Massimo Trucco, MD
Hillman Professor
Division of Immunogenetics, Department of Pediatrics
School of Medicine, University of Pittsburgh

Committee Member:
William Rudert, MD/Ph.D
Research Associated Professor
Division of Immunogenetics, Department of Pediatrics
School of Medicine, University of Pittsburgh

Committee Member:
Jon Piganelli, Ph.D
Assistant Professor
Department of Pediatrics
School of Medicine, University of Pittsburgh

Committee Chairman:
Robert Ferrell, Ph.D
Professor
Department of Human Genetics
Graduate School of Public Health, University of Pittsburgh

Massimo Trucco, MD

EXPERIMENTAL EVIDENCE FOR THE PEPTIDE COMPETITION BETWEEN TYPE 1 DIABETES ASSOCIATED HLA-DQ8 AND DR4 MOLECULES

Xinhui Ge, PhD

University of Pittsburgh, 2006

Abstract

Among the public health relevant disorders, Type 1 Diabetes (T1D) is a degenerative disease affecting almost 2 million Americans. It is characterized by the loss of insulin-producing β-cells due to a T cell-mediated autoimmune response. The risk to develop T1D is HLA associated. HLA-DQ8-DR4 has been identified as the most prevalent HLA haplotype in the Caucasian T1D population. Although DQ8 has been demonstrated to be the primary genetic determinant of disease susceptibility, its predisposing effect is likely modulated by the expression of closely linked DR4 alleles. As one of hypotheses to explain the role of DR4 molecules in T1D etiology, the peptide competition model holds that DR4 competes to bind diabetogenic peptides with DQ8 and thus affects DQ8-restricted autoreactive CD4 T cell responses. However, the evidence of the competition is insufficient due to the lack of detection reagents and the difficulty of segregating the expression of DR4 from DQ8. In this study, we investigated the competition of peptides derived from Glutamic Acid Decarboxylase 65 (GAD65) – a putative β-cell autoantigen. A panel of DQ8-restricted T cell lines was generated to serve as detection reagents to evaluate the peptide occupancy of DQ8. After demonstrating that a single peptide derived from GAD65 could bind both HLA-DQ8 and HLA-DR4, we compared

Massimo Trucco, MD

CD4 T cell responses elicited by antigen presenting cells expressing DQ8 alone with those expressing DQ8 and DR4 simultaneously. Results indicated that the co-expression of HLA-DR4 diminished DQ8-restricted T cell responses. In addition, distinct DR4 subtypes were demonstrated to affect DQ8-restricted T cell responses differently, suggesting the variable degrees of peptide competition potentials. Taken together, this study provides the evidence that DR4 is able to compete for peptides with DQ8. The outcome of this competition decreases DQ8-restricted CD4 T cell responses, which may hence contribute to a peripheral tolerance mechanism and explain the modulating role of DR4 to the DQ8-conferred T1D susceptibility.

TABLE OF CONTENTS

LIST OF TABLES

LIST OF FIGURES

xi

ACKNOWLEDGEMENTS

1.0   INTRODUCTION

HLA-DQ and HLA-DR are MHC class II molecules constitutively expressed on the surface of human antigen presenting cells (APCs) such as B cells, macrophages, and dendritic cells. The function of HLA-DQ and DR is to present antigenic peptides and initiates CD4 T cell responses (1). Both DQ and DR molecules are composed of an α-chain and a β-chain. Genes encoding DQ and DR subunits are located at the short arm of chromosome 6. DR α-chain gene is non-polymorphic, whereas DR β-chain and DQ α-/β- chain genes are highly polymorphic.

Specific HLA-DQ-DR haplotypes are associated with various autoimmune diseases such as human Type 1 Diabetes (T1D), which is characterized as the cell-mediated destruction of insulin-producing pancreatic β-cells (2, 3). It has been demonstrated that a single amino acid polymorphism at the position 57 of DQ β-chain (Asp57β *vs.* non-Asp57β) is associated with increased risk to develop T1D (4, 5). Asp57β alleles such as DQB1*0602 and DQB1*0301 confer dominant disease resistance, whereas non-Asp57β alleles such as DQB1*0302 and DQB1*0201 render disease susceptibility.

Among the Caucasian T1D population, HLA-DQ8 (DQA1*0301/DQB1*0302)-DR4 (DRB1*0401) is the most prevalent haplotype (6). Current understanding of this haplotype in the progression of the disease is that the non-Asp57β DQ8 molecule is defective in directing efficient negative selection of autoreactive CD4 T cells during the T cell development in the thymus (7). Some of these CD4 T cells are potentially reactive against β-cell autoantigens such as insulin and glutamic acid decarboxylase 65 (GAD65). In a concert with certain types of viral infection or other poorly identified environmental factors, these autoreactive CD4 T cells are activated in the periphery and initiate β-cell specific autoimmune responses, which cause insulitis and β-cell death. When majority of β-cell mass is lost, diabetes occurs.

The role of DR molecules in the disease progression, however, is defined quite differently. Although the frequency of DRB1*0401 is high in diabetic patients, it is mainly due to its strong linkage disequilibrium with highly susceptible DQ8 alleles (6). Results from DQ8-matched case-control studies have indicated that different DQ8-DRB1*04 haplotypes are associated with variable risks in a hierarchical rank of DQ8-DRB1*0405 > DQ8-DRB1*0402 > DQ8-DRB1*0401 > DQ8-DRB1*0404 (*RR=1*)> DQ8-DRB1*0403 or 0406 (8, 9). DQ8-DRB1*0405/0402/0401 are susceptible, DQ8-DRB1*0404 is neutral and DQ8-DRB1*0403/0406 are strongly resistant. This rank suggests that DR4 subtypes composed of different DRB1*04 alleles provide variable degrees of protection to T1D in the order of 0405 < 0402 < 0401 < 0404 < 0403 or 0406. In addition, by using HLA transgenic mice that also transgenically express the co-stimulatory molecule CD80 in β-cells, it has been demonstrated that the co-expression of DR4 (DRB1*0401) with DQ8 diminishes the incidence of spontaneous diabetes (10). Taken together, these studies suggest that DR4 molecules modulate the T1D susceptibility conferred by DQ8. However, the mechanisms by which those DR4 manifest the effect are still under investigation.

A peptide competition model has been proposed to address the combined effect of DQ8 and DR4 to the risk of T1D (11). It hypothesizes that DR4 competes with DQ8 for β-cell-derived peptides responsible for the activities of autoreactive CD4 T cells, which escape from negative selection due to the defect of DQ8. The outcome of DR4-DQ8 competition results in reduced peptide occupancy of DQ8 on the surface of APCs and diminishes peptide-driven autoreactive CD4 T cell responses. Hence, it provides a straightforward explanation to the hierarchical association between T1D and those DQ8-DRB1*04 haplotypes. It is noteworthy that polymorphic residues among this panel of DRB1*04 alleles are mostly located in the peptide binding site and directly involved in peptide presentation. Thus, these polymorphisms might render distinct DR4 subtypes variable peptide competition potentials that differently affect DQ8-restricted autoreactive CD4 T cell activities. A strong DR competitor is associated with decreased T cell activities, whereas a weak DR competitor is associated with increased T cell activities.

This study aimed to develop an *in vitro* experimental system and provide the evidence to define the role of DR4 molecules regarding their peptide competition capabilities. We started from preparing reagents that were required to evaluate the peptide occupancy of DQ8 molecules. It was accomplished by generating a panel of T cell lines and hybridomas from HLA-DQ8 transgenic mice that were immunized by candidate peptides. These T cell reagents were also characterized regarding their specificities and purities to ensure that the quality satisfied the requirement of peptide presentation evaluation. Four steps were then applied to test the hypothesis of DR4-DQ8 competition. In the first step, a candidate peptide – $hGAD65_{206-220}$ was demonstrated to be capable of binding to both DQ8 and DR4. The second step was to examine whether the presence of DR4 (0401) would diminish DQ8-restricted T cell responses. This was achieved by comparing T cell responses elicited by $DQ8^+DR4^-$ to $DQ8^+DR4^+$ APCs, which were obtained from different HLA transgenic mice since they were the most available sources of APCs segregating DQ8 from DR4 expression. To further confirm the role of DR4 competition, another T cell assay was applied in the presence of a peptide blockade that occupied DR4 peptide binding sites to neutralize DR4 peptide binding activity. We observed that T cell responses were partially recovered. The third step was to evaluate effects of different DRB1*04 alleles. With the comparison of T cell responses induced by a panel of human B cell lines that expressed distinct DQ8-DRB1*04 haplotypes, we demonstrated that B cells bearing T1D resistant DQ8-DRB1*0403/0406 haplotype and neutral DQ8-DRB1*0404 were less capable of triggering T cell responses than those expressing susceptible DQ8-DRB1*0402 and DQ8-DRB1*0401 haplotypes. In the end, we attempted to deliver a candidate peptide $hGAD65_{539-547}$ into intracellular compartments where HLA-DQ8 and DR4 were synthesized. It was accomplished by forcing an artificial APC – COS7 cell line to synthesize the candidate peptide endogenously from the transfected recombinant invariant chain cDNA that carried the peptide coding sequence. This endogenously synthesized peptide was presented by DQ8 onto the surface and caused the T cell response. However, in the presence of DR4, the T cell response was reduced.

In summary, we not only provided the evidence to demonstrate that DR4 was able to compete for peptides with DQ8, but also showed that the potential of competition was associated with polymorphisms (within the peptide binding site) that distinguished high risk DQ8-DRB1*04 haplotypes from low risk ones. With this improved understanding to the role of DR4

in affecting DQ8 peptide presentation in this *in vitro* system, it is tantalizing to use the HLA transgenic mouse model to further pursue the outcome of DR4-DQ8 peptide competition under the *in vivo* system regarding the generation, activation and regulation of DQ8-restricted autoreactive T cells. These events all depend on the amount of peptide:DQ8 complexes. Given the DQ8-DR4 is the most common haplotype in the Caucasian population, the knowledge toward the overall effect of this haplotype should always be considered in the attempt to develop immunotherapeutic strategies to interfere in the progression of autoimmune diabetes.

2.0   REVIEW OF RELEVANT LITERATURE

2.1   Etiology of T1D

2.1.1   Clinical manifestation

Type 1 Diabetes (T1D) or insulin-dependent diabetes mellitus (IDDM) is by far the most common serious metabolic disorder in children (12). It is characterized as the hyperglycemia and absolute lack of insulin production due to the loss of pancreatic β-cells. Although exogenous insulin administration prevents death caused by insulin-deficiency, it is not able to cure the disease and leads to a variety of life-span complications such as T1D-related eye disease, kidney dysfunction, cardiovascular disease and neuropathy syndromes. As a consequence of microvascular pathology in the retina and renal tissues, T1D is now the leading cause of new cases of blindness in people aged 20-74. T1D patients are the fastest growing group of recipients for renal dialysis and kidney transplantation. Over 60% of these patients are affected by neuropathy. In conjunction with lower extremity arterial disease, T1D accounts for 50% of all non-traumatic amputations in the United States. Furthermore, the risk for developing cardiovascular complications is increased 2-fold to 6-fold in subjects with T1D (13). Their life expectancy is about 7-10 years shorter than normal healthy subjects (14).

2.1.2   T1D is an autoimmune disease

Distinguished from Type 2 Diabetes (or non-insulin-dependent diabetes mellitus, NIDDM) that is defined as either insufficient insulin-secretion by pancreatic β-cells or improper taking up of insulin by peripheral tissues, T1D is characterized as the selective autoimmune destruction of insulin-producing β-cells. By the onset of T1D, the β-cell mass is mostly destroyed and the C-

5

peptide (a post-translation side-product of proinsulin) level in the blood is below detection, indicating that no insulin is produced.

T1D shares several common features (2) with other autoimmune diseases. First, the disease state can be transferred to a healthy subject by the patients' antibodies or T cells. It was supported by a report of an accidental transmission of the disease to a 29-year-old aplastic anemia-affected woman who developed T1D 4 years after receiving bone marrow transplantation from her HLA-identical diabetic brother (15, 16). The circulating leukocytes (B lymphocytes and T lymphocytes) were confirmed to be male-donor type by chromosomal analysis. It indicated that the disease was not spontaneous but was caused by the lymphocytes from the donor's bone marrow.

More details about the role of lymphocyte subsets have been further elucidated by studies using animal models of T1D such as the non-obese diabetic mouse (NOD). NOD is one of the most intensively investigated animal models of T1D (17). This strain was originally established in Japan by inbreeding of Jcl:ICR progenitors in 1980 (18). Many sub-strains are now available, though they differ from each other with certain variation of spontaneous diabetes incidence. In high-incidence colonies, 80-90% of female NOD mice are diabetic by 24 weeks of age, whereas incidence of male NOD mice is lower and more fluctuating, typically >40 % by the age of 30 weeks. Similar to human T1D, the onset of diabetic symptoms in NOD mice is preceded by insulitis, a process defined as a mixed population of leukocyte infiltrating into islets and subsequent disruption of islet structure and function. CD4 and CD8 T cells are major "invaders". Normally, the number of CD4 T cells is dominant over CD8 T cells (19, 20). In addition, B cells, macrophages, and dendritic cells are also found at the site of infiltration (21).

It was also demonstrated that the disease was able to be transferred in mice by diabetic NOD spleen T cells including CD4 and CD8 T cell subsets to the irradiated non-diabetic young NOD or NOD*scid* recipients (NOD*scid* mice are immunodeficient because a genetic mutation leads to the failure of T cell and B cell development) (22, 23). CD4 T cells are so-called helper T cells. They respond to antigens presented by MHC Class II molecules and secrete cytokines such as IL-2, IFN-γ, TNF-α, IL-4, IL-10, etc. These cytokines induce further proliferation and/or activation of lymphocytes/monocytes. Alternatively, CD4 T cells also express membrane-bound

CD40 ligand (CD40L) and Fas ligand (FasL). CD40L triggers the activation of target cells such as B cells and macrophages, whereas FasL triggers the apoptosis of Fas-expressing cells. CD8 T cells are cytotoxic (or killer) cells. Unlike CD4 T cells, CD8 T cells engage with cells expressing specific antigens in the context of the MHC Class I molecule. Once activated, CD8 T cells are armed with FasL, perforin and granzyme to kill target cells instead of helping other leukocytes. Meanwhile, activated CD8 T cells also secrete IFN-γ and TNF-α/β to sensitize the targets for killing machinery equipped by CD8 T cells. Neither the purified CD4 nor the CD8 T cell subset from diabetic NOD spleens alone is able to transfer the disease to young NOD or NOD*scid* recipients (24). Without the help of CD4 T cells, CD8 T cells from diabetic NOD cannot home to islets of NOD*scid* recipients (22). In addition, the disease cannot be transferred by diabetic NOD spleen T cells (including CD4 and CD8 T cells) to NOD*scid* recipients that also carry the β2-microglobulin mutation (25). As the β2-microglobulin mutation leads to a deficiency of MHC Class I expression in recipient islet cells, thus they cannot not serve as CD8 T cell targets. Therefore, both CD4 and CD8 T cells are required for diabetes development. Although B cells are also observed at the site of islet infiltration, they are generally not considered as primary mediators of β-cell destruction. Without T cells, B cells alone cannot induce diabetes in NODscid recipients. B cell-depleted diabetic NOD splenocytes transfer disease as well as the non-depleted spleen cell population. The role of B cells in accelerating or postponing the disease is mainly achieved by modulating antigen presentation and T cell immunity instead of directly targeting the pancreas (26, 27).

The second feature shared by T1D and other autoimmune diseases is that the disease can be slowed or prevented by immunosuppressive therapy. Typical chemicals for this therapeutic regimen include cyclosporine (28, 29), FK506 (30, 31), steroids (31), and Azathioprine (32). They are all immunosuppressive medicines. However, the administration of these agents is limited by their toxicity to peripheral tissues, especially kidneys. A promising strategy was achieved with the administration of an anti-CD3 monoclonal antibody to block T cell responses without toxic effects to other tissues (33). It is noteworthy that all of these regimens are targeting T cell activities regardless of T cell antigen specificities. In addition, they are only effective at the early stage of the disease progression before the β-cell mass is completely destroyed.

A third feature is that the cell-mediated autoimmunity only targets against self-tissues. In the scope of T1D, pancreatic β-cells are the ultimate target, whereas glucagon-producing α-cell and somatostatin-producing δ-cells are spared. The overt clinical symptom is preceded by insulitis. Autoantibodies (secreted by infiltrated B cells with the help of CD4 T cells) (34, 35) and self-reactive CD4/CD8 T cells (36, 37) are specific to the β-cell products such as insulin (38-40), glutamic acid decarboxylase 65 (GAD65) (27, 35, 41, 42) and other β-cell-derived antigens (43), which are collectively considered as T1D-related autoantigens. Conceptually, insulitis is composed of two phases, concluded from the observation from NOD mice. During the first phase, autoantigen-specific naïve CD4 and CD8 T cells are activated in pancreatic lymph nodes (PLNs). In the second phase, activated T cells or diabetogenic T cells migrate to the islets and specifically kill β-cells. The damage further accelerates lymphocyte infiltration.

In the PLNs, the activation of diabetogenic T cells requires antigen presenting cells (APC) – mainly tissue-resident macrophages and dendritic cells (DCs) to present β-cell- derived autoantigenic peptides to T cell receptors (TCRs). The initial release of autoantigens is due to the physiological β-cell death. Evidence from rodent models has revealed that a wave of physiological β-cell death takes place in islets during the juvenile stage, peaking at 14-17 days after birth, regardless of normal or diabetes-prone strains (44-47). This wave of β-cell death could be due to tissue remodeling during the development, which involves apoptosis (48). Alternatively, during the weaning stage, the pancreatic tissue undergoes stress due to massive metabolic changes such as the rate of glycogenolysis, gluconeogenesis, lipogenesis and hormone production (49). For reasons unknown, β-cells are very sensitive to the stress. Cellular components released from dead β-cells are engulfed by APCs, particular DCs, and subsequently induce DC maturation. Matured DCs migrate to the PLN. Meanwhile, several critical phenotype changes such as upregulation of the antigen processing/presentation machinery and co-stimulatory expression render matured DCs further competent to activate β-cell-reactive T cells. The activation signal not only drives T cells to proliferate, but also induces naïve T cell to become armed effector T cells. Naïve CD4 T cells become Th1 or Th2 cells. Naïve CD8 T cells become Tc cells.

The physiological wave of β-cell death alone is not sufficient to cause diabetes. The massive, specific destruction of β-cells is caused by activated T cells that infiltrate into the islets. As a part of activation, activated T cells increase the expression of adherent molecules such as LFA-1 and ICAM-1, thus enhancing the mobility within tissues. In the islet, activated T cells encounter their cognate antigens and manifest their effects. Two major cellular mechanisms are involved in T cell mediated β-cell death (50, 51). First, the "cell-cell contact" is the principal approach undertaken by self-reactive Tc cells. It is triggered by the engagement between the TCRs and the self-peptide:MHC Class I complex on the surface of β-cells. Thus, Tc cells either use the Fas/FasL (52, 53) or the perforin/granzyme (54, 55) pathway to induce β-cell apoptosis. Activated CD4 T cells, especially Th1 cells, however, manifest their killing effect indirectly. Tissue-resident macrophages present islet antigens in the context of MHC Class II molecules and induce Th1 cells to secrete cytokines such as IL-2, IFN-γ and TNF-α. IL-2 mainly enhances CD4/CD8 T cell proliferation. IFN-γ, on the other hand, not only upregulates MHC, co-stimulatory molecule expression in the APCs and β-cells that enhance β-cell antigen exposure, but also activates macrophages that subsequently secrete soluble mediators to accelerate β-cell apoptosis (56). The second mechanism – "soluble mediators" is more complicated and less specific than the "cell-cell contact" mechanism since it involves multiple cytokines (IFN-γ, TNF-α, IL-1, IL-6, and NO) generated by a variety type of cells. **Figure 1** briefly illustrates the pathways described above.

2.1.3   Epidemiological statistics

According to the statistics provided by the National Institute of Diabetes and Digestive and Kidney Diseases, by 2005, 20.8 million people in the United States (7 % of the population) have diabetes (http://diabetes.niddk.nih.gov/dm/pubs/statistics/index.htm). T1D accounts for 5-10% of all diagnosed cases of diabetes. Additionally, 13,000 children are diagnosed annually with T1D.

Worldwide, the incidence of T1D is varied among different countries, ranging from the highest 35/100,000 per year in Finland to the lowest < 0.1/100,000 per year in the People's

Republic of China (57). The enormous geographic variation for the risk to develop T1D is due to combined effects of genetic and environmental factors.
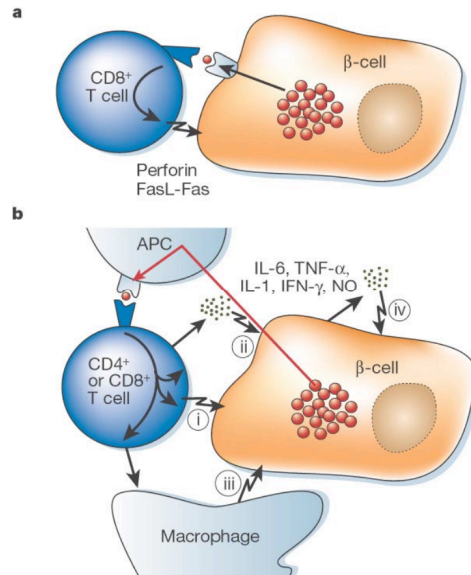
Figure 1. Cellular mechanisms of β-cell death.

(a). The CD8 T cell is activated by direct recognition of β-cell antigens presented by MHC Class I molecules on the surface of the β-cell. Activation induces CD8 T cells to express FasL and perforin/granzymes and trigger β-cell apoptosis. (b). Activated CD8 T cells (by direct engagement to the β-cell) and CD4 T cells (recognize β-cell antigens presented in the context of MHC Class II complex on the surface of tissue-resident macrophages and other APCs) express FasL or membrane-bound TNF-α and trigger β-cell death *via* FasL/Fas and TNF-α/TNF-R pathways (i); activated T cells also secrete cytokines and other soluble death mediators to induce β-cell death directly (ii); macrophages are activated by T cells and elicit their cytocoidal activities (iii); the intracellular stress induces the β-cell endogenous apoptotic pathway (iv) (adapted from reference (57)).

2.1.4 Genetics of T1D

The feature of familial clustering is a landmark to determine whether a disorder is an inherited disease. The overall risk for developing T1D in North American Caucasian siblings, parents and offspring of an individual with T1D varies from 1-15%, as compared to 0.12% in the general population (58-63). In addition, twin studies have revealed stronger disease concordance rates among monozygotic than dizygotic twins (64). Thus, it is very clear that T1D is a genetically associated disorder. However, data from the same study also suggests that T1D is affected by

10

environment factors since the concordance rate for T1D development between monozygotic twins is less than 50 %.

According to the information collected by the T1DBase (65), a Type 1 Diabetes specific bioinformatics resource founded by the Juvenile Diabetes Research Foundation (JDRF) and the Welcome Trust, at least 20 genomic loci have been identified to be associated with the disease (**Table 1**).

The strongest genetic determinant – *IDDM1* is located at chromosome 6p21, the Human Leukocyte Antigen (HLA) cluster (66), which accounts for over 40 % of the familial clustering of T1D (67). This region, approximately 3.5 Mb in length, harbors three different MHC Class I α-chain genes – HLA-A, -B, -C, three different sets of MHC Class II α/β-chain genes – HLA-DP, -DQ, -DR, and genes encoding a variety of antigen processing/presentation related products (**Figure 2**) (1).
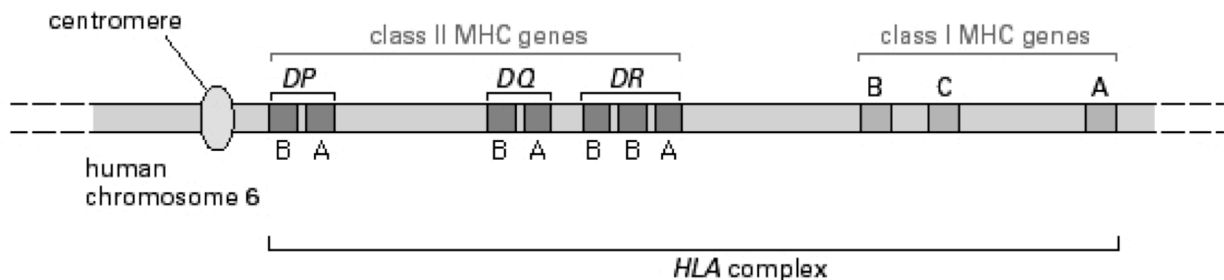
Figure 2. The organization of human HLA gene cluster.

The simplified diagram illustrates the location of the genes that encode the α–chain subunits of class I MHC, and α/β-chains of class II MHC molecules. Genes shown encode three types of class I proteins (HLA-A, HLA-B and HLA-C) and three types of class II MHC proteins (HLA-DP, HLA-DQ, and HLA-DR). An individual can therefore make six types of Class I HLA (three encoded by maternal chromosome and three by paternal chromosome) and more than six types of class II HLA proteins. The number of class II HLA molecules that can be made is increased because 1) there is more than one DR β-chain gene; 2) the DQ, DP β-chains expressed from maternal chromosome can pair with the α-chains expressed from either *cis*-position and *trans*-position. (adapted from reference (1))

Table 1. Human T1D gene linkage summary

Region name	Candidate genes or markers
IDDM1	HLA (DQA1, DQB1, DRB1)
IDDM2	5' INS-VNTR, TH
IDDM3	D15S107
IDDM4	FGF3,D11S1917, MDU1, ZFM1, RT6, ICE, CD3, LRP5
IDDM5	ESR, a046Xa9, MnSOD
IDDM6	D18S487, D18S64, JK
IDDM7	D2S152, D2S326, GAD1
IDDM8	D6S281, D6S264, D6S446
IDDM9	D3S1303
IDDM10	D10SS193, D10S208, GAD2
IDDM11	D14S67
IDDM12	CTLA-4, CD28
IDDM13	D2S137, D2S164, IGFBP2, IGFBP5
IDDM15	IDDMFYN, D6S283, D6S434, D6S1580
IDDM17	D10S554, D10S592
IDDM18	IDDMIL12B, IL12B
Unnamed Chr1	D1S1617
Unnamed Chr16	IDDMICSBP1, D16S3098
Unnamed Chr8	D8S198
Unnamed ChrX	DXS991, DXS999

source: data from T1DBase (http://T1Dbase.org)

HLA-A, -B, and -C are all polymorphic. Each allele encodes a 44 KDa MHC Class I α-chain that non-covalently associates with a 12 KDa non-polymorphic β2-microglobulin (**Figure 3A**), which is encoded by the β_{2m} gene outside of HLA region. Class I HLA molecules are

expressed virtually on every nucleated cell surface. Their function is to present intracellular antigenic peptides (normally derived from viral products or mis-folded endogenous proteins) to CD8 T lymphocytes.
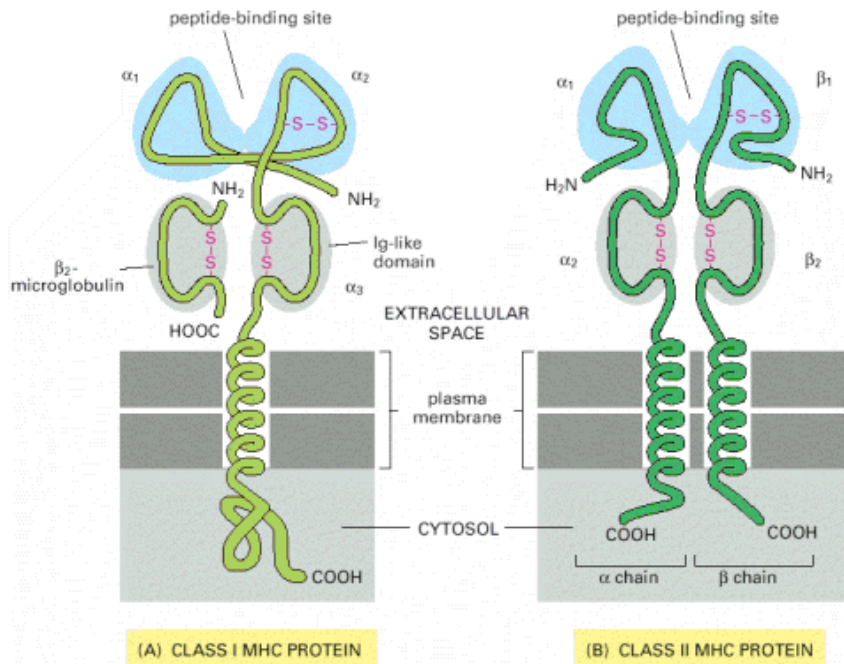
Figure 3. Class I and Class II MHC molecules.
(**A**) The α-chain of a class I molecules has three extracellular domains, α1, α2, α3, encoded by distinct exons. It is non-covalently associated with a smaller polypeptide chain, β2-microglubolin, which is not encoded within the MHC cluster region. The α3 domain and β2-microglobulin are Ig-like. While β2-microglobulin is monomorphic, the α-chain is extremely polymorphic, mainly in the α1 and α2 domains that form the peptide binding site. (**B**) For an MHC class II molecule, both α-chain and β-chain are polymorphic (except α-chain for HLA-DR), mainly in the α1 and β1 domains. Meanwhile, α1 and β1 domains form the peptide binding site. The α2 and β2 domains are Ig-like (adapted from reference (1)).

HLA-DP, -DQ, and -DR molecules consist of two non-covalently associated glycoproteins – an approximate 34 KDa α-chain and an approximately 29 KDa β-chain (**Figure 3B**). They are expressed on the surface of professional antigen presenting cells (APCs) such as B lymphocytes, macrophages, and dendritic cells. Their function is to present engulfed soluble extracellular protein antigen fragments to CD4 T lymphocytes. Activated human T cells also express Class II HLA (mouse T cells don't express any MHC Class II molecules). Both the α-

chain and β-chain of HLA-DP (DPA1, DPB1) and HLA-DQ (DQA1, DQB1) are polymorphic. The HLA-DR β-chain gene is polygenic and polymorphic. Several loci within the DR-subregion encode functional β-chains to pair with a non-polymorphic α-chain from the DRA1 locus. The complexity of human HLA gene organization has evolved to improve the immune recognition against a diversified pathogen invasion. Another feature of HLA genomic organization is the linkage disequilibrium, particularly between DQB1-DQA1 and DRB1 loci (68). During meiosis, the recombination between DQ and DR loci is very rare. The parental DQ-DR haplotypes instead of randomly segregated DQA1, DQB1, and DRB1 alleles are stably transmitted to the next generation. Therefore, distinct DQ-DR combinations are unevenly distributed in the population. In distinct ethnic groups or geographic areas, the frequency of each haplotype is different.

Not all genes within this 3.5 Mb region are genetically associated with T1D. In the early stage of familial studies, serological approaches were widely used to determine those common HLA haplotypes shared by diabetic parents and children. Historically, HLA-B8, B15 and B18 were first observed with increased frequency in T1D patients as compared to a non-diabetic control population (69, 70). Then, serological typing for class II HLA loci revealed a stronger association between HLA-DR and T1D than the association between HLA-B and T1D (71-73). Approximately 95% of T1D patients in most populations have DR3 and/or DR4. Expression of HLA-DR2, however, was generally considered to be associated with T1D resistance, and the protective effect of DR2 was dominant over DR3 or DR4 alleles. Later on, it was realized that serological methods were limited by the availability and the resolution of HLA specific anti-serums. The advent of molecular biology techniques, especially the Polymerase Chain Reaction (PCR) and the DNA sequencing based Sequence Specific Oligonucleotide Probing (SSOP) or Single Nucleotide Polymorphism (SNP) increased the resolution of HLA typing and simplified the procedure. By analyzing HLA alleles in a variety of racial and ethnic groups, it was revealed that the presence of a specific human DQ β-chain polymorphism encoding a neutral amino acid (alanine, valine, or serine) other than aspartic acid at the position 57 (so-called non-Asp57β) was strongly associated with T1D (4, 5). In contrast, a negatively charged aspartic acid at the position 57 of the DQ β-chain (Asp57β) appeared to confer "resistance" to T1D progression. The association between non-Asp57β DQ allele and T1D is stronger than the HLA-DR3, -DR4. Meanwhile, the investigation of the association between the DQ α-chain and the disease

suggested that an arginine residue at position 52 of the DQ α-chain was found in high frequency in the T1D population (74). Common non-Asp57β alleles in the Caucasian T1D population include DQB1*0302 and DQB1*0201, whereas Asp57β alleles include DQB1*0301 and DQB1*0602. Arg52α alleles normally refer to DQA1*0301 and DQA1*0501, whereas non-Arg52α alleles refer to DQA1*0102, etc. Those haplotypes composed of a non-Asp57β allele and an Arg52α allele encode high risk "diabetogenic" heterodimers (7) such as the DQB1*0302/DQA1*0301 haplotype (DQ8) and the DQB1*0201/DQA1*0501 haplotype (DQ2). The DQB1*0602/DQA1*0102 haplotype (DQ6) is protective. It is noteworthy that DQ8 and DQ2 are stably transmitted with DR4 and DR3 to the next generation due to the strong linkage disequilibrium between DQ and DR loci. Interestingly, individuals with heterozygosity for DR3/DR4 (also heterozygous for DQ8/DQ2) are more susceptible to the disease than a DR3 or DR4 homozygote. It has been suggested that individuals with both DQ8 and DQ2 are able to produce four different non-Asp57β/Arg52α heterodimer combinations, whereas DQ8 homozygous or DQ2 homozygous subjects are only able to form one non-asp57β/Arg52α heterodimer. In addition, the expression of Asp57β DQ6 confers predominant protection since DQ8/DQ6 heterozygous individuals are resistant to the disease. It is consistent with the notion mentioned above that the protective effect of DR2 is dominant over susceptible DR3/DR4 haplotypes because DQ6 is closely linked with DR2. Additional evidence from NOD mice also supports the predisposing role of DQ in the progression of T1D, because NOD mice only express an $H2-A^{g7}$ MHC Class II heterodimer that is regarded as the human HLA-DQ homologue. The NOD $H2-A^{g7}$ β-chain shares the non-Asp57β feature with HLA-DQ8 β-chain (75). Two amino acid mutations from $H2-A^{g7}$ β57 serine $\rightarrow$ aspartic acid and β56 histidine $\rightarrow$ proline render this NOD mutant ($NOD.H2-A^{g7PD}$) free from diabetes (76). It is still challenging to pursue whether and how DR molecules are also involved in disease predisposition. Although DR molecules are not the primary factor in conferring T1D susceptibility, they may play an independent role other than DQ in T1D progression. This notion is driven by at least two observations. First, like many other autoimmune diseases, all antigen-specific CD4 T cells cloned from peripheral blood of T1D patients are exclusively restricted to HLA-DR instead of HLA-DQ (77-79). Second, DQ8-matched case-control studies demonstrated that the risk for T1D development was modulated by the expression of closely linked DR4 (8, 9). It was suggested that different DR4 subtypes might be associated with variable degrees of protection. As the HLA-DR molecules are similar to

HLA-DQ regarding the structure and the function, DR molecules should manifest their effect through influencing CD4 T cell reactivity.

In NOD mice, the MHC gene cluster is also the first reported genetic determinant associated with spontaneous diabetes (80). Located on mouse chromosome 17, the cluster encompasses genes encoding mouse MHC Class I/II, and other antigen processing/presenting related proteins. The unique MHC haplotype in NOD mice, termed $H2^{g7}$ consists of $H2\text{-}K^d$ and $H2\text{-}D^b$ –two MHC Class I α-chain genes, plus $H2\text{-}A^{g7}$ – MHC Class II α/β-chain genes. NOD mice are deficient in H2-E expression due to a deletion in Eα promoter region. $H2\text{-}K^d$ and $H2\text{-}D^b$ alleles are also shared by diabetes-resistant strains such as BALB/C and C57BL/6, respectively. The α-chain of $H2\text{-}A^{g7}$ is identical to the α-chain of $H2\text{-}A^d$ from BALB/C, however, the β-chain of $H2\text{-}A^{g7}$ in NOD is unique and differs from the β-chain of $H2\text{-}A^d$ only at the first external domain (75). The NOD $H2\text{-}A^{g7}$ β-chain contains a histidine at position 56 and a serine at position 57, whereas BALB/C $H2\text{-}A^d$ β-chain has a proline and an aspartic acid at residues 56-57 instead. The polymorphism of two residues renders different peptide binding affinity and preference. It also confers the $H2\text{-}A^{g7}$ T1D susceptibility and the $H2\text{-}A^d$ T1D resistance. It is noteworthy that the non-Asp57β feature of NOD $H2\text{-}A^{g7}$ is similar to human T1D susceptible HLA-DQ8 (DQA1*0301/DQB1*0302) in the Caucasian population. In addition, it is well acknowledged that both homozygous expression of the $H2\text{-}A^{g7}$ and the H2-E deficiency are required for spontaneous diabetes development in the NOD. The transgenic expression of $H2\text{-}E^d$ in NOD background diminishes the diabetes incidence in a dose-dependent pattern (81). The mechanism of the protection provided by $H2\text{-}E^d$ expression is very complicated and is still under investigation.

Another putative genetic predisposing factor of T1D – *IDDM2* is briefly illustrated here, for it accounts for ~10 % of familial clustering of T1D (82, 83). The *IDDM2* refers to the variable number of tandem repeats (*VNTR*) at the 5'-region of human insulin genes. The 5' *INS-VNTR* polymorphisms are categorized into three classes. Class I represents approximate 26-63 repeats, up to 570 bases in length. Class III represents 140-200 repeats up to 2,200 bases in length. Class II is defined as the length between Class I and Class III (84). The *VNTR* polymorphism was demonstrated to influence insulin expression, especially in the thymus (84,

85). The protective Class III allele expresses a higher level of insulin than the susceptible Class I allele. It has been suggested that high insulin expression in the thymus enhances antigen-driven negative selection of insulin-specific autoreactive T cells.

It is noteworthy that neither diabetogenic HLA haplotypes nor alleles are fully penetrated, so that not every individual who inherits susceptible haplotypes/alleles from diabetic parents will necessarily develop T1D. It actually implies the role of environmental factors in the etiology of T1D.

2.1.5 Environmental factors

Strong evidence of environmental factors linked to the progression of T1D include the discordant disease onset rate between monozygous twins who inherited identical genetic materials from their parents (64) and enormous geographic variation of the disease incidence that has been observed in world-wide epidemiological studies (86). These differences are not simply due to ethnical differences since migrants from countries with low T1D frequency to countries with a high frequency are more susceptible to the disease than their compatriots (87).

Viral infection is one of the first etiological hypotheses (88-92). Particular attention has been paid to rubella virus and Coxsackie B virus. The involvement of Coxsackie B virus derived superantigens in triggering islet specific T cell expansion was identified in severe leukocyte infiltrated pancreatic tissues from a child who died from acute-onset T1D related ketoacidosis (93). The consumption of cow's milk or infant formula has also been suspected to be a critical environmental trigger or modulator to the progression of T1D. This notion was supported by the presence of anti-BSA (bovine serum albumin) antibodies in 100% of subjects affected by T1D (94), but it was challenged by the opposite observation (95). In addition, it is also suggested that the T1D incidence appears to be influenced by the degree of a society's cleanliness. The "hygiene hypothesis" holds that the improvements in health care delivery and sanitation have lead to the rise in autoimmune disorders including T1D (96, 97). Likewise, this hypothesis lacks sufficient evidence.

In summary, T1D is a degenerative disease. Genetic predisposing factors (susceptible HLA haplotypes) are further complicated by a variety of unveiled environmental factors to generate autoimmune responses against b-cells and ultimately cause b-cell death.

2.2   The establishment/maintenance of antigen specificity and self-tolerance

Although certain HLA/MHC alleles are associated with spontaneous diabetes in human and NOD mice, these alleles don't directly cause β-cell death. Nevertheless, they are responsible for the generation of autoreactive T cells and T cell-mediated autoimmunity causes β-cell death.

2.2.1   The binding between a peptide and an MHC molecule

Structurally, a peptide:MHC Class II complex exists as a three-chain complex composed of an α-chain and a β-chain of class II heterodimer plus an antigenic peptide associated with the peptide binding groove. Class II molecules without associated to peptides have been previously demonstrated to be vulnerable to aggregation and sensitive to proteolytic degradation (98). It suggests that the association of class II MHC with a peptide is required for structural integrity and stability.

Crystal structure studies have indicated that an MHC Class II heterodimer has two membrane-proximal immunoglobulin-like domains within each subunit (α- and β-chain), and a membrane-distal peptide-binding site formed by an eight-stranded β-sheet and two α-helical regions (**Figure 4**)(99, 100). The β-sheet acts as the "floor" to provide the support for the bound peptide, while two α-helixes act as two "clamps" to hold the bound peptide. Both the α-chain and the β-chain are involved in the formation of the binding region. Polymorphic residues in each human HLA allele are clustered in the peptide-binding region. They are responsible for the peptide binding specificity and affinity. Unlike an MHC Class I molecule, which has closed ends at both sides and normally accommodates peptides with 8-10 residues (101-103), an MHC Class II heterodimer is open at both sides of the binding region so that there is less restriction to the

length of the peptide. The peptide stays in the Class II binding site in a straight extended conformation, like a hot dog in a hot dog roll. It has been suspected that this conformation allows the most residues of the peptide to be exposed outward, which maximizes the interaction with T cell receptor (TCR).
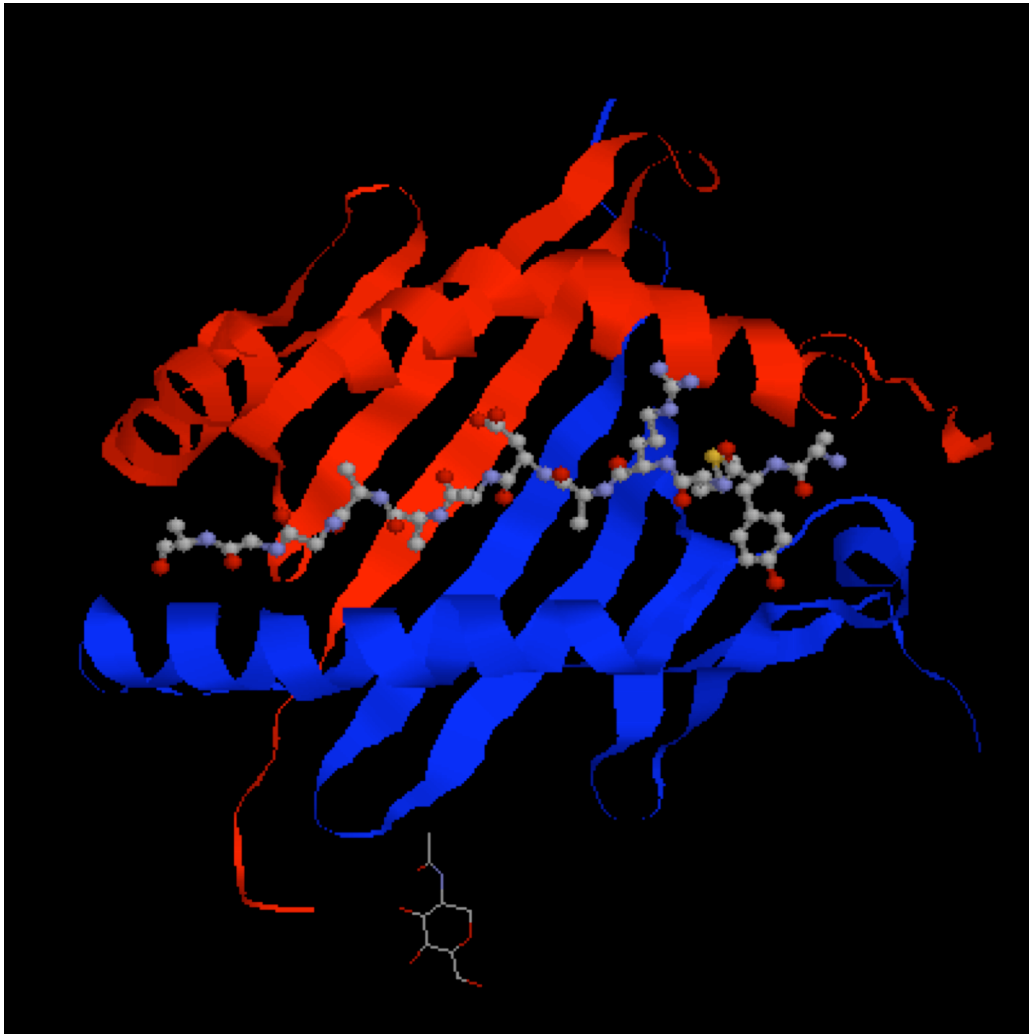
Figure 4. The illustration of HLA-DR4:Collagen$_{1168\text{-}1179}$ complex crystal structure.
The peptide binding site formed by the α-chain and the β-chain of HLA-DR4 is simplified as the ribbons in dark color and light color, respectively. The peptide of Callagen$_{1168\text{-}1179}$ is fitting in the middle of the DR4 binding site as illustrated in a ball-stick style (adapted from PDB file 2SEB with slight modification (101)).

Two different types of interaction contribute to the formation of a stable peptide:Class II complex – the hydrogen bond interaction and pocket interaction. Hydrogen bonds are formed between atoms along the main-chain peptide and side-chains of conserved amino acid residues in α-helixes and the β-sheet of the MHC. Therefore, the hydrogen bond interaction is independent of peptide sequence. Pocket interactions are formed between side-chains of the bound peptide and side-chains of residues in the Class II binding region. The β-sheet "floor" is actually not "flat". Due to the difference in size and direction of side-chains of different residues within the "floor" and "clamps", the surface of the "floor" has several "humps" and several "holes" or "pockets". Apparently, a "pocket" provides more possibility to accommodate a residue with a long point-out side-chain than a "hump". Normally, a peptide anchors into a Class II binding site at 5 principle "pockets" named P1, P4, P6, P7 and P9 according to the position of the residues (along the peptide) that interact with the Class II binding site. P1 and P9 locate near the end of the binding groove on each side, whereas P4, P6 and P7 cluster in the center of the binding site. The pocket interaction is not only determined by the size of the pocket, but also influenced by the polarity of the amino acid residues that form the pocket. The amino acid residues within both β-sheet "floor" and α-helix "clamps" contribute the polarity and the size of "pockets". Thus, distinct HLA molecules manifest different preferences for peptide binding. The degree of a difference is then determined by the similarity of the amino acid sequence along the binding groove.

2.2.2 The structure of TCR – the receptor of peptide:MHC complex

The nature of hydrogen bonds and pocket interactions allows a single MHC molecule (Class I and Class II) to bind a variety of distinct peptides, though the affinity is different (depending on peptide sequence and the polymorphisms within the MHC binding groove). An individual maximally expresses 6 different Class I and 20 different Class II molecules when he/she carries two distinct HLA haplotypes. Any given protein can be degraded into many different fragments by proteolytic enzymes in the antigen processing compartment, and in most cases, at least one of these peptides is able to bind one or more of MHC molecules and be presented on the surface of the cell (104). Thus, the immune system requires a well-tuned recognition system, not only to detect all kinds of pathogens, but also to distinguish the foreign from the self so that it avoids

eliciting immune responses to self-tissues. One major class of such recognition apparatuses (a second category is immunoglobulin that doesn't interact with HLA) is T cell receptor (TCR), which is only expressed on the T cell surface. The antigen recognition is accomplished by the TCR/CD3 complex and the co-receptor -- either CD4 or CD8. A TCR/CD3 complex consists of two parts – a TCR heterodimer and a CD3 complex (**Figure 5**), part of which associates with the intracellular tail of the TCR. The TCR is only responsible for the antigen recognition. The CD3 complex converts the TCR:antigen engagement event to the intracellular signals (such as the activation of phorsphotyrosine kinases, the cleavage of phosphatidylinositol (PIP2), calcium flux, etc), which ultimately induce T cell activation. $CD4^+$ T cells recognize antigenic peptides presented by MHC Class II complexes, whereas $CD8^+$ T cells recognize antigenic peptides in the context of MHC Class I molecules. The co-receptor CD4 and CD8 are also involved in antigen recognition by directly interacting with the non-polymorphic portion of the MHC molecules (**Figure 6**) (105, 106). Both CD4 and CD8 are believed to transduce signals independently from CD3 complex (107, 108).
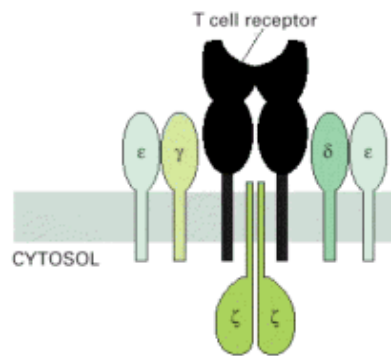
Figure 5. The TCR and its associated CD3 complex.

The TCR heterodimer is composed of two transmembrane glycoprotein chains, α- and β-chain. Both α- and β-chain have large external domains and small cytoplasmic tails that associate with four other polypeptides, collectively called CD3 complex. (Adapted from reference (1))
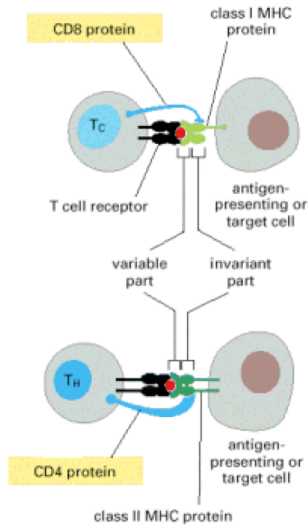
Figure 6. CD4 and CD8 co-receptors on the surface of T cells.

T_C cells express CD8, which interacts with the MHC Class I complex, whereas T_H cells express CD4, which interacts with MHC Class II proteins. It is noted that co-receptors bind to the same MHC protein that the TCR has engaged, so that they are brought together with TCRs during the antigen recognition process. Whereas the TCR binds to the variable part of the MHC protein that form the peptide binding groove, the co-receptor binds to the invariant part, far away from the MHC peptide binding groove (Adapted from reference (1)).
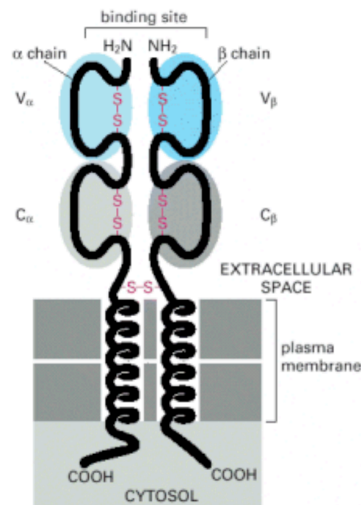
Figure 7. Schematic diagram to illustrate that the TCR is composed of an α- and a β-chain.

Each chain is about 280 amino acids long and has a large extracellular portion that is folded into two Ig-like domains – one variable (V) and one constant (C). The antigen binding site is formed by a V_α and a V_β domain, thus each TCR heterodimer has one binding site for antigen engagement. The α-chain and the β-chain are covalently associated to each other through a disulfide bond. A T cell typically has about 30,000 such receptors on its surface. (Adapted from the reference (1))

22

Most T cells express αβTCRs that consist of an α-chain and a β-chain. Only a small subset of T cells express γδTCRs. External portions of TCR α- and β-chains have two domains – a variable domain and a constant domain, respectively (**Figure 7**). Variable domains from α-chain and β-chain together form the antigen recognition site, which directly interacts with the combination structure of the antigenic peptide:MHC complex.
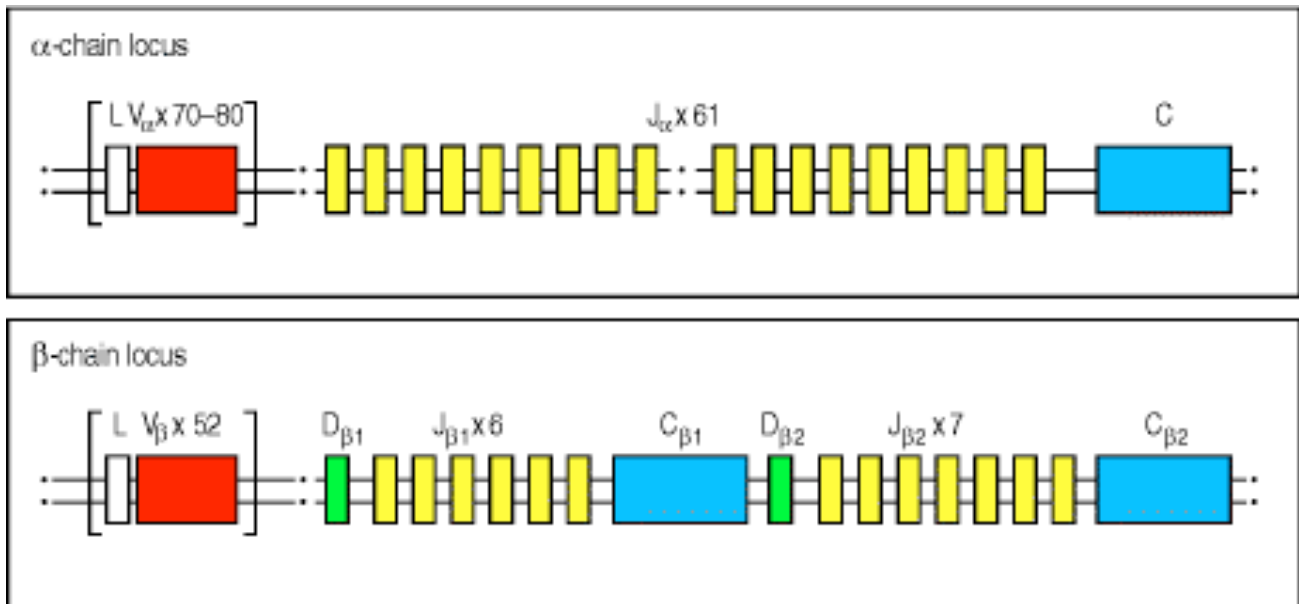
Figure 8. The organization of mouse TCR α-/β-chain genes.

In the mouse, the α-chain cluster consists of 70-80 V-segments categorized into 13 subfamilies (defined as groups of V gene segments that share greater than 75 % nucleotide sequence homology), though some of them are not functional (Pseudo-gene). Each functional V-segment contains a promoter, one exon encoding a leading sequence and one exon encoding the V-region. A cluster of ~60 J-segments is located a considerable distance from the V-segment cluster. The J-segment cluster is then followed by a single constant-domain gene. The α-chain gene cluster is actually interrupted between the J and V-segment loci by another TCR gene cluster – the δ-chain cluster (not shown here) The β-chain gene cluster is located on a different chromosome and the organization is slightly different. About 50 functional V-segments out of 17 subfamilies are located distantly from two separate clusters that each is composed of a single D gene segment, together with 6 or 7 J gene segments and a single constant-region gene. The two C_β genes are very similar to each other. (Adapted from reference (109))

The genomic organization of TCR α-/β-chain genes, however, is extremely complicated (**Figure 8**). Both the α-chain and the β-chain are encoded by genes constructed by rearrangement of discontinuous germline TCR gene segments for variable (V), diverse (D) (only existing in β-

23

chain), joining (J), and constant (C) regions (**Figure 9**). The rearrangement is catalyzed by DNA recombinases that are encoded by the recombinant activity genes –RAG1 and RAG2. Products of
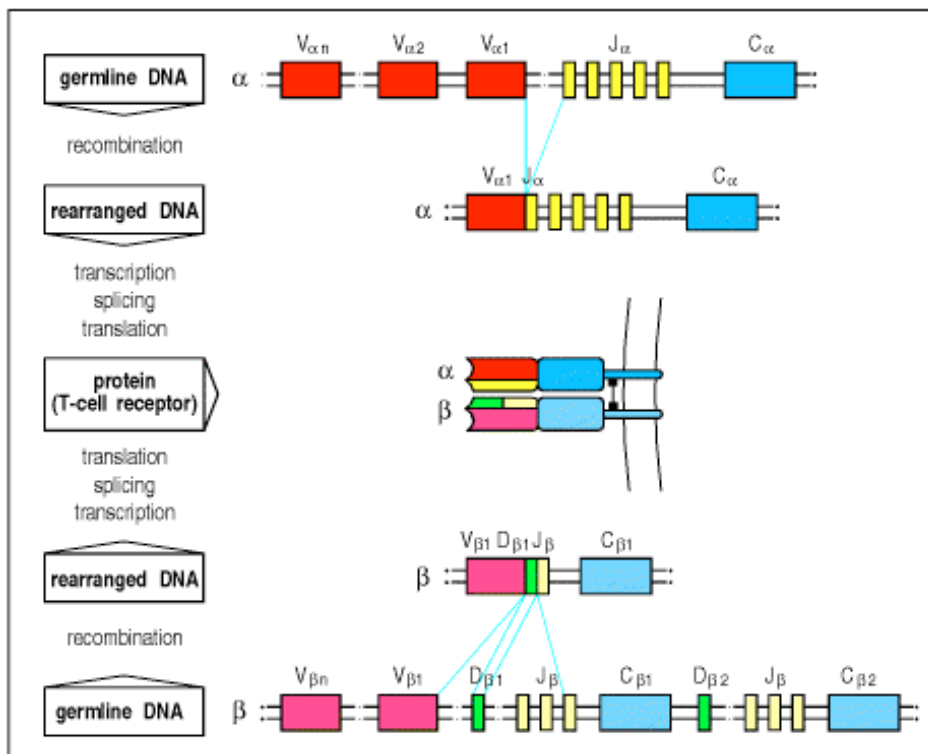
Figure 9. TCR α-/β-chain gene rearrangement and expression.
Both α-/β-chain genes are composed of discrete segments that are joined by somatic recombination during development of the T cell in the thymus. For the α-chain, a V_α gene segment joins to a J_α gene segment to create a functional exon. Transcription and splicing of the $V_\alpha J_\alpha$ exon to C_α generates the mRNA that is translated to yield the T cell receptor α-chain polypeptide. For the β-chain, the variable domain is encoded in three gene segments, V_β, D_β, and J_β. Rearrangement of these gene segments generates a functional $V_\beta D_\beta J_\beta$ exon that is transcribed and spliced to join to C_β. The resulting mRNA is translated to yield the T cell receptor β-chain. The α- and β-chain pair to each other to generate a functional TCR (Adapted from reference (110)).

the RAG-1/2 recognize specific recombination signaling sequences flanking each individual TCR gene V, (D), J segment and bring them together during particular periods of T cell development. Each rearrangement is believed to be an independent event so that the V(D)J recombination is individually randomized and collectively creates all possibilities of V(D)JC rearrangements among a whole T cell population. Additional diversities of rearrangement are also obtained at the V-(D)-J joint by the random introduction of nucleotides not encoded in the

germline, or deletion of nucleotides encoded in the germline. Theoretically, the total diversity of T cell receptors is about 10^{16}. It ensures that all possible peptide:MHC complexes can be recognized by one or some TCRs, as long as the affinity between the TCR and its ligand achieves a threshold. It is very likely that the generation of such a huge size TCR repertoire has co-evolved with the MHC system to form a comprehensive recognition system and provide the host with a mighty defense system against the invasion of all possible foreign pathogens.

2.2.3 T cell maturation and central tolerance

All T cells are developed from bone marrow pluripotent hematopoietic stem cells that do not express TCRs. In the thymus, with special intercellular signaling, these bone marrow-derived precursors then differentiate into thymocytes expressing TCRs. Therefore, the T cell development is actually the process of TCR repertoire generation. Three events are critical to T cell ontogeny: 1) the up-/down-regulation of RAG expression and the germline DNA rearrangement of TCR α-/β-chain genes; 2) the expression of co-receptor CD4/CD8 and lineage commitment; 3) thymic selection and central tolerance establishment.

The differentiation starts from the expansion of precursor cells to form the population of CD4$^-$CD8$^-$ double negative thymocytes (DN). The expression of RAG-1/2 is upregulated very briefly in a subset of DN thymocytes. At the DN stage, only β-chain gene rearrangement occurs (110). The rearrangement starts from one chromosome. Once a productive rearrangement is achieved, that β-chain then pairs with a surrogate α-chain –pTα to form a preTCR, which has been demonstrated to prevent further β-chain rearrangement from the second chromosome (111). If first rearrangement fails to generate a functional β-chain polypeptide because of the non-sense mutation introduced by randomly inserting or deleting nucleotides, the process continued allowing a second rearrangement from other chromosome. If both rearrangements fail to generate a functional β-chain to form a preTCR, the thymocyte clone is unable to receive survival signals and undergoes apoptosis. The allelic exclusion of further rearrangement is known as "β-selection" and allows each T cell to express a single TCR β-chain. A successful "β-selection" renders the thymocytes transition from DN into CD4$^+$CD8$^+$ double positive (DP)

thymocytes. At this stage, RAG-1/2 expression is activated again and allows rearrangement of α-chain gene elements. The allelic exclusion of the α-chain is not strictly enforced since two distinct TCR α-chains have been detected in T cell clones and hybridomas, though in most cases only one αβ heterodimer renders antigen specificity (112, 113). The functional α-chain then pairs with a previously matured β-chain to form a mature TCR heterodimer and translocates to the cell surface, where they are engaged with self-peptide:MHC complexes expressed on the surface of thymic cortical epithelia and undergo a process termed positive selection. Only the DP thymocytes bearing TCRs with enough avidity to self-peptide:MHC complex can survive. It is noted that the avidity is not only determined by the affinity of the interaction between a single TCR and its ligand, but also determined by the density of TCR:peptide:MHC engagements between the thymocytes and antigen presenting cells (114). Most DP thymocytes fail to be positively selected due to the weak interaction between TCR and self-MHC and undergo apoptosis. Therefore, the positive selection generates a TCR repertoire restricted by self-MHC and consequently ensures that all TCRs are able to detect foreign pathogens presented only in the context of self-MHC molecules. The successful positive selection also down-regulates RAG expression to prevent further α-chain rearrangement. Meanwhile, the lineage commitment is determined as DP thymocytes transit into a CD4 or CD8 single positive thymocyte stage (SP). The mechanism of CD4 and CD8 commitment is still not clear. Prior to obtaining full maturation and entering the periphery for immune surveillance, SP thymocytes encounter another checkpoint – the negative selection. Those SP thymocytes that bear TCRs interacting with self-peptide:MHC complex with high avidity are deleted from the repertoire. Thus, clonal deletion ensures that matured T cells are not able to recognize self-antigen in the periphery and protect self-tissue from autoimmune attack. Apparently, the negative selection is also self-peptide:MHC dependent. It occurs mainly at the thymic medulla, apart from the compartment for positive selection. Therefore, the intercellular signals are very different.

Theoretically, the size of the TCR repertoire can be as great as 10^{16} (1, 109). However, positive and negative selections dramatically reduce the size. Positive selection only allows thymocytes bearing "useful" TCRs (self-MHC restricted) to survive. Negative selection removes the thymocytes bearing "harmful" TCRs (reactive to self-peptide) from the repertoire and establishes central tolerance. The efficiency of negative selection is affected by several factors.

1) As negative selection is to delete thymocytes that recognize self-antigens, the expression of self-antigen in the thymus is required and the degree of expression may generate very different outcomes. In addition to the report that the risk to develop diabetes is weakly associated with the relative expression level of insulin in the thymus (82-85), recent studies of the *aire* gene provide substantial evidence regarding the association between thymic expression of self-antigen and the efficiency of negative selection. Aire is a transcription factor specifically expressed in thymic medullary epithelial cells (MECs) – the same cell population directing negative selection. Aire-deficient MECs have diminished expression of peripheral tissue-specific genes (115, 116), and Aire-deficient mice develop multi-organ autoimmune responses (115, 117), which indicate the complete loss of self-tolerance. In addition, in a study using hen-egg-lysosome (HEL)-specific TCR transgenic mice in conjunction with transgenic expression of HEL under the control of an insulin promoter, it was found that thymocytes were deleted in the presence of Aire, whereas they failed to be deleted in the absence of Aire (118).

2) As negative selection is TCR engagement dependent, the stability of the TCR ligand can also affect the efficiency of negative selection. Structural studies have showed that the presence of a non-Asp57b is shared by human T1D susceptible HLA-DQ8/DQ2 and the mouse spontaneous diabetes susceptible gene H2-A^{g7}. It distinguishes them from other diabetes resistant alleles such as HLA-DQ6 in humans and H2-A^{d} in mice, which have an aspartic acid residue at the position 57 of HLA/MHC Class II b-chain. It has been noticed that the non-Asp57b confers the predisposing HLA/MHC Class II molecules a unique P9 structure (119). The presence of aspartic acid at the position 57 in disease resistant alleles allows the formation of a salt-bridge – two hydrogen bonds between the Asp57b side-chain and the Arg76a side-chain. However, in the HLA-DQ8/DQ2 or H2-A^{g7}, the aspartic acid is replaced by an alanine residue that has a non-polar side-chain. Therefore, different from most Asp57b heterodimers, DQ8/DQ2 and H2-A^{g7} fail to form the salt-bridge with the arginine residue at the a-chain position 76 and thus leave a big open P9 pocket at the end of the peptide-binding groove. This unique feature disenables non-Asp57b alleles to bind a peptide with high affinity and is associated with impaired negative selection (120). Consequently, more thymocytes bearing self-reactive TCRs pass the checkpoint and enter the periphery. Once they re-encounter cognate peptides derived from tissue-specific

antigens, autoimmune responses will occur. The contrasting outcome of the non-Asp57b *vs*. Asp57b has been strongly supported by the observation of a reduced incidence of spontaneous diabetes in NOD mice transgenically expressing mutated H2-A^{g7} (Ser->Asp57) instead of wild type H2-A^{g7} (121). In addition, studies using HLA transgenic mice (devoid of murine endogenous MHC Class II but expressing co-stimulatory molecule B7.1 in the b-cells) also demonstrated that the expression of non-Asp57b HLA-DQ8 led to the progression of insulitis and spontaneous diabetes while the expression of Asp57b HLA-DQ6 inhibited the lymphocytes infiltration to islets and abolished the onset of diabetes (122).

2.2.4 T cell activation and peripheral tolerance

Mature SP thymocytes, so-called naïve T cells, leave the thymus and enter the periphery for immune surveillance. They circulate between peripheral blood and secondary lymph organs until they encounter antigens. Upon antigen engagement, they are activated and manifest their effects such as clonal expansion, cytokine secretion and/or cell-mediated cytotoxicity. The lymph node is the venue where T cell activation occurs. At least three checkpoints are required for T cell activation (123). The first checkpoint is the cell-cell contact, which is mostly provided by intergrins expressed by both T cells and antigen presenting cells (APCs). The second checkpoint is the engagement of peptide:MHC complex to the TCR. The co-receptor (CD4 or CD8) is also involved in the engagement and independently transduces signals that eventually merge with signals from TCR/CD3 complex. It is noteworthy that the T cell and the APC are brought close enough by adhesion molecules so that the TCR has a chance to find its ligand, however, the outcome is affinity dependent. Every mature T cell has one rearranged β-chain gene and at most two rearranged α-chain genes. Thus, most T cells have only one kind of TCR on their surface while some may have two kinds with different a-chains. The numerous T cells matured from the thymus thus represent a huge TCR repertoire. From within, only a very limited number of TCRs (or T cells bearing these TCRs) are able to interact with a specific peptide:MHC complex with an affinity that is high enough to reach a threshold and initiate signal transduction. Presumably, this process starts from a few TCR molecules and few peptide:MHC complexes. It induces events such as tyrosine phosphorylation, cytoplasmic Ca^{++} flux, which is required to redirect cytoskeleton organization toward the site of engagement to facilitate the recruitment of more

TCR/CD3 complexes and accessory molecules to the spot of initial contact. The last checkpoint is the maintenance of a stable contact synapse, which is the fundamental signaling unit to reach a full activation. It depends heavily on the number of TCR ligands on the surface of the APC to maintain the TCR/CD3 complex clustering on the surface of the T cell and constant signaling transduction. This is a positive feedback or self-strengthening system because increasing TCR engagements continuously bring more and more TCR/CD3 complexes to the site where T cell interact with the APC and stabilize the TCR:peptide:MHC synapse (surrounding accessory molecules are also included in the synapse structure). Hence, the T cell will have enough time to transduce the signal constantly to the nucleus to accomplish activation-associated gene transcription. It has been estimated that ~8,000 TCRs are required to be engaged to achieve a successful activation in the absence of co-stimulation (CD28-CD80 interaction)(124). Even with the co-stimulation, ~2,000 TCRs are still required.

The first checkpoint implies a pre-inflammatory condition in the LN so that increased cell-cell contact is feasible due the upregulation of adhesion molecules under that condition. The second checkpoint requires an initial antigen exposure and the availability of T cell recognition. The third checkpoint demands the abundance of both antigens and MHC molecules. Not fulfilling any of these checkpoints leads to non-signaling or partial signaling, and the naïve T cell stays in resting or anergic status. It actually provides the premise for peripheral tolerance, which is a complementary mechanism to thymic negative selection (so-called central tolerance) in preventing autoimmunity.

During negative selection, most thymocytes bearing self-reactive TCRs are deleted to avoid comprehensive autoimmune activities. This event depends on the presentation of self-peptides derived from peripheral self-proteins expressed in the thymus. Although a large scope of peripheral tissue proteins are expressed in MECs under the control of Aire (115), certain tissue-specific self-proteins may still not be expressed or only expressed at very low levels. It is possible to allow a certain number of thymocytes bearing potentially self-reactive TCRs to escape deletion and enter the periphery. In addition, as just mentioned, there are defects in the establishment of central tolerance with the expression of certain MHCs (such as HLA-DQ8, DQ2 in human and H2-A^{g7} in mouse) and many autoreactive T cells escape deletion. In fact, some

evidence indicated that autoreactive T cells existed even in the periphery of healthy individuals and non-autoimmune-prone experimental animals (125, 126). However, they have to be fully activated prior to breaking self-tolerance and causing tissue damage (127, 128). In a normal physiological condition (a non-inflammatory situation, no foreign pathogen infiltration), peripheral tissue cells (endothelia) and antigen presenting cells express a low level of adhesion molecules, MHC molecules, and co-stimulation molecules. Most autoreactive T cells, if not all, fail to be activated either because they can't access the targets without the help of adhesion molecules or because they are not able to form stable TCR:peptide:MHC synapses without the help of co-stimulation (129) and enough autoantigens. It should be noted that the inflammation caused by pathogen invasion possibly facilitates the breakage of peripheral tolerance in a bystander style. Normal anti-pathogen immune responses induce the secretion of inflammatory cytokines such as IFN-γ and TNF-α. Both of these upregulate the expression of adhesion molecules and antigen processing/presenting machineries in APCs. On the other hand, anti-pathogen responses inevitably cause tissue damage and increase the release of self-proteins that might be taken up by APCs and act as autoantigens for autoreactive T cells. Since it takes time for the immune system to clear the invasion of pathogens, the exposure of self-proteins persists to an extent that is sufficient to activate autoreactive T cells.

Another important peripheral tolerance realm is contributed by naturally occurring T regulatory cells (T_{reg}) (130, 131). Like other CD4 T cells, T_{reg} cells mature in the thymus. Unlike other CD4 T cells, they constitutively express CD25, the α-chain of the IL-2 receptor, which normally is not expressed in naïve CD4 T cells until they are activated (132). T_{reg} cells express diverse $\alpha\beta$TCR. The specificity of T_{reg} cells is mysterious. It has been suggested that they are likely to be reactive to self-peptides with a relatively high avidity (133). The importance of T_{reg} in maintaining self-tolerance has been demonstrated by the severe autoimmunity in *foxp3*-deficient mice and human individuals with a nonsense mutation in the *foxp3* gene (134-136). The *foxp3* gene encodes a transcription factor specifically expressed in the CD4$^+$CD25$^+$ T_{reg} population and it has been demonstrated to be the master gene directing the development and the function of T_{reg} cells (137, 138). The TCR engagement is required for the induction of *foxp3* expression and T_{reg} cell lineage commitment in the thymus. However, the details bridging the TCR signal and T_{reg} cell maturation are still missing. T_{reg} cells dominantly suppress other T cell

responses by mechanisms that have not been completely understood. Both inhibitory cytokine secretion (IL-10, TGF-β) and cell-cell contact (CTLA-4, mTGF-β) might be involved (132, 139-142). In addition, it has also been suggested that T$_{reg}$ cells not only inhibit IL-2 secretion by effector cells but also compete for IL-2 with other effector cells so that the expansion of those effector cells is diminished (143-145).

2.3   DQ8 and DR4

As mentioned in the previous section of *Genetics of T1D*, DQ8 has been identified as the major genetic determinant associated with T1D (4, 5). Results from crystal structure studies also provide fundamental evidence that DQ8 differs from other T1D resistant alleles (such as DQ6) at the structure of the binding groove (119). This structural feature confers DQ8 less capable of deleting autoreactive T cells during negative selection than other protective DQ alleles. The data from HLA-DQ8 *vs.* DQ6 transgenic mouse models confirms that DQ8 is responsible for the break of central tolerance to β-cell antigens (122).

However, it is not crystal clear how HLA-DR is also involved in disease progression, either independently from DQ8 or in conjunction with DQ8. The structure of HLA-DR4 (DRB1*0401) doesn't reveal the defect that could be responsible for inefficient negative selection. Previous genetic studies suggested that the high frequency of DR4 in Caucasian T1D population was due to the strong linkage disequilibrium between DR loci and DQ loci. However, other results from DQ8-matched case-control studies indicated that different DQ8-DRB1*04 haplotypes were associated with variable risk to develop T1D, depending on which DRB1*04 allele was carried by the haplotype (8, 146). It suggested that different DR4 subtypes provide variable degrees of protection to disease onset, in the order of DRB1*0405<0402<0401<0404<0403, 0406. Briefly, DQ8-DRB1*0403 and DQ8-DRB1*0406 provide strong resistance, whereas DQ8-DRB1*0405, 0402, 0401 confer susceptibility and DQ8-DRB1*0404 is a neutral haplotype. The role of the DR4 allele was further highlighted by a result using HLA-DQ8/DR4 transgenic mice (10). With transgenic expression of the co-stimulatory molecule B7.1 in β-cells, 75 % of HLA-DQ8 transgenic mice developed spontaneous

diabetes incidence, whereas only 25 % of HLA-DQ8DR4 (DR4 co-expression) transgenic mice became diabetic. This suggested that DR4 (0401) had a certain regulatory role to the disease susceptibility conferred by DQ8, though DQ8-DRB1*0401 was defined as a high risk haplotype. In another study, H2-E transgenic NOD mice were protected from disease in a dose-dependent manner (81). An interesting observation from this study was that H2-E expression didn't account for clonal deletion of autoreactive T cells since the continuous presence of H2-E expression in the periphery was required to keep the animal free from diabetes in bone marrow transferring experiments.

Therefore, the involvement of DR4 alleles in the progression of T1D is not as simple as a linkage mark to susceptible DQ8.

Structurally, DR4 and DQ8 are similar. The first domain of HLA-DR4 α/β-chains associate together to form the peptide binding site as well as any other DQ molecule does. Functionally, just like the DQ8 molecule, DR4 is also responsible for presenting peptides to CD4 T cells. As for biosynthesis, DQ and DR also share many similarities. They are restrictedly expressed in antigen presenting cells (APCs) such as B cells, macrophages and dendritic cells (human activated T cells also express MHC Class II). The cell-specific expression pattern is controlled at the transcription level by the transactivator CIITA that is constitutively expressed in APCs (147). The α/β-chain of DQ or DR are transcribed and translated independently. The assembly of DQ and DR heterodimers occurs in the lumen of the endoplasmic reticulum. For both DQ and DR, a newly assembled heterodimer must avoid clogging their peptide binding groove prematurely with peptides derived from endogenously synthesized proteins in the ER lumen. A special polypeptide – invariant chain (Ii) ensures this by associating with heterodimer's peptide binding groove by a fragment spanning amino acid residues from 89-104 along the Ii (148). This fragment, also called MHC Class II-associated invariant chain peptide or CLIP, blocks the peptide-binding groove from binding other peptides in the lumen of the ER. Three αβIi complexes then associate with each other to the C-terminal fragment of Ii to form a complex that actually consists of 9 polypeptides. The complex is subsequently translocated from the ER to the trans-Golgi network, then to a late endosomal compartment (**Figure 10**). Here, the invariant chain is cleaved by proteases, leaving CLIP alone still in the peptide-binding groove of the MHC protein. Another molecular chaperon -- HLA-DM (H2-M in mice) facilitates the

release of CLIP and the uploading of peptides derived from endocytosed exogenous soluble proteins to the Class II peptide binding site. The peptide:Class II MHC complex is then translocated from the endosomal compartment to the cell surface.
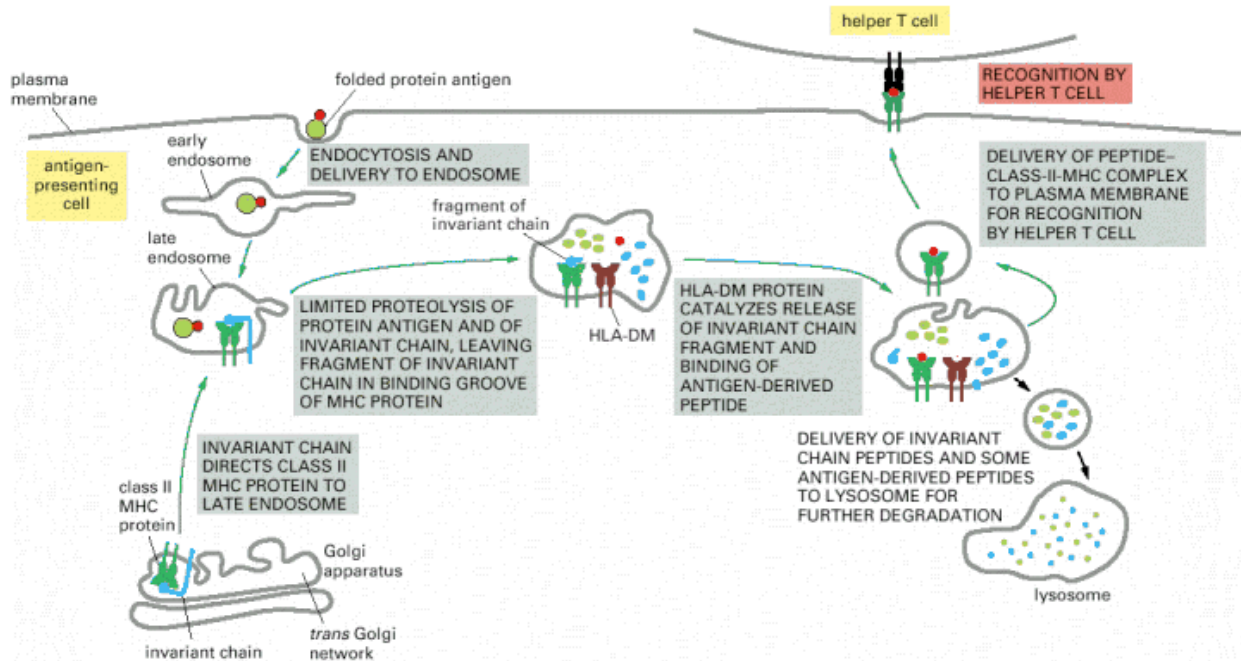
Figure 10. The biosynthesis of an MHC Class II molecule and the processing of an extracellular protein antigen for presentation to a helper T cell.

This cartoon illustrates a newly synthesized MHC Class II heterodimer that associates with an Ii and translocates from the lumen of the ER through trans-Golgi network to the late endosome, where Iis are degraded and replaced by antigenic peptide derived from extracellular proteins that are taken up by the cell through endocytosis. Matured peptide:MHC Class II complexes then translocate to the cell membrane and are ready to engage T cells (adapted from reference (1))

As DR4 shares similarities with DQ8 regarding their structure, function and biosynthesis, they are thus potentially capable of binding to the same peptide. This promiscuous binding activity was experimentally demonstrated by the evidence that peptides derived from a *Mycobacterium tuberculosis* antigen were found to be bound with multiple HLA alleles including HLA-DR4 (DRB1*0401) and HLA-DQ8 (DQA1*0301/DQB1*0302) (149). Additionally, peptide binding assays in cell-free conditions also indicated that several peptides derived from the T1D related autoantigen, GAD65, were capable of binding DQ8 and DR4 (150).

A unified peptide competition model has been proposed to address a possible mechanism for the DR4-directed (or H2-E-mediated in the H2-E transgenic NOD mouse model mentioned early) peripheral tolerance that may provide an explanation for the role of DR4 and variable degrees of protection conferred by distinct DR4 subtypes (11). It hypothesizes that the protection is due to the co-expression of DR4 alleles manifesting stronger peptide binding affinity than T1D susceptible DQ8 molecules. The premise of the competition is that HLA-DQ8 and HLA-DR4 are able to bind the same diabetogenic peptides (though it is not necessary to use identical anchoring residues from target peptides). As a consequence of the competition, the abundance of self-peptide:DQ8 complex on the surface of antigen presenting cells is lower than in the situation where there is no strong competitor. Thus, the corresponding T cell response is diminished since the number of TCRs engaged by peptide:DQ8 complex may be decreased proportionally (151). Alternatively, an increased antigenic peptide concentration is required as compensation. Hence, the risk to develop T1D is increased when a diabetogenic peptide (derived from islet antigens such as insulin or GAD65) prefers binding with DQ8 better than other DQ or DR molecules. In contrast, when DQ8 is co-expressed with a DR manifesting strong peptide binding affinity, the chance of the binding between DQ8 and peptide is reduced.

3.0   MATERIALS AND METHODS

3.1   Animals

B6.129-H2$^{dlAb1-Ea}$/J (The Jackson Laboratory, Bar Harbor, ME)

HLA-DQ8 and HLA-DR4 transgenic mice (courtesy of Dr. Li Wen, Yale University)

The animals were housed and bred under pathogen-free conditions in the Animal Facility of the Rangos Research Center at the Children's Hospital of Pittsburgh. The usage for generating HLA-DQ8 transgenic mice for antigen-specific CD4 T cell lines was approved by the Children's Hospital of Pittsburgh Animal Research and Care Committee (ARCC) protocol #16-03. The usage of HLA-DQ8/DR4 transgenic mice and MHC Class II deficient C57BL/6 mice was approved by the ARCC protocol #25-04.

3.2   Immunofluorescence staining for flow cytometry analysis or cell sorting

Materials

FACS Staining buffer

　　1 x PBS, pH7.4 (Gibco/Invitrogen, Carlsbad, CA)

　　0.1 % Na$_3$N (w/v) (Sigma, St. Louis, MO)

　　1 % BSA (w/v) (Sigma, St. Louis, MO)

FACS Fixation buffer

　　1 x PBS, pH7.4

　　1 % Paraformaldehyde (w/v) (Sigma, St. Louis, MO)

Fluorescence-conjugated mAbs and isotype controls

5-ml polystyrene tubes (Cardinal Health, McGraw Park, IL)

Glass Pasteur Pipette (Cardinal Health, McGraw Park, IL)

Sorvall RT7-plus, Centrifuge (Newtown, CT)

BD FACSCalibur Flow Cytometer (Becton Dickinson, Palo Alto, CA)

BD FACSVantage SE DIVA Cell Sorter (Becton Dickinson, Palo Alto, CA)

1) Typically, 5×10^5 cells are required for staining process for a regular flow cytometry analysis to inspect the expression of a surface marker.*

2) Centrifuge 1,000 rpm x 10 minutes at room temperature.

3) Resuspend the cell pellet in 50 ul of FACS staining buffer and add 10 ul antibody with proper dilution, vortex for 5 seconds.

4) Incubate the cell suspension on ice for 30 minutes, protect from light.

5) Add 2 ml FACS staining buffer to wash the cells.

6) Centrifuge at 1,000 rpm x 10 minutes at room temperature.

7) Repeat step 5) and 6) once.

8) Resuspend the cell pellet in 500 ul FACS fixation buffer. **

9) Analyze staining results with a flow cytometry.

For cell sorting to separate distinct cell subpopulations according to surface marker expression, the amount of reagents (such as buffer, and antibodies) needs to be adjusted proportionally.

**For cell sorting experiment, use the staining buffer instead of the fixation buffer to resuspend the cell pellet prior to applying the sample to the cell sorter.*

3.3   Transgenic mice HLA genotyping

Materials

Weanling mice (3-week old) required for genotyping

Heparinized microhematocrit tube (Fisher Scientific, Pittsburgh, PA)

0.9 % Saline, 1 mM EDTA (Sigma, St. Louis. MO)

Red blood cell lysis buffer (Sigma, St. Louis, MO)

FACS staining buffer and fixation buffer

FITC-conjugated anti-HLA-DQ mAb, Leu-10; PE-conjugated anti-HLA-DR mAb, L243; APC-conjugated rat anti-mouse CD45R/B220 mAb, RA3-6B2; purified anti-mouse CD16/CD32 antibody (mouse Fc blockade), 2.4G2; isotype control antibodies (BD/Pharmingen, San Diego, CA)

5-ml polystyrene tubes

Glass Pasteur pipettes

Centrifuge

BD FACS*Calibur* Flow Cytometer

1). Manually restrain the animal (as illustrated in **Figure 11)**. Introduce the end of the microhematocrit tube at the medial canthus of the orbit. Carefully advance the tip of the microhematocrit tube gently towards the rear of the socket until blood (~200 ul) flows into the tube. Discharge the blood into a 5-ml polystyrene tube containing 2 ml of 0.9 % saline-EDTA solution. Dab excess blood from the site with a clean tissue paper. Place the tube on ice while collecting blood from other animals.
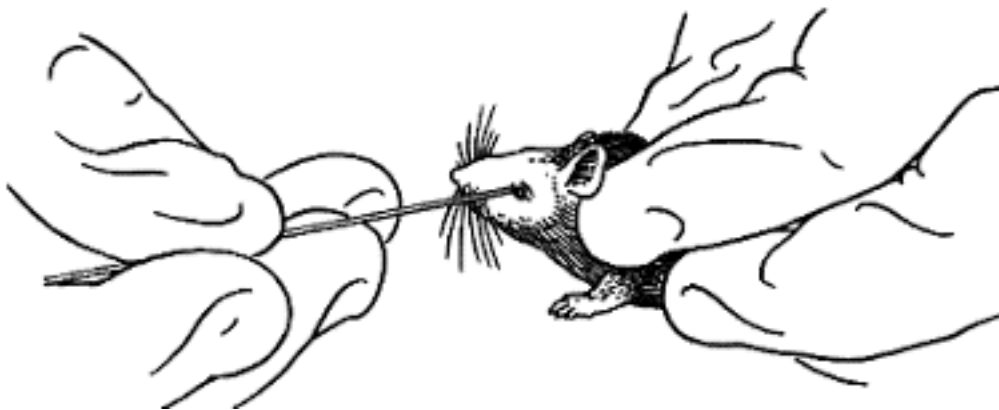
Figure 11. Collect peripheral blood from a weanling mouse (152).

2). Centrifuge the blood suspension, 1,000 rpm x 5 minutes at 4 °C. Aspirate the solution carefully without disturbing the cell pellet, resuspend the cell pellet in 1 ml of red blood cell lysis buffer and incubator the suspension for 5 minutes at room temperature.

3). Repeat step 2 once.

4). Centrifuge, 1,000 rpm x 5 minutes at 4 °C. Add 10 ul of purified anti-mouse CD16/CD32 antibody to block Fc receptors expressing on white blood cell surface. Incubate the suspension at room temperature for 15 minutes.

5). Stain the cell suspension with fluorescence-conjugated anti-HLA mAb(s), and anti-mouse CD45R/B220 mAb.

6). Flow cytometry analysis to examine mAb staining results.

3.4 Prepare single cell suspension from mouse lymph nodes, spleen, and thymus

Materials:

Mice with identified transgenic HLA genotype

Red blood cell lysis buffer

10 % FBS (v/v)-supplemented DMEM completed Medium, 0.22 um filter sterilization

DMEM medium, high glucose (Invitrogen, Carlsbad, CA)

10 % heat-inactivated fetal bovine serum (FBS) (Invitrogen, Carlsbad, CA)

2 mM L-glutamine (Invitrogen, Carlsbad, CA)

5 mM HEPES buffer (Invitrogen, Carlsbad, CA)

1 mM non-essential amino acid solution (Invitrogen, Carlsbad, CA)

1 mM Sodium Pyruvate (Invitrogen, Carlsbad, CA)

100 U/ml Penicillin, 100 ug/ml Streptomycin (Invitrogen, Carlsbad, CA)

*50 uM β-mercaptoethanol (*Sigma, St Louis, MO*)*

2 % NMS (v/v)-supplemented DMEM complete medium, 0.22 um filter sterilization

DMEM medium, high glucose

2 % Normal mouse serum (NMS) (Cedarlane, Westbury, NY)

2 mM L-Glutamine

5 mM HEPES buffer

1 mM non-essential amino acid solution

1 mM Sodium Pyruvate

100 U/ml Penicillin, 100 ug/ml Streptomycin

50 uM β-mercaptoethanol

70 % Ethanol

Trypan-blue (Sigma, St. Louis. MO)

Scissors and forceps (Cardinal Health, McGaw Park, IL), autoclave sterilization

Glass homogenizer (Cardinal Health, McGaw Park, IL), autoclave sterilization

Hemocytometer (Fisher Scientific, Pittsburgh, PA)

50-mL conical tubes (Cardinal Health, McGaw Park, IL)

Cell restrainer, 40 um (Cardinal Health, McGaw Park, IL)

250-ml and 500-ml Filter unit, 0.22 um (Cardinal Health, McGaw Park, IL)

Centrifuge

Inverted and upright microscopes

1). Mice were euthanized through CO_2 inhalation followed by cervical dislocation.
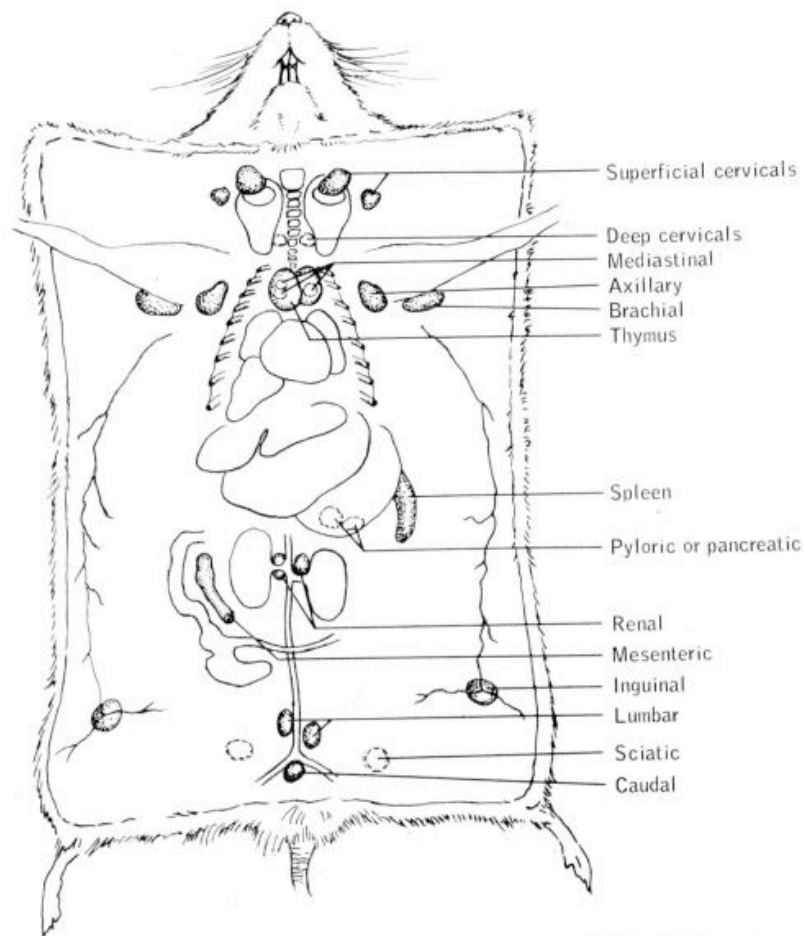
Figure 12. Illustration of mouse lymph organs.

2). In a bio-safety hood, lay the mouse on a clean blue pad. Rinse the abdomen with 70 % ethanol. Make a "V" shape incision on the abdomen with scissors, carefully remove the lymph nodes, spleen or thymus with a sterile set of forceps and scissors. The illustration of mouse lymph organs (except for bone marrow) is shown in **Figure 12**.

3). Keep the tissue(s) in ice-cold DMEM complete medium (For primary *in vitro* T cell culture, use 2 % NMS DMEM medium rather than 10 % FBS DMEM medium to avoid non-specific T cell responses. For other applications, such as preparing antigen presenting cells for restimulation, or preparing thymocytes as feeder cells for T hybridoma generation, use 10-20 % FBS DMEM medium)

4). Pour the tissue(s) and 5 ml medium into a glass homogenizer, grind the tissue(s) into a single cell suspension, then the single cell suspension is transferred from the homogenizer through a cell strainer to a 50-ml conical tube. Wash the homogenizer with 5 ml medium once, and transfer the washing medium to the 50 ml conical tube. Centrifuge, 1,000 rpm x 5 minutes,

5). Carefully aspirate the liquid by a glass pipette without disturbing the cell pellet. For the cell pellet prepared from the lymph nodes, resuspend the pellet in 5 ml medium, and count cells with hemocytometer under a upright microscope, (20x objective). Trypan-blue is used to exclude the dead cells. Adjust the density to 10×10^6 cells/ml

6). For a single cell suspension prepared from spleen or thymus, resuspend the pellet in 3 ml red blood cell lysis buffer per spleen/thymus. Incubate the cell suspension at room temperature for 5 minutes.

7). Add an equal volume of medium, mix well, and centrifuge for 1,000 rpm x 5 minutes at 4 °C. Resuspend the cell pellet in 10 ml medium per spleen or thymus. Count cells and adjust the density to 10×10^6 cells/ml

3.5 Generation of primary CD4 T cell responses to soluble peptide antigens by immunization

Materials

Mice with identified transgenic HLA genotype

Synthesized peptides (>95 % purity), **see Table 2** (Sigma-Genosys, Woodlands, TX)

Hank's Balanced Salt Solution (Invitrogen, Carlsbad, CA)

DMSO (Sigma, St. Louis, MO)

Complete Freund's Adjuvant (Difco, Detroit, MI)

Table 2. Peptides used to prime HLA-DQ8 and HLA-DQ8/DR4 transgenic mice.

	Amino acid sequence
hGAD65$_{101-115}$	CDGERPTLAFLQDVM
hGAD65$_{121-140}$	YVVKSFDRSTKVIDFHYPNE
hGAD65$_{206-220}$	TYEIAPVFVLLEYVT
hGAD65$_{536-550}$	RMMEYGTTMVSYQPL

Red blood cell lysis buffer

Trypan-blue

2 % NMS supplemented DMEM complete medium

Hamilton gastight syringes, 1 ml (Fisher, Pittsburgh, PA)

Double-hub Micro-Emulsifying needles, 18 G (Fisher, Pittsburgh, PA)

B-D hypodermic needles, 25 G (Fisher, Pittsburgh, PA)

Autoclaved scissors and forceps

Autoclaved glass homogenizer

250-ml filter unit, 0.22 um

50-ml and 15-ml conical tubes

Cell strainer, 40 um

Hemocytometer

Costar 24-well cell culture plate (Cardinal Health, McGaw Park, IL)

Centrifuge

Inverted and upright microscope

37 ℃, 10 % CO_2, Incubator

1). Dissolve the peptides hGAD65$_{101-115}$, hGAD65$_{121-140}$, hGAD65$_{536-550}$ in HBSS buffer to a final concentration of 2 mg/ml. Dissolve the peptide hGAD65$_{206-220}$ in DMSO to a final concentration of 10 mg/ml for storage, and dilute this peptide with HBSS buffer to final concentration of 2 mg/ml prior to immunizing.

2). Mix peptide solution with an equal volume of CFA (Normally, 100 ug of peptide is required for each mouse, and 4 mice will be assigned as a group to receive immunization with the same antigen). In order to improve emulsification, transfer the mixture into two gastight syringes connected by a double-hub micro-emulsifying needle and repeatedly force peptide/CFA mixture through the double-hub needle.

3). Inject mice subcutaneously at the base of the tail, 100 ul emulsion per mouse.

4). One week after immunization, sacrifice the mice and remove draining inguinal and periaortic lymph nodes and spleens.

5). Prepare lymph node/spleen single cell suspension in 2 % NMS supplemented DMEM complete medium.

6). Mix an equal number of lymph node cells and spleen cells, transfer cell suspension into 24-well cell culture plates at 2 ml/well, with 10 ug/ml of cognate peptide. Incubate the plates in a humidified 37 °C 10 % CO_2 incubator for 7 days.

3.6 *In vitro* antigen-specific CD4 T cell culturing

Materials
Cells from previous *in vitro* culture
Single cell suspension prepared from syngenic mouse spleen
Peptide stocking solution
Recombinant mouse interleukin-2 (rmIL-2) (Roche, Indianapolis, IN)
10 % FBS supplemented DMEM complete medium
T25 cell culture flask (Cardinal Health, McGaw Park, IL)
Hemocytometer
Centrifuge
Shepherd Mark I ^{137}Cs-sourced irradiator
Incubator
Inverted and upright microscopes

1). Prepare single cell suspension from syngenic mouse spleen

2). With the cell suspension incubating on ice, irradiate the splenocytes with 2, 500 *rads* using a ^{137}Cs-sourced irradiator.

3). Centrifuge 1,000 rpm x 5 minutes at 4 °C. Aspirate the liquid, resuspend the cell pellet in 10 % FBS DMEM complete medium. Count cells, adjust the density to 10 x 10^6 cells/ml.

4). Establish a 20-ml restimulation culture in a T25 flask containing 25 x 10^6 irradiated splenocytes, 1 x 10^6 cells harvested from previous culture, 5-10 ug/ml of cognate peptide, 2.5-5 unit/ml of recombinant mouse IL-2.

5). Place the T25 flask in an upright position in a humidified 37 °C 10 % CO_2 incubator.

6). Repeat the restimulation protocol every two weeks.

3.7   Characterizing *in vitro* T cell culture – examining CD4, CD8 and TCR V**β** expression

Materials

T cells from day-12~14 restimulation culture

FACS staining buffer and fixation buffer

FITC-conjugated anti-mouse TCR Vβ panel; PE-conjugated rat anti-mouse CD4 mAb, GK1.5; APC-conjugated rat anti-mouse CD8 mAb, 53.6.7; purified anti-mouse CD16/32 mAb, 2.4G2 and antibody isotype controls (BD/Pharmingen, San Diego, CA)

BD FACS*Calibur* Flow Cytometer

1). Harvest the cells by centrifuging

2). Wash the cell pellet once with FACS staining buffer

3). Resuspend the cell pellet in 50 ul of anti-CD16/32 mAb solution for 15 minutes at room temperature

4) Aliquot an equal volume of the cell suspension into different tubes, label the cell suspension with anti-CD4, -CD8 and TCR Vβ mAb panel.

5). Analyze staining results with flow cytometer to determine the expression of CD4, CD8 and TCR Vβ.

3.8   MACS and FACS for T cell fractionation (*optional protocol*)

Materials

T cells from day-12~14 restimulation culture

MACS anti-mouse CD8a (Ly-2) Microbeads (Miltenyi, Auburn, CA)

MACS staining buffer

1x PBS, pH7.2

0.5 % BSA

2 mM EDTA

FACS staining buffer and fixation buffer

FITC-conjugated anti-mouse TCR Vβ panel; PE-conjugated rat anti-mouse CD4 mAb, GK1.5; APC-conjugated rat anti-mouse CD8 mAb, 53.6.7; purified anti-mouse CD16/32 mAb, 2.4G2 and antibody isotype controls

Centrifuge

MACS LS and MS column (Miltenyi, Auburn, CA)

MACS separator (Miltenyi, Auburn, CA)

BD FACS*Calibur* Flow Cytometer

BD FACS*Vantage* DIVA Cell Sorter

The purpose of this optional protocol is to obtain a relatively pure CD4 T cell subset from an in vitro T cell culture that contains CD4$^+$ and CD8$^+$ T cells, or CD4$^+$ T cells expressing distinct TCR Vβs. Steps from 3) to 9) are used to pre-clear CD8+ T cell contamination (if it is applied). Cell sorting is eventually required to separate each individual subset to obtain a highly homogeneous cell population. It is not necessary if the T cell culture is composed of a homogeneous CD4 T cell population.

1). Harvest the cells from day-12~14 restimulation culture by centrifuging.

2) Wash the cell pellet with FACS staining buffer once and count cells.

3). Resuspend the cell pellet in MACS staining buffer at a volume of 40 ul buffer/1x10^7 cells, add the CD8a microbead suspension at a concentration of 10 ul microbeads/1x10^7 cells.

4). Incubating at 4-8 ºC for 15 minutes

5). Wash the cell suspension with MACS buffer (10-20 fold of labeling volume)

6). Centrifuge and resuspend the cell pellet with 0.5 ml MACS staining buffer

7). During the centrifugation, place a MACS LS or MS column in magnetic field of a MACS separator, and rinse the column (0.5 ml for MS column and 3 ml for LS column).

8). Apply the cell suspension onto the column, wait till entire cell suspension passes through the column by gravity, then wash the column with a 3-fold rinsing volume of MACS staining buffer.

9). Collect/combine total effluent, and centrifuge to remove the MACS buffer.

10). Resuspend the cell pellet with FACS buffer and label the cells with anti-CD4, -CD3, or TCR Vβ antibody panel.

11). Apply labeled cells onto a cell sorter to separate the subpopulations that differ from each other by their surface marker expression.

12). Confirm the result of sorting by analyzing a small volume of sorted subpopulations on a regular flow cytometer.

13). Once the purity is assured, use sorted cell populations for next round of restimulation culturing.

3.9 *In vitro* CD4 T cell assay using irradiated mouse splenocytes as antigen presenting cells

Materials
T cells from day-12~14 restimulation culture
Irradiated mouse splenocytes
Peptides
10 % FBS DMEM complete medium
^{3}H-TdR, 1mCi/ml stock solution, 6.7 Ci/mmol (Perkin Elmer, Wellesley, MA)

Ultima Gold Scintillation Fluid (Perkin Elmer, Wellesley, MA)

Costar round-bottom 96-well cell culture plate (Cardinal Health, McGaw Park, IL)

OmniFilter-96 microplate (Perkin Elmer, Wellesley, MA)

Glass fiber filters (Perkin Elmer, Wellesley, MA)

MiscoBeta FilterMate – 96-well cell harvester (Perkin Elmer, Wellesley, MA)

Microplate Scintillation Counter (Packard, Meriden, CT)

1). Prepare irradiated splenocyte suspension in 10 % FBS DMEM complete medium, and adjust the density to 10×10^6 cells/ml.

2). Harvest T cells from the restimulation culture, wash once with complete medium, adjust the density to 2×10^5 cells/ml.

3). Setup the peptide recall assay in a round-bottom 96-well plate. Each assay well contains 0.5×10^6 irradiated splenocytes, $20\text{-}50 \times 10^3$ T cells from the restimulation culture, and indicated amount of peptide. The assay is normally applied in triplication.

4). Setup control wells either containing responder T cells only, and responder T cells together with splenocytes.

5). To detect the cytokine production, harvest 150 ul of assay supernatant at 48 hours for IL-4 measurement, or 66 to 72 hours supernatant for IFN-γ measurement.

6). ELISA is performed to determine the cytokine production. (*See next section*)

7). To evaluate the cell proliferation, 66 to 72 hours co-culture is pulsed with 1 uCi ^{3}H-TdR (dilute 50-fold from 1 mCi/ml stock solution) for 6 hours followed by freezing down whole assay plate at -20 ºC.

8). On the next day, thaw the assay plate, harvest contents of each assay well to a glass fiber filter using a 96-well cell harvester.

9). Align the fiber filter onto an OmniFilter-96 microplate, add 25 ul of scintillation fluid to each assay well.

9). Mount the microplate onto a Microplate Scintillation Counter to measure the incorporation of the ^{3}H-TdR.

3.10   Enzyme-linked immunosorbent assay (ELISA)

Materials

T cell assay supernatant

Coating buffer: *50mM NaHCO₃, pH9.6*

Blocking buffer

1 x PBS, pH7.4

3 % BSA (w/v)

0.02 % Na₃N (w/v)

25x DELFIA Washing concentrate; DELFA assay buffer; DELFIA enhancement solution; DELFIA Europium-Streptavidin; DELFIA 96-well yellow microtiter plate (Perkin Elmer, Wellesley, MA)

ELISA capture antibodies: anti-mouse IFN-γ, R4-6A2; anti-mouse IL-4, BVD-1D11; anti-mouse IL-2, JES6-1A12 (BD/Pharmingen, San Diego, CA)

ELISA detection antibodies: anti-mouse IFN-γ, XMG1.2; anti-mouse IL-4, BVD-24G2, anti-mouse IL-2, JES6-5H4 (BD/Pharmingen, San Diego, CA)

ELISA recombinant cytokine standards: recombinant mouse IFN-γ, IL-4, IL-2 (BD/Pharmingen, San Diego, CA)

Microtiterplate Washer (Bio-Rad, Hercules, CA)

VICTOR² MicrotiterPlate Reader (Perkin Elmer, Wellesley, MA)

DeltaSoft 3 (Bio-Rad, Hercules, CA)

1). Coat a 96-well DELFIA yellow microtiterplate with capture antibody (cap) dilutent, 100 ul/well, 4 °C incubation over night.

   10 ul 0.5 mg/ml anti-IL-2(cap) stock into 10 ml coating buffer, final conc. 0.5 ug/ml

   30 ul 1.0 mg/ml anti-IFN-γ (cap) stock into 10 ml coating buffer, final conc. 3 ug/ml

   10 ul 0.5 mg/ml anti-IL4 (cap) stock per 10 ml coating buffer, final conc. 0.5 ug/ml

2). Discard the antibody solution, add 300 ul of blocking buffer to each well and incubate at 37 °C for 2 hours

3). Wash the plate with washing buffer 3 times.

4). Add 100 ul sample and recombinant protein standard into assigned wells, triplication or duplication is required, 4 °C incubation overnight.

Standard starting solution:

10 ul 2 ug/ml IL-2 into 2 ml blocking buffer, final conc. 10 ng/ml

25 ul 2 ug/ml IFN-γ into 2 ml blocking buffer, final conc. 25 ng/ml

2 ul 50 ug/ml IL-4 into 2 ml blocking buffer, final conc. 50 ng/ml

1: 2 series dilution is applied to dilute the standard.

5).Discard the liquid, wash the plate 4 times with washing buffer.

6). Dilute secondary antibody (det) with blocking buffer, pipette 100 ul/well, incubate the plate at room temperature for 1 hour.

10 ul 0.5 mg/ml anti-IL-2(det) into 10 ml blocking buffer, final conc. 0.5 ug/ml

10 ul 0.5 mg/ml anti-IFN-γ (det) into 10 ml blocking buffer, final conc. 0.5 ug/ml

10 ul 0.5 mg/ml anti-IL-4 (det) into 10 ml blocking buffer, final conc. 0.5 ug/ml

7). Wash the plate with washing buffer and add 100 ul of 1: 1000 diluted Eu-conjugated Streptavidin (use DELFIA assay buffer to dilute), incubate the plate at room temperature for one hour with slow shaking and protect from light.

8). Wash the plate and add 200 ul DELFIA enhancement solution to each well and shake the plate with a plate shaker for 5 minutes.

9). Measure the fluorescence on the VICTOR^2 MicrotiterPlate Reader under time-resolved fluorometer module.

10). Raw data is processed by DeltaSoft 3 for standard curve and cytokine concentration calculations.

3.11   T hybridoma generation

Material

T cells from day-5 restimulation culture

BW5147α$^-$β$^-$ T lymphoma (courtesy of Dr. Willi Born, University of Colorado Health Science Center)

Mouse thymocyte suspension

50 % PEG-1500 (v/v, in non-supplemented DMEM medium), pH neutral (Sigma, St. Louis, MO), autoclave sterilization

Non-supplemented DMEM medium

20 % FBS supplemented DMEM complete medium

50x HAT supplement (Invitrogen, Carlsbad, CA)

100x HT supplement (Invitrogen, Carlsbad, CA)

Trypan blue

Flat-bottom 96-well cell culture plate

12-well cell culture plate

Hemocytometer

Inverted and upright microscopes

Centrifuge

37 °C water bath

Incubator

1). Euthanize 4-week old syngenic mice, prepare a single cell suspension of thymocytes at a density of 10 x 10^6 cells/ml in 20 % FBS supplemented DMEM complete medium. Place the thymocyte suspension in a 37 °C water bath.

2).Harvest CD4 T cells from day-5 restimulation culture by centrifugation 1,000 rpm x 5 minutes at room temperature. Wash the cells twice with 37 °C pre-warmed DMEM medium (without serum supplements) to remove residual amount of serum and antibiotics.

3). Resuspend T cells in non-supplemented DMEM medium. Use trypan-blue to determine the viability. Normally, 95 % viability is required for a successive cell fusion reaction. Place the CD4 T cell suspension in the 37 °C water bath.

4). Harvest exponential growth phase BW5147$\alpha^-\beta^-$ lymphomas by centrifuge, wash the cells twice with DMEM, determine the viability with the aid of trypan blue. 95 % viability is required.

5). Mix the lymphomas and activated CD4 T cells at a ratio of 5:1 in a 50 ml conical polypropylene tube and add 20 ml of 37 °C pre-warmed DMEM.

6). Centrifuge the cell mixture, 2,000 rpm x 5 minutes at room temperature.

7). Aspirate the liquid from the mixed-cell pellet

8). Add 1 ml of 37 °C pre-warmed 50 % PEG solution in drop-wise manner to the mixed cell pellet, with gentle stirring of the pellet with the pipette tip following each drop.

9). Drop-wise, add 2 ml of pre-warmed DMEM to the PEG/cell mixture over a period of 2 minutes, gently stirring after each drop. Likewise, add an extra 7 ml of pre-warmed DMEM to the mixture over a period of 3 minutes.

10). Centrifuge 2,000 rpm x 5 minutes at room temperature.

11). Aspirate the liquid and use a 10-ml pipette to forcefully discharge 10 ml of thymocyte suspension onto the cell pellet.

12). Add the rest of the thymocytes until the desired volume is reached (10 ml for each plate).

13). Plate 100 ul cell suspension to each well of a flat-bottom 96-well plate (an estimating density of the T cells is around 100-500 cells/well). Place the plates in a humidified 37 °C 10 % CO_2 incubator.

14). After 1 day of incubation, add 100 ul of DMEM complete medium supplemented with 20 % FBS and 2x HAT supplement to each well of the culture plates. Return the plates to the incubator.

15). On day 3 after fusion, monitor the cells under an inverted microscope. At this point, most non-hybrid cells should be dead while hybrids have not yet had a chance to grow out.

16). On day 7 after fusion, aspirate 100 ul supernatant of each well and discard it. Feed the hybridomas by adding 100 ul of freshly prepared DMEM complete medium containing 20% FBS and 2 X HAT supplement.

17). On day 10 after fusion, check the plates daily for the need to expand. Expand the content of the wells that have become slightly yellow by transferring the cells to the wells of a 12-well cell culture plate. Add 3 ml of DMEM complete medium with 10 % FBS and 1x HT supplement to each well.

3.12 Screening for hybridomas with biological phenotype and function

Materials

T Hybridomas from the 24-well expansion plates

Syngenic mouse splenocytes suspension, 2,500 *rads* irradiated

Peptide

Round-bottom 96-well tissue culture plates

Fluorescence-conjugated anti-mouse CD3 mAb, anti-mouse CD4, anti-mouse TCR Vß panel

Reagents for surface staining

Reagents for IL-2 ELISA

BD FACS*Calibur* Flow Cytometer

Microtiter Plate Washer

Microtiter Plate Reader

Incubator

1). Around 2-3 days after expansion, collect 2 ml of the cell suspension from wells that appear to be expanding for primary screening for the TCR/CD3 complex and CD4 expression using PE-conjugated anti-CD3 mAb, APC conjugated anti-CD4 mAb, and FITC-conjugated anti-specific-TCR-Vβ mAb (if the usage of TCR Vβ by parental T cell line is known).

2). Only a portion of the hybridomas identified in the primary screening as $CD3^+CD4^+TCR^+$ will be qualified for the next round of screening.

3). Secondary screening consists of Ag-specific *in vitro* T cell assay using selected hybridomas as responder cells.

4). Candidate hybridomas were plated into round-bottom 96-well culture plates in duplicate at 50,000 cells/well, in the presence of 500,000 cells/well of irradiated syngenic splenocytes and 10 ug/ml of cognate peptide. Negative controls that contain only hybridomas and splenocytes but no peptide are also required for the assay.

5). Incubate the 96-well plates for 24 hours in a humidified 37 °C 5 % CO_2 incubator.

6). Harvest and combine 150 ul of supernatant from the wells with the same contents. Freeze the supernatant at -20 °C for >1 hour to kill any of the hybridoma cells that may have been transferred with the supernatant.

7). Thaw the supernatant, and perform ELISA to determine the IL-2 production.

8). Expand the hybridomas (that are capable to produce IL-2 upon cognate peptide restimulation) for freezing and re-cloning by limiting dilution.

3.13 *In vitro* T hybridoma assay using mitogenically inactivated human B-LCL as antigen presenting cells

Materials

Human B Lymphoblast Cell Line (B-LCL): WT51, FS, KT17, BM92

Exponential growth phase T Hybridoma

Peptides

Mitomycin C, 50 ug/ml, in non-supplemented DMEM

10 % FBS supplemented RPMI complete medium

   RPMI 1640 medium (Gibco/Invitrogen, Palo Alto, CA)

   10 % Heat inactivated fetal bovine serum (FBS) (v/v)

   2 mM L-Glutamine

   5 mM HEPES buffer

   1 mM non-essential amino acid solution

   1 mM Sodium Pyruvate

   100 U/ml Penicillin, 100 ug/ml Streptomycin

   50 uM β-mercaptoethanol

10 % FBS DMEM complete medium

Round-bottom 96-well plates

1). Human B-LCLs are normally maintained in RPMI 1640 complete medium supplemented with 10 % FBS and passaged once a week with 1:10-20 dilution.

2). Harvest human B-LCLs and inspect the viability with the aid of trypan-blue. Normally, 95 % viability is required. Dead cells can be removed by centrifugation over Ficoll-Hyaque.

3). Centrifuge 1,000 rpm x 5 minutes at room temperature.

4). Aspirate the liquid and resuspend the pellet in 50 ug/ml Mitomycin C. Place the cell suspension in a 37 ºC water bath for 20 minutes

5). Wash the B-LCLs twice with DMEM complete medium and resuspend the cells in 10 % FBS DMEM complete medium at the density of 0.8×10^6 cells/ml

6). Harvest T hybridomas. Likewise, 95 % viability is required.

7). Setup the assay in a round-bottom 96-well tissue culture plate. Each well contains 40 $\times 10^3$ Mitomycin C inactivated B cells as antigen presenting cells, 20×10^3 T hybridomas as effector cells, and a variable amount of cognate peptide or un-relevant control peptide.

8). Place the assay plate in a humidified 37 °C 5 % CO_2 incubate for 24 hours

10). Harvest the supernatant and perform ELISA to determine the IL-2 production.

3.14   cDNA synthesis

Materials
Cells harvested from the cell culture
TRIzol reagent (Invitrogen, Carlsbad, CA)
Chloroform (Fisher, Pittsburgh, PA)
Glycogen (Roche, Indianapolis, IN)
Isopropanol (Sigma, St. Louis, MO)
DEPC-treated water (RNase-free) (Ambion, Austin, TX)
75 % Ethanol (v/v, in DEPC treated water)
DNA-Free kit (Ambion, Austin, TX)
SuperScript II First Strand cDNA Synthesis kit (Invitrogen, Carlsbad, CA)
0.5-ml, 1.5-ml RNase-free microcentrifuge tubes (Ambion, Austin, TX)
Spectrophotometer (LKB)
Microcentrifuge (Kendro, Newtown, CT)

DNA Thermal Cycler (Perkin Elmer, Wellesley, MA)

1). Harvest the cell culture by centrifugation. For adherent cells, it requires to dissociate the cells from tissue culture flask or dish with trypsin or cell dissociation buffer. Wash the cell pellet once with 1x PBS

2). Centrifuge and remove the PBS. Resuspend the cell pellet in TRIzol reagent (1 ml TRIzol reagent is sufficient for $10x10^6$ eukaryotic cells) and transfer contents to a 1.5 ml RNase-free tube. Incubate the tube at room temperature for 2 minutes.

3). Add 0.2 ml chloroform and incubate at room temperature for 3 minutes

4). Centrifuge at 4 °C, 11,500 rpm x 15 minutes. Transfer aqueous phase to a new 1.5-ml RNase-free tube, add 1 ul of glycogen to facilitate precipitation, then add 0.5 ml isopropanol and incubate the sample on ice for 10 minutes.

5). Centrifuge at 4 °C, 11,500 rpm x 15 minutes

6). Descant the supernatant and use 75 % ethanol to wash the pellet once. Air-dry the pellet (<5 minutes at room temperature). Add 20 ul DEPC-treated water to dissolve the pellet.

7). (*Optional*) Use DNase treatment to remove the DNA contamination. Briefly, transfer 15 ul of the RNA sample from step 6) to a new 0.5 ml RNase-free tube containing 2 ul 10x DNA-free buffer and 1 ul of DNase (provided by DNA-free kit), add 2 ul of DEPC-treated water to make total volume up to 20 ul. Incubate the reaction tube at 37 ºC for 45 minutes. The reaction is then terminated by the addition of 2 ul DNase inactivation reagent provided by the same kit. Incubate the tube at room temperature for 2 minutes. Briefly centrifuge and transfer the aqueous fraction to a new 0.5 ml tube. The RNA sample is then ready for cDNA synthesis.

8). Determine the yield of total RNA by examining the $O.D_{260}$ absorbance using a spectrophotometer.

9). Normally, 1-5 ug of total RNA is required as the template for cDNA synthesis using the reagents provided by the Superscript II First Strand cDNA Synthesis Kit.

RNA sample	*5 ug*
10 mM dNTPs	*1 ul*
oligo dT	*1 ul*
DEPC-treated H₂O	*up to 10 ul*

10). Incubate the sample in the DNA Thermal Cycler at 65 ºC for 5 minutes. Then place the sample on ice for 2 minutes, then add reagents listed below:

10 x RT buffer	*2 ul*
25 mM MgCl2	*4 ul*
0.1 mM DTT	*2 ul*
RNase inhibitor	*1 ul*

11). Incubate the sample at 42 ºC for 2 minutes, then add 1 ul of reverse transcriptase. Incubate the sample at 42 ºC for 50 minutes.

12). Increase the temperature to 70 ºC for 15 minutes to inactivate the reverse transcriptase.

13). Transfer the sample onto ice for 5 minutes, then add 1 ul of RNase H. Incubate the sample at 37 ºC for 20 minutes.

14). cDNA synthesis is then accomplished. The sample is ready for PCR.

3.15 Human HLA-DQA1*0301, DQB1*0302, DRA1*0101, DRB1*0401, and Ii (p33) cDNA cloning

Materials

cDNA prepared from WT51 (human B-LCL)

BD Advantage cDNA PCR polymerase mix (BD/Clontech, Palo Alto, CA)

Oligo-nucleotides for PCR primers (**Table 3**) (IDT, Inc., Coralville, IA)

1Kb and 100 bp DNA ladder (Invitrogen, Carlsbad, CA)

Agarose (Roche, Indianapolis, IN)

50x TAE buffer

242 g	*Trizma*
100 ml	*0.5 M EDTA, pH8.0*
57.1 ml	*Acetic Acid (glacial)*
1000 ml	*in total volume with addition of water*

Qiagen PCR cloning kit (Qiagen, Valencia, CA)

Bacteria: DH5α competent cell (BD/Clontech, Palo Alto, CA)

IPTG (Stratagene, La Jolla, CA)

X-gal (Stratagene, La Jolla, CA)

Bacto Agar (BD, Palo Alto, CA)

LB broth (Invitrogen, Carlsbad, CA)

Ampicillin (Roche, Indianapolis, IN)

QIAquick PCR purification kit (Qiagen, Valencia, CA)

QIAprep MiniPrep plasmid DNA purification kit (Qiagen, Valencia, CA)

Electrophoresis apparatus: power suppler/combs/trays/tank, etc. (Bio-Rad, Hercules, CA)

GeneAmp PCR system 9600 (Perkin Elmer, Wellesley, MA)

Spectrophotometer

DNA Thermal Cycler

3130 Genetic Analyzer (ABI, Fost City, CA)

Sequencher v4.5 Software (Gene Codes Corporation, Ann Arbor, MI)

1). WT51 (human B cell line) cDNA is prepared by SuperScript II First Strand cDNA Synthesis Kit.

2) 50 ul PCR reaction is performed. A similar reaction without cDNA template is also setup as a negative control.

0.5 ul	*WT51 cDNA template*
5 ul	*10 x Advantage cDNA polymerase buffer (BD/Clontech, Palo Alto, CA)*
1 ul	*dNTPs mixture, 10 mM for each (Roche, Indianapolis, IN)*
1 ul	*Advantage cDNA polymerase (BD/Clontech, Palo Alto, CA)*
0.5 ul	*Forward strand primer (20 uM)(Table I)*
0.5 ul	*Reverse strand primer (20 uM) (Table I)*
41.5 ul	*ddH$_2$O*
50 ul	

3). PCR program setup

1 cycle of 95 ºC incubation for 2 minutes

    *30 cycles of 15 seconds incubation at 95 ºC, followed by 15 seconds incubation at annealing temperature (**Table 3**), and 60 seconds incubation at 68 ºC.*

1 cycle of 10 minutes incubation at 72 ºC

Table 3. PCR primers for cDNA cloning

Gene	Forward primer	Reverse primer	Annealing temp (ºC)	PCR product
DQA1*0301	ACT GCT GAG GCT GCC TTG	CCG CTG CTG TAG ATG GTG	61	821bps
DQB1*0302	CCA AGC TGT GTT GAC TAC C	GGC GTT ACA GAA AAG TGA	54	861bps
DRA1*0101	AAC AGA GCG CCC AAG AAG A	CCA TCA CCT CCA TGT GCC T	64	786bps
DRB1*0401	CTG GTC CTG TCC TGT TCT C	GGT CAT CTT CAC TTC AGC TC	57	818bps
Ii (p33)	CTC TTC CTT GGG GAG TGA TG	GAT GTT GAA GAC CGC CTC TG	61	723bps

4). Apply electrophoresis to inspect and separate PCR products.

5). Excise a single band PCR product from the agarose gel and extract the double-strand DNA from the gel by using QIAquick PCR purification kit.

6). Measure the DNA concentration of purified PCR product.

7). The ligation reaction is performed using a QIAgen PCR cloning kit. Briefly, 10 ul of ligation reaction composed by 5 ul of 2 x Master ligation mixture provided by the kit, and the mixture of PCR product and pDriver vector. Adjust the ratio of the molecule of PCR product to vector as 5:1.

8). Perform the ligation reaction at 16 º for 30 minutes.

9). Transform DH5α competent cells with ligation product and spread the bacterial suspension evenly on an LB agar plate contain 60 ug/ml Ampicillin and IPTG/X-gal.

10). On the next day, pick 10 white colonies from each plate and inoculate into 3 ml ampicillin-supplemented LB medium. Grow the bacterial overnight.

11). Harvest 1.5 ml bacteria culture and purify the plasmid DNA using QIAamp MiniPrep plasmid DNA purification kit.

12). Apply DNA sequencing and analyze the results with the aid of Sequencher v4.5 software to identify correct clones.

3.16 Cloning strategies to generate bicistronic constructs for HLA-DQ8 and HLA-DR4 cDNA expression in COS7 cell line

Material

pDriver-DQA1*0301, pDriver-DQB1*0302, pDriver-DRA1*0101, pDriver-DRB1*0401

pDriver-eIF4-IRES (courtesy of Dr. William Rudert, University of Pittsburgh)

pcDNA3.1/Zeo (+), pcDNA3.1 (Invitrogen, Carlsbad, CA)

Restriction enzymes and reaction buffers: BamH I, EcoR I, EcoR V, Kpn I, Hind III, Pst I, Sal I, Xho I (Roche, Indianapolis, IN)

Other enzymes: Klenow fragment (Roche, Indianapolis, IN), DNA ligase (Qiagen, Valencia, CA)

dNTP mixtures, 10 mM for each (Roche, Indianapolis, IN)

DH5α competent cells

Low salt LB broth

10 g	*Bacto-tryptone (Difco, Detroit, MI)*
5 g	*Bacto-yeast extract (Difco, Detroit, MI)*
5 g	*NaCl (Sigma, St. Louis, MO)*

Adjust volume to 1000 ml with deionized distilled H$_2$O, autoclave sterilization

Zeocin (Invitrogen, Carlsbad, CA)

1). For constructing DQ8 expression vector (**Figure 13**), DQB1*0302 cDNA (encoding HLA-DQ8 β-chain) and IRES were cloned into pcDNA3.1/Zeo(+) vector between Kpn I and Pst I sites through a three-fragment ligation reaction. DQA1*0301 cDNA (encoding HLA-DQ8 α-chain) was then cloned into intermediated vector between the EcoR V (located at immediate downstream of IRES) and Xho I sites. The "sticky" ends generated by Xho I and Sal I (underlined) digestion are mutually complement and can anneal to each other. The "blunting" in the bracket indicates a klenow fragment-mediated blunting reaction is applied after primary digestion reaction.
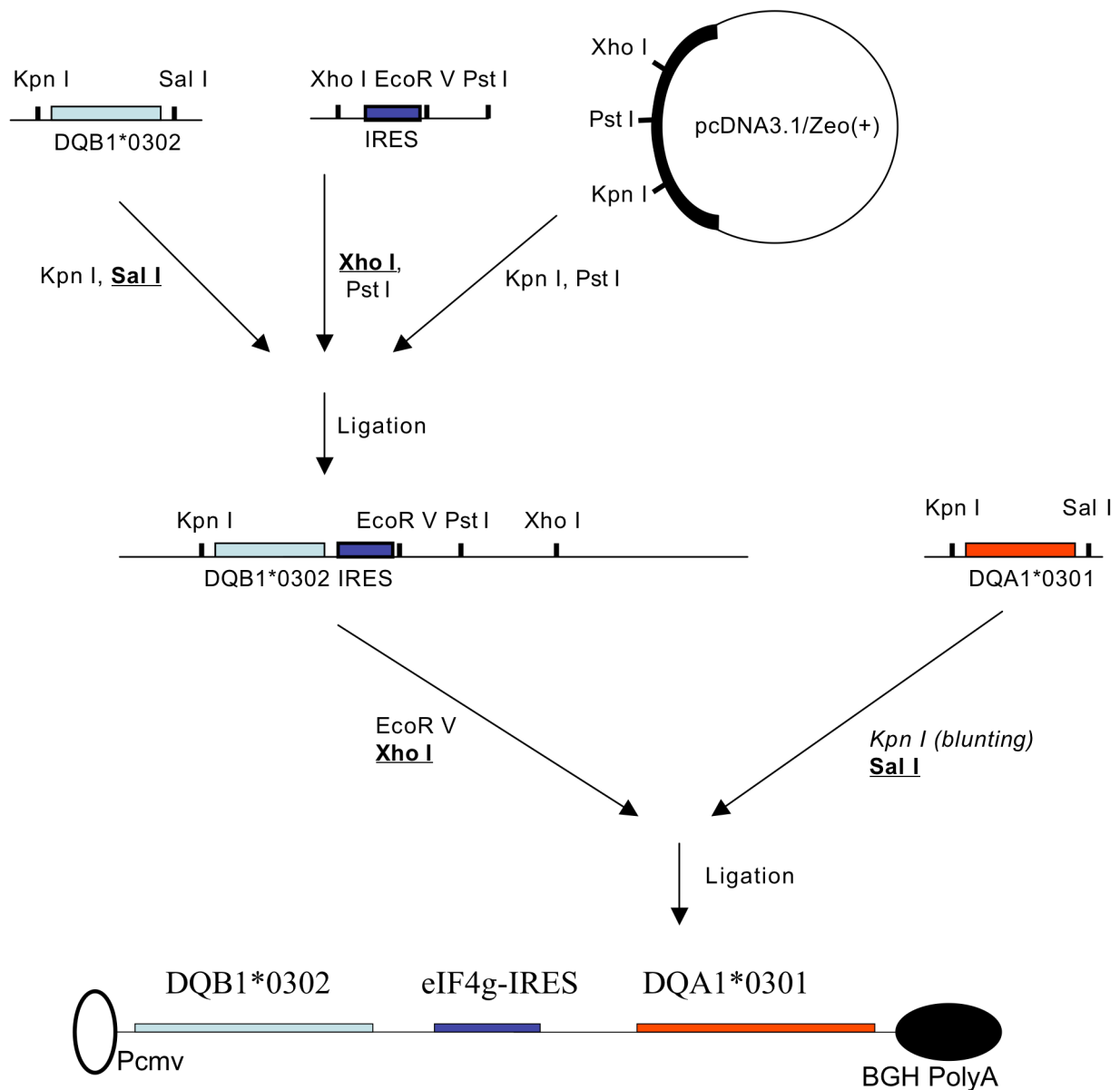
Figure 13. A bicistronic construct for HLA-DQ8 cDNA expression

2). For constructing the HLA-DR4 expression vector (**Figure 14**), DRA1*0101 cDNA (encoding HLA-DR4 α-chain) was cloned into the pDriver-eIF4-IRES vector between EcoR V and Kpn I sites. DRB1*0401 cDNA (encoding HLA-DR4 β-chain) and the IRES-DRA1*0101 fragment were subsequently cloned into pcDNA3.1 (+) expression vector between Nhe I and Kpn I sites through a three-fragment ligation reaction. The "blunting" in the bracket indicates a klenow fragment-mediated blunting reaction is applied after primary digestion reaction.
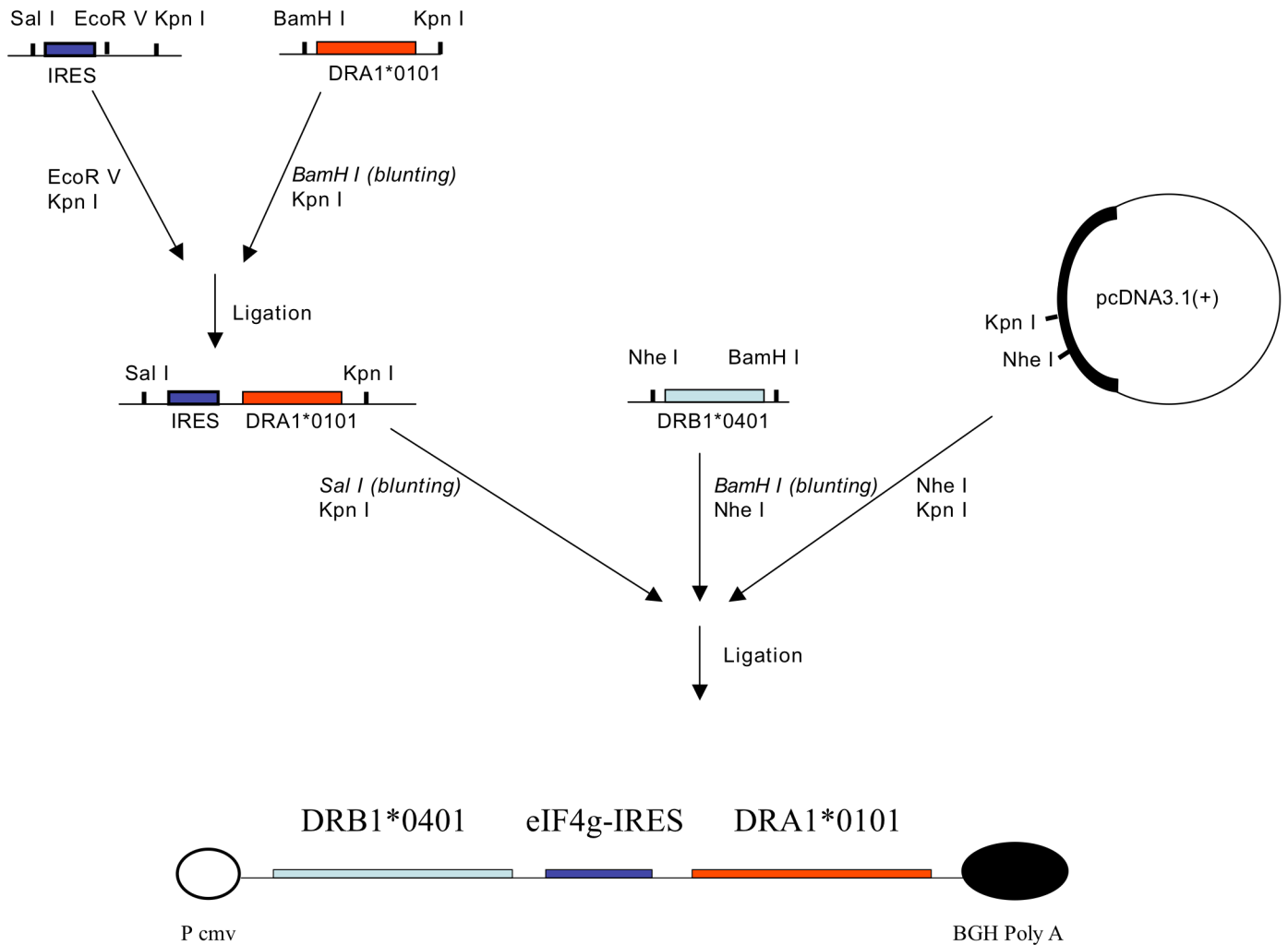
Figure 14. A bicistronic construct for HLA-DR4 cDNA expression

3). The DQ8 expression vector was transformed into DH5α competent cells and selected on the low salt LB agar plate containing 25 ug/ml Zeocin. The DR4 expression vector was transformed into DH5α competent cells and selected on regular LB agar plate containing 60 ug/ml Ampicillin.

4). Plasmids purified from selected clones were examined by performing PCR and DNA sequencing to ensure the sequence of essential elements.

3.17   Introduce HLA-DQ8 cDNA into COS7 cells by stable transfection

Materials

COS7 cell line (ATCC, Manassas, VA)

pDQ8-Zeo (the bicistronic construct for HLA-DQ8 cDNA expression)

Restriction enzyme and reaction buffer: Pvu I (New England BioLabs, Ipswich, MA)

Agarose

QIAquick PCR purification kit

1x PBS, pH7.4

Superfect transfection reagent (Qiagen, Valencia, CA)

DMEM medium, without supplement

10 % FBS supplemented DMEM complete medium

6-well tissue culture dish (Cardinal Health, McGaw Park, IL)

Electrophoresis apparatus

1). One day before the transfection, seed the COS7 cells at 20% confluence in a 6-well cell culture dish to ensure a 40-60% confluence will be reached on the day of transfection.

2). On the same day, apply Pvu I restriction enzyme digestion to linealize the pDQ8-Zeo expression vector.

pDQ8-Zeo	*20 ug*
Buffer H, 10 x	*20 ul*
Pvu I	*10 ul*
ddH$_2$O	*up to 200 ul in total volume, 37 ºC incubation for 2 hours*

3). Apply 1% agarose gel electrophoresis and extract the 7.5 Kb band from agarose gel with the aid of QIAquick PCR purification kit.

4). On the day of transfection, mix 2 ug of linealized pDQ8-Zeo DNA with 100 ul of DMEM medium. Add 10 ul of Superfect transfection reagent into the DNA mixture, gently pipetting the mixture two times. Incubate the tube at room temperature for 10 minutes and avoid of further disturbing.

61

5). During the incubation (the process in which DNA binds transfection reagent particles), aspirate the culture medium from the COS7 cells and wash the COS7 cells with 1 x PBS twice without dislodging the monolayer.

6). Add 400 ul 10% FBS supplemented DMEM complete medium to the DNA/Superfect mixture, gently pipetting twice to mix the content evenly, then drop-wise transfer the transfection mixture onto the COS7 monolayer. Place the cells at the 37 ºC 5% CO_2 incubator for 5 hours.

7). Remove the transfection mixture from the COS7 cells and wash the monolayer twice with 1x PBS. Add 3 ml 10 % FBS supplemented DMEM complete medium and place the cells in the 37 ºC incubator for 24 hours prior to selecting stable transfected clones.

3.18   Select and identify pDQ8-Zeo stable-transfected COS7 cells

Materials
Transfected COS7 cells
TH536.1 T Hybridoma
hGAD65$_{536-550}$ peptide
Zeocin
Trypsin-EDTA (Invitrogen, Carlsbad, CA)
10 % FBS-supplemented DMEM complete medium
TRIzol reagent
Reagents for RT-PCR
FACS staining buffer and fixation buffer
FITC-conjugated anti-HLA-DQ mAb and isotype control
IL-2 ELISA reagents
Cloning disc, 3 mm (ID) (Fisher, Pittsburgh, PA)
Autoclaved fine-tip forceps
10 cm cell culture dish (Cardinal Health, McGaw Paw Park, IL)
Flat-bottom 96-well cell culture dish (Cardinal Health, McGaw Paw Park, IL)
12-well cell culture dish
T25 cell culture flask

Inverted microscope

1). After 24 hours of transfection, dissociate the monolayer with trypsin-EDTA. Centrifuge to remove the culture medium. Resupend the cell pellet in 11 ml of DMEM complete medium.

2). Apply a series of 10-fold dilutions starting from 10^0 to 10^{-1}, 10^{-2}, 10^{-3} and 10^{-4} in individual 10 cm cell culture dishes containing 10 ml DMEM complete medium, supplemented with 400 ug/ml of Zeocin. Place the dishes in the 37 ºC 5 % CO_2 incubator.

3). Monitor the monolayer everyday and replace the selection medium every 4 days. After one week, in highly diluted dishes, some new-formed colonies will be observed.

4). Mark the position of the colonies at the bottom of the dishes with the aid of an inverted microscope. Transfer the marked colonies to the wells of a flat-bottom 96-well plate with a trypsinized cloning disc.

8). On the next day, remove the cloning disc from each individual well. Maintain the cell clones in 96-well plates under Zeocin selection and monitor the growth of the colonies every two days after one week. Dissociate the cells from the wells reaching 60 % confluence and transfer the cells to a 12-well cell culture dish for expansion. Further expansion to a T25 flask is required when the cells growing in the 12-well dishes reach full confluence.

9). Identify the selected colonies for the expression of transfected cDNA by RT-PCR the assembly of DQ8 α-/β-chain by FACS surface staining, and the function of DQ8 by T hybridoma assay (Functional DQ8 should be able to present peptide and induce antigen-specific T cell responses).

3.19 Cloning strategies for generating a CLIP-substituted recombinant invariant chain that carries hGAD65$_{539-547}$ coding sequence

Materials
pDriver-hIi
Restriction enzyme and reaction buffer: Hind III, EcoN I, PinA I, Nde I, Kpn I, Not I (New England Biolabs, Ipswich, MA) (Roche, Indianapolis, IN)
Other enzymes: DNA ligase (Qiagen, Valencia, CA)

Oligo-nucleotides: (IDT, Inc., Coralville, IA)

5ARM-adaptor (+): 5'-AGC TTC CCA AAG CCT CCC AAA CCG GTG-3'

5ARM-adaptor (-): 5'- AAT TCA CCG GTT TGGGAG GCT TCC CA-3'

3ARM-adaptor (+): 5' AAT TCT GCC CCA TAT GGG AGC CCT GC-3'

3ARM-adaptor (-): 5'-GGC AGG GCT CCC ATA TGG GGC AG-3'

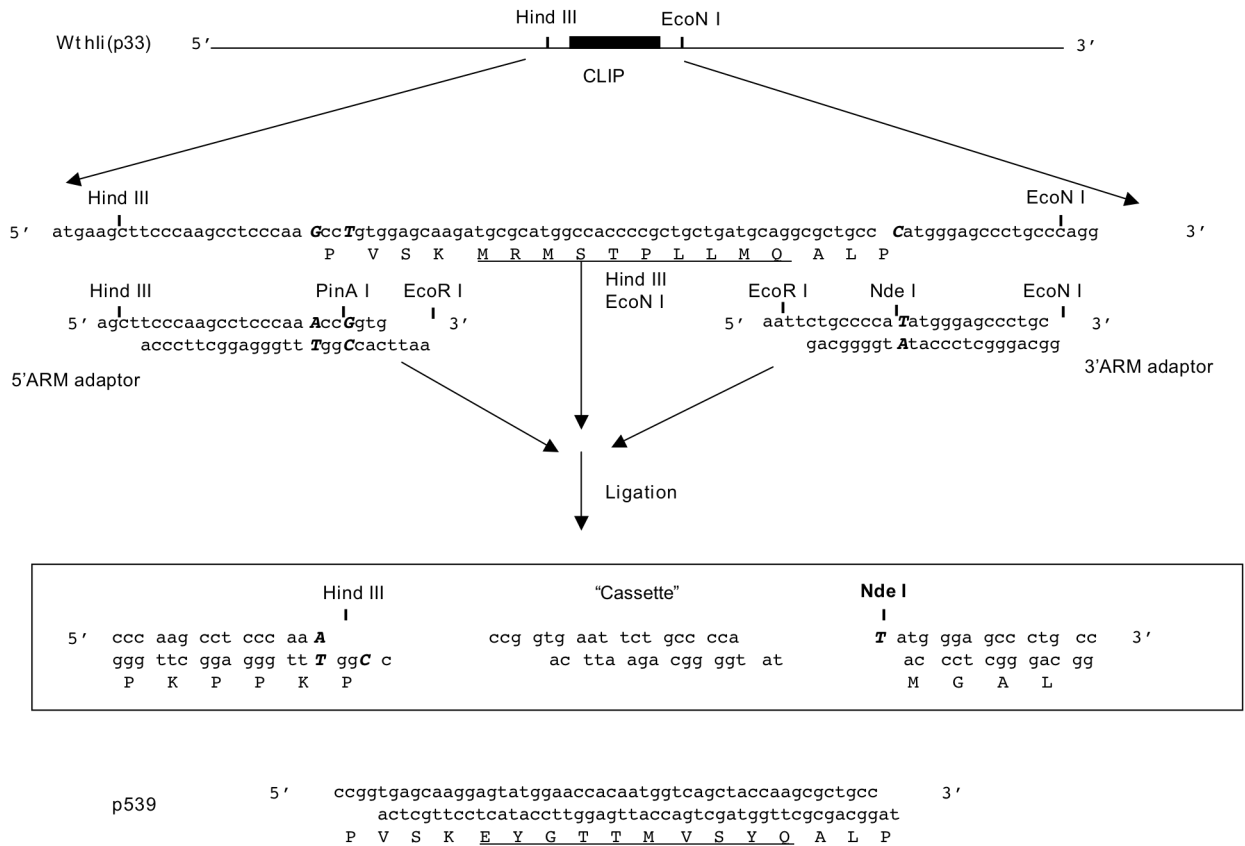DH5α competent cells

pcDNA3.1 (+)

Figure 15. The generation of CLIP-substituted recombinant invariant chain (rIi) "cassette"

1). Original CLIP coding sequence was removed from Ii (p33) between Hind III and EcoN I sites (**Figure 15**), and replaced by a "cassette" created from two double-strand oligo-nucleotides (5'ARM adaptor and 3'ARM adaptor) that partially overlapped with Ii cDNA

64

through a three-fragment ligation reaction. The 5'ARM adaptor and 3'ARM adaptor introduced a G→A mutation, a T→A mutation and a C→T mutation so that a PinA I and an Nde I site were generated in the place where the original CLIP was but not affecting the Ii coding sequences flanking the CLIP region. In order to generate a CLIP –substituted rIi, the PinA I-Nde I fragment – a DNA "cassette" was then replaced by a double-stranded oligo-nucleotide a carrying peptide coding sequence such as p539 (hGAD65$_{539-547}$) and "sticky" ends complemented to the single strand DNA extruded-ends generated by PinA I and Nde I.

2). The CLIP-substituted hrIi-539 that encodes the hGAD65$_{539-547}$ sequence was cloned into the pcDNA3.1 (+) expression vector between Kpn I and Not I sites. DNA sequencing was applied to confirm the sequence of the recombinant invariant chain.

3.20 Transient transfect CLIP-substituted hrIi-539 into DQ8^{+} COS7 cells and T hybridoma responses

Materials

DQ8^{+} COS7 cell (DQ8#114)

TH536.1

hrIi-539 (CLIP was replaced by hGAD65$_{539-547}$ coding sequence)

Superfect transfection reagents

DMEM medium (without supplements)

10 % FBS supplemented DMEM complete medium

Trypsin-EDTA

1x PBS

Trypan-blue

6-well cell culture dish

Flat-bottom 96-well cell culture plate

Inverted and upright microscope

1). One day before the transfection, seed the DQ8^{+} COS7 into a 6-well cell culture dish at 40 % confluence to ensure 60-80 % of confluence on the day of transfection

2). Apply transfection with 2 ug of circular hrIi-539 plasmid DNA together with 10 ul of Superfect transfection reagent.

3). Dissociate the transfected monolayer 24 hours later and re-seed the cell to a flat-bottom 96-well plate at the density of 5,000 cells/well in triplicate

4). Place the plate in a 37 ºC incubator overnight, then add TH536.1 hybridomas.

5). Harvest the supernatant 24 hours later for ELISA to determine the IL-2 production.

3.21   Statistics

The results were analyzed using Prism 4 software (GraphPad Software, Inc., san Diego, CA). The difference of T cell responses elicited by DQ8 vs. DQ8/DR4 transgenic splenocytes were assessed by one-tailed unpaired *t* test. The results of T hybridoma responses against a panel of B-LCLs were analyzed by one-way ANOVA. A *p*-value < 0.05 was considered statistically significant.

4.0   RESULTS/FINDINGS

4.1   Generation of antigen-specific CD4 T cell lines and hybridomas

4.1.1   Breeding and genotyping mice with human HLA-DQ8 and/or -DR4 transgenes

An important step of this study was to obtain an antigen presenting system that segregated DQ8 from DR4. This was impossible to achieve by using human samples since human APCs expressed DQ and DR simultaneously. Thus, two previously (and also independently) generated HLA transgenic mouse strains were used instead (10, 153). As the DQ8 and DR4 transgene were not located on the same chromosomes, they would be transmitted independently to the offspring generation during the interbreeding process. Therefore, by crossing DQ8 transgenic mice with DR4 transgenic mice, we expected to obtain mice expressing:

1) DQ8 and DR4 together
2) DQ8 alone
3) DR4 alone
4) Neither DQ8 nor DR4

Mice were genotyped for HLA expression at 3-4 weeks of age, by determining the HLA expression on the surface of B cells. Briefly, peripheral blood was collected and stained by fluorescence-conjugated monoclonal antibodies specific for the HLA-DQ, HLA-DR and B cell surface marker CD45R (B220). Staining results of $DQ8^+DR4^+$ (**Figure 16C**), $DQ8^+DR4^-$ (**Figure 16D**), $DQ8^-DR4^+$ (**Figure 16E**), and $DQ8^-DR4^-$ mouse (**Figure 16F**) were revealed by flow cytometry analysis, respectively. The fluorescence intensity was utilized to quantitate the relative expression level of DQ8 or DR4, which was required for subsequent experiments in this study.

4.1.2 Generation and characterization of antigen-specific primary CD4 T cell lines

Four candidate peptides -- $GAD65_{101-115}$, $hGAD65_{121-140}$, $hGAD_{206-220}$, and $hGAD65_{536-550}$ were chose to generate CD4 T cell lines, which expressed TCRs only recognizing cognate peptides in the context of DQ8 binding site. These peptides were derived from human GAD65 — a putative autoantigen of human T1D. They were previously demonstrated to be able to bind HLA-DQ8 molecules (154). Four groups of HLA-DQ8 transgenic mice were immunized by an individual peptide. After a week, an *in vitro* primary T cell culture was established followed by biweekly cognate peptide restimulation (**Figure 17A**)(155). Within the first few days after restimulation, antigen-specific T cells were activated and manifested an enlarged morphology (**Figure 17B**) that could be easily monitored by microscopic observation. In contrast, the size of non-activated T cells was relatively small and undistinguishable from other splenocytes (**Figure 17C**). Repeated restimulation was actually a selection process. Since only those antigen-specific T cells received activation signals through their TCRs that engaged the peptide:DQ8 complex on the surface of APCs, they survived and expanded in culture. In contrast, non-specific T cells were eliminated for the lack of the activation signal and negligible after six rounds of restimulation. In this way, four primary DQ8-restricted CD4 T cell lines were obtained, named DQ8p101, DQ8p121, DQ8p206, and DQ8p536, respectively. Results from *in vitro* proliferation assays showed that DQ8p101 (**Figure 18A**), DQ8p121 (**Figure 18B**), DQ8p206 (**Figure 18C**), and DQ8p536 (**Figure 18D**) specifically responded to their cognate peptides.

4.1.3 T206, T536.1 and T536.2 – CD4 T cell lines with clonal phenotypes

Although all four DQ8-restricted T cell lines specifically responded to their cognate peptides, the background of DQ8p101 and DQ8p121 responses were relatively higher than that of DQ8p206 and DQ8p536 (**Figure 18A, B, C** and **D**). It implied poor quality of the cell line, probably due to a small fraction of non-specific T cell contamination that was kept alive by the IL-2 secreted from specific T cells. The DQ8p206 and DQ8p536 lines, manifesting low background responses upon antigen restimulation, were further characterized for the TCR β-chain expression. This was accomplished by flow cytometric analysis with a panel of fluorescence-conjugated anti-TCR Vβ monoclonal antibodies including Vβ2, 3, 4, 5.1/5.2, 6, 7, 8.1/8.2, 8.3, 9, 10, 11, 12, 13 14 and 17.

Staining results showed that the DQ8p206 cell expressed a single TCR Vβ6 (**Figure 19A**). It was likely that the DQ8p206 line was derived from a single naïve CD4 T cell precursor (Each T cell only expresses one functional TCR β-chain). To further confirm this observation, the cDNA was prepared and RT-PCR (with Vβ6-specific primer paired with a common Cβ primer) was used to clone the DQ8p206 TCR β-chain VDJC joint fragment into a cloning vector for sequencing analysis. Sequence results showed all colonies were identical (**Figure 19B**). Therefore, DQ8p206 represented a clonal phenotype and was renamed as T206. Cytokines produced by T206 upon antigen recall were also evaluated by IFN-γ and IL-4 ELISA. Results indicated T206 predominantly secreted IFN-γ, but no IL-4 (**Figure 19C**). It suggested that T206 was a Th1-like CD4 T cell line.

Staining result of DQ8p536 cell line showed that 50 % of CD4 T cells were Vβ11$^+$ (**Figure 20A**), whereas the remaining population could not be unambiguously verified by 14 other different Vβ antibodies. It suggested that this cell line was composed of T cells derived from different precursors and Vβ11$^-$ subset could express some rare β-chains that were not covered by the commercially available Vβ antibody panel. Hence, the Vβ11$^-$ subset was separated from the Vβ11$^+$ subset by cell sorting. RT-PCR was then applied with a panel of Vβ-specific primers (**Table 4**) covering 24 different Vβ segments to identify the TCR β-chain of the Vβ11$^-$ DQ8p536 subset (156). Confirmed by sequencing analysis, this subset dominantly expressed Vβ1 (**Figure 20B**). The Vβ11$^-$ subset was then named T536.1. ELISA results indicated that T536.1 secreted both the Th1 cytokine IFN-γ and the Th2 cytokine IL-4 (**Figure 20C**).

The Vβ11$^+$ DQ8p536 subset (**Figure 21A**) was also confirmed for the clonal phenotype by sequencing the TCR β-chain (**Figure 21B**), and was named T536.2. T536.2 secreted a Th2 profile cytokine – IL-4, but not IFN-γ (**Figure 21C**).

Table 4. Oligo-nucleotides used as RT-PCR primers to screen TCR Vβ usage (156)

Mouse TCR V-segment-specific oligo-nucleaotides	
V -segment	Sequence in forward direction
Vβ1	CT GAA TGC CCA GAC AGC TCC AAG C
Vβ2	TC ACT GAT ACG GAG CTG AGG C
Vβ3.1	CCT TGC AGC CTA GAA ATT CAG T
Vβ4	GCC TCA AGT CGC TTC CAA CCT C
Vβ5.1	CAT TAT GAT AAA ATG GAG AGA GAT
Vβ5.2	AAG GTG GAG AGA GAC AAA GGA TTC
Vβ5.3	AG AAA GGA AAC CTG CCT GGT T
Vβ6	CT CTC ACT GTG ACA TCT GCC C
Vβ7	TAC AGG GTC TCA CGG AAG AAG C
Vβ8.1	CAT TAC TCA TAT GTC GCT GAC
Vβ8.2	CAT TAT TCA TAT GGT GCT GGC
Vβ8.3	T GCT GGC AAC CTT CGA ATA GGA
Vβ9	TCT CTC TAC ATT GGC TCT GCA GGC
Vβ10	ATC AAG TCT GTA GAG CCG GAG GA
Vβ11	G CAC TCA ACT CTG AAG ATC CAG AGC
Vβ12	C ATG GTG GGG CTT TCA GGG ATC
Vβ13	AGG CCT AAA GGA ACT AAC TCC CAC
Vβ14	AC GAC CAA TTC ATC CTA AGC AC
Vβ15	CCC ATC AGT CAT CCC AAC TTA TCC
Vβ16	C ACT CTG AAA ATC CAA CCC AC
Vβ17	AG TGT TCC TCG AAC TCA CAG
Vβ18	C AGC CGG CCA AAC CTA ACA TTC TC
Vβ19	CT GCT AAG AAA CCA TGT ACC A
Vβ20	TC TGC AGC CTG GGA ATC AGA A
Mouse TCR C-segment-specific oligo-nucleotide	
CTT GGG TGG AGT CAC ATT TCT C	

4.1.4 Cell fusion – to obtain T hybridomas

A second class of T cell reagents prepared in this study was T hybridoma (157). They were generated by fusing activated primary T cells with a T lymphoma that didn't express functional CD3/TCR complex. Unlike its parental T cell lines, T hybridoma can be maintained in culture medium without the requirement of antigen presenting cells and peptide restimulation. Meanwhile, it is also capable of responding to cognate antigen recall and secreting IL-2 (or IL-4,

depending on the nature of fusion partners). In addition, for unknown reasons, IL-2 secretion of T hybridoma upon antigen recall is less depended on the co-stimulation than primary T cell (158). It thus provides the convenience and the advantage for studying antigen presentation in the absence of co-stimulation.

In this study, BW5147$\alpha^-\beta^-$, a mouse T lymphoma devoid of the endogenous CD3 complex and TCR α/β-chain was used as a fusion partner. Since this lymphoma does not express endogenous TCR, it guaranteed that the antigen specificity was limited to the TCR from primary T cell (159). Fused cells were selected with hypoxanthine/aminopterin/thymidine (HAT) supplemented medium followed by a two-step screening procedure. The first step was to screen for the TCR/CD3 expression by flow cytometry analysis. As BW5147$\alpha^-\beta^-$ doesn't express a functional TCR/CD3 complex, only those hybridomas expressing CD3 and TCR identical to the parental T cell line would be selected for subsequent studies. Accordingly, TCR/CD3$^+$ T hybridomas were screened for the ability of antigen-specific responses, and this procedure required both APCs and the cognate peptide (and a non-related peptide as control). A panel of CD4$^+$Vβ6$^+$ TH206 hybridomas was generated from T206 (**Figure 22A**). They all responded to cognate peptide hGAD65$_{206-220}$ recall (**Figure 22B**). TH206#2 was empirically chosen for subsequent study since this clone manifested a highly uniform morphology under the microscope. TH536.1 hybridomas were obtained from T536.1, and they were selected by antigen recall assay (**Figure 23**) and RT-PCR for Vβ1 expression. TH536.2 hybridomas were obtained from T536.2. They were screened by Vβ11 expression (**Figure 24A**) and antigen-specific response (**Figure 24B**). TH536.1#36 and TH536.2#62 were chose for subsequent experiments.

4.2 Evidence that DR4 (DRA1*0101/DRB1*0401) competes for peptides with DQ8 (DQA1*0301/DQB1*0302)

4.2.1 DQ8 and DR4 can bind same peptide

In addition to the panel of DQ8-restricted CD4 T cell lines, another CD4 T cell line was generated from hGAD65$_{206-220}$ immunized DQ8$^+$DR4$^+$ transgenic mice. Unlike other DQ8-

restricted T cell lines, this cell line, named DR4p206, was maintained/selected by restimulation using DR4$^+$ spleen cells as APCs. Results from *in vitro* restimulation assay showed that DR4p206 responded to the cognate peptide – hGAD65$_{206-220}$ presented by both DR4$^+$ and DQ8$^+$DR4$^+$ spleen cells but not DQ8$^+$ spleen cells (**Figure 25**). It indicated that hGAD65$_{206-220}$ was associated with the DR4 peptide binding site to form the ligand that induced DR4p206 response. It was noteworthy that hGAD65$_{206-220}$ was the cognate peptide of the DQ8-restricted T206 cell (**Figure 19C**). Therefore, it was clear that the same hGAD65$_{206-220}$ peptide was able to bind both DQ8 and DR4 molecule.

4.2.2 Co-expression of DR4 with DQ8 diminished DQ8-restricted T cell responses

As DQ8 and DR4 were demonstrated to bind the same peptide, they potentially would compete for the source of peptide when DQ8 and DR4 were co-expressed on the same APC. In order to test this hypothesis, we then evaluated the relative peptide occupancy of DQ8 by comparing the CD4 T cell responses elicited by DQ8$^+$ APCs (in the absence of DR4 expression) with DQ8$^+$DR4$^+$ APCs (in the presence of DR4 co-expression), using DQ8-restricted T206, T536.1 and T536.2 as responding T cells. Since these T cell lines manifested homogeneous compositions, they were reliable to serve as detection reagents. Splenocytes from selected DQ8 single transgenic and DQ8/DR4 double transgenic mice were used as APCs. FACS analysis was performed to ensure splenocytes from selected HLA transgenic mice expressing similar levels of HLA-DQ8 (**Figure 26A**). Both DQ8$^+$ and DQ8$^+$DR4$^+$ splenocytes induced the T206 response for IFN-γ secretion, whereas in the presence of DR4, IFN-γ secretion was decreased (**Figure 26B**). A similar reduction in cytokine secretion was also observed using the T536.1 line as the responding T cell (**Figure 26C**). However, when T536.2 cells were used as responders, the result of *in vitro* restimulation assay showed that there was a slight difference in IL-4 release between the responses elicited by DQ8 APCs and DQ8/DR4 APCs (**Figure 26D**). This could be due to a relatively low proliferation rate shared by most Th2-like T cells such as T536.2. It responded to its cognate peptide by producing IL-4, but manifested limited expansion without the addition of exogenous IL-2 administration (**Figure 27A**). In contrast, T536.1 – the Th1 cell line expanded rapidly upon restimulation (**Figure 27A**), particularly in the absence of DR4 expression (**Figure**

27B). Rapid expansion certainly synergized the cytokine production since increasing numbers of T cells were involved in the assay. In summary, these results indicated that DR4 co-expression affected DQ8-restricted Th1 cell responses and led to diminished clonal expansion and IFN-γ production, whereas the response of the Th2 cell line T536.2 was less affected. Since the DQ8 and DQ8/DR4 transgenic mice used in this comparison were from the same litter, the genetic differences (except DR4 expression) between these two transgenic groups were minimized, and should not account for the observed differences.

4.2.3 A peptide blocking DR4 peptide binding site was able to partially recover DQ8-restrcited T cell responses.

The peptide competition requires a free DR4 peptide binding site. Diminished T cell responses observed in previous experiments thus suggested that a significant amount of peptide was able to access the DR4 binding site. In order to confirm this interpretation, we investigated $hGAD65_{206-220}$ and $hGAD65_{536-550}$ presentation efficiency in the presence of blocking peptide – $hGAD65_{554-566}$, which was demonstrated previously to bind DR4 with a high affinity, but was not able to bind DQ8 at all (150). A human B cell line WT51 (expressing both DQ8 and DR4) was used as the APC and T hybridomas TH206 (**Figure 28A**), TH536.1 (**Figure 28B**), and TH536.2 (**Figure 28C**) were used as detection reagents. Results showed that with increasing amounts of blocking peptide, T hybridoma responses were increased accordingly. It indicated that the peptide occupancy of DQ8 was at least partially recovered due to the saturation of the DR4 binding site with the blocking peptide.

4.3 Different DR4 subtypes (DRB1*0401, 0402, 0403, 0404, and 0406) manifested different levels of modulation of DQ8-restricted CD4 T cell responses

We next examined effects of other DR4 subtypes (DRB1*0401, 0402, 0403, 0404, and 0406) on DQ8-restricted CD4 T cell responses. It is noteworthy that DQ8-DRB1*04 haplotypes carrying distinct DRB1*04 alleles are associated with variable susceptibility to T1D (8, 146). These

DRB1*04 alleles differ from each other only by a few amino acid residues within peptide binding groove regions (**Figure 29**)(100). We thus suspected that the polymorphisms within the peptide binding groove would confer variable peptide competition potentials for these DR4 subtypes.

As transgenic mice expressing DR4 alleles other than DRB1*0401 have not been developed, the most available sources of antigen presenting cells are Epstein-Barr virus transformed human B cells – WT51, FS, BM92 and KT17 (International Histocompatibility Working Group (http://www.ihwg.org). These four B cell lines express distinct DQ8-DRB1*04 haplotypes (**Table 5**). It should be noted that they are homozygous at DQ-DRB1 loci except that KT17 heterozygously expresses DRB1*0403 and 0406 at DRB1 locus. However, since the amino acid sequence within the DR peptide binding groove is identical between 0403 and 0406, it is presumed that HLA-DR4 (0403) and HLA-DR4 (0406) manifest an identical affinity for peptide binding.

Table 5. DQ-DRB1 haplotypes of selected B-LCLs

	WT51	FS	KT17	BM92
DQA1	0301	0301	0301	0301
DQB1	0302	0302	0302	0302
DRB1	0401	0402	0403/0406	0404

Primary T cells (T206, T536.1 and T536.2) were not ideal to evaluate antigen presenting efficiencies of human B cells, because human B cells could not provide proper co-stimulation that had been demonstrated to be needed for primary T cell activation (158). Hence, the T hybridomas – TH206, TH536.1 and TH536.2 were used for this purpose.

We also noticed that TH206 was similar to its un-fused parental T cell line T206 and responded better to truncated hGAD65$_{209-217}$ 9-mer than cognate hGAD65$_{206-220}$ 15-mer (**Figure**

30). We thus decided to use truncated 9-mer hGAD65$_{209-217}$ as antigen for subsequent T hybridoma response to obtain optimal sensitivity.

Given a sufficient quantity of peptide, all of these human B cell lines were able to raise TH206, TH536.1 and TH536.2 responses (**Figure 31A, B, C**). However, the magnitude of T cell responses elicited by human B-LCLs was variable and ranked from high to low in the order of FS ≥ WT51 >BM92 >KT17. These variable T hybridoma responses were not correlated with the level of HLA-DQ8 expression (**Figure 32**). The lower DQ expressing B cell line FS (homozygous for DQ8-DRB1*402) always caused strong T cell responses. In contrast, those higher DQ-expressing cells such as BM92 (homozygous for DQ8-DRB1*0404), and KT17 (homozygous for DQ8, heterozygous for DRB1*0403/0406) were less capable to induce T cell responses than FS. This indicated that the peptide presenting efficiency of DQ8 in the presence of distinct DRB1*04 alleles were different. Effects of these DRB1*04 alleles were in the rank of 0402 ≤ 0401 < 0404 < 0403/0406. The DRB1*0403/0406$^+$ KT17 always required 5-10 fold more peptide to achieve an equivalent T cell response as DRB1*0402$^+$ FS did. It suggested that DRB1*0403/0406 alleles had a much stronger competition for these peptides than the DRB1*0402 allele. To further confirm this observation, the KT17 was mixed with FS to stimulate TH536.1. The group with the mixed presenter (20,000/well FS + 10,000/well KT17) caused a reduced level of IL-2 secretion in comparison with the group of pure FS (20,000/well) (**Figure 33**). It indicated that in the KT17/FS mixture, the number of available hGAD65$_{536-550}$:DQ8 complex was decreased, though more DQ8 input was provided.

4.4   DR4 also competed with DQ8 for the peptide delivered by CLIP-substituted recombinant invariant chain

In addition to using synthesized peptides as the source of antigen, we also attempted an alternative peptide delivery method for T cell assay. It was accomplished by transfecting a recombinant MHC Class II-associated invariant chain cDNA that carried peptide coding sequence to DQ8$^+$ target cells. Previous studies demonstrated that a recombinant Ii (rIi) with its original CLIP replaced by an antigenic peptide coding sequence could successfully deliver

antigenic peptide to the MHC Class II (160, 161). It allowed target cells to generate antigen endogenously so that it provided the possibility to investigate the peptide competition within the intracellular compartment.

DQ8#114, a DQ8-transfected COS7 cell clone was used as the target cell. This clone was qualified to serve as antigen presenting cell not only because it stably expressed DQ8 heterodimer on the surface (**Figure 34A**), but also was able to present exogenous cognate peptide hGAD65$_{536-550}$ to TH536.1 hybridoma (**Figure 34B**). DQ8#114 was transfected by rIi-539 – the recombinant invariant chain bearing TH536.1 hybridoma cognate peptide coding sequence (**Figure 15**). TH536.1 was added into the culture 24 hours later. IL-2 secretion indicated that rIi-539 could be endogenously processed and presented to the surface to trigger T cell response. When DQ8*114 was co-transfected by rIi-539 and DR4, the IL-2 secretion level was decreased (**Figure 35**). The input of TH536.1 hybridomas was titrated down from 10^5 cells/well to 10^4 cells/well. The rIi-539/DR4 co-transfection group consistently elicited lower hybridoma responses than the group without DR4 expression. It indicated that the efficiency of hGAD65$_{539-547}$ presentation was reduced in the presence of DR4.
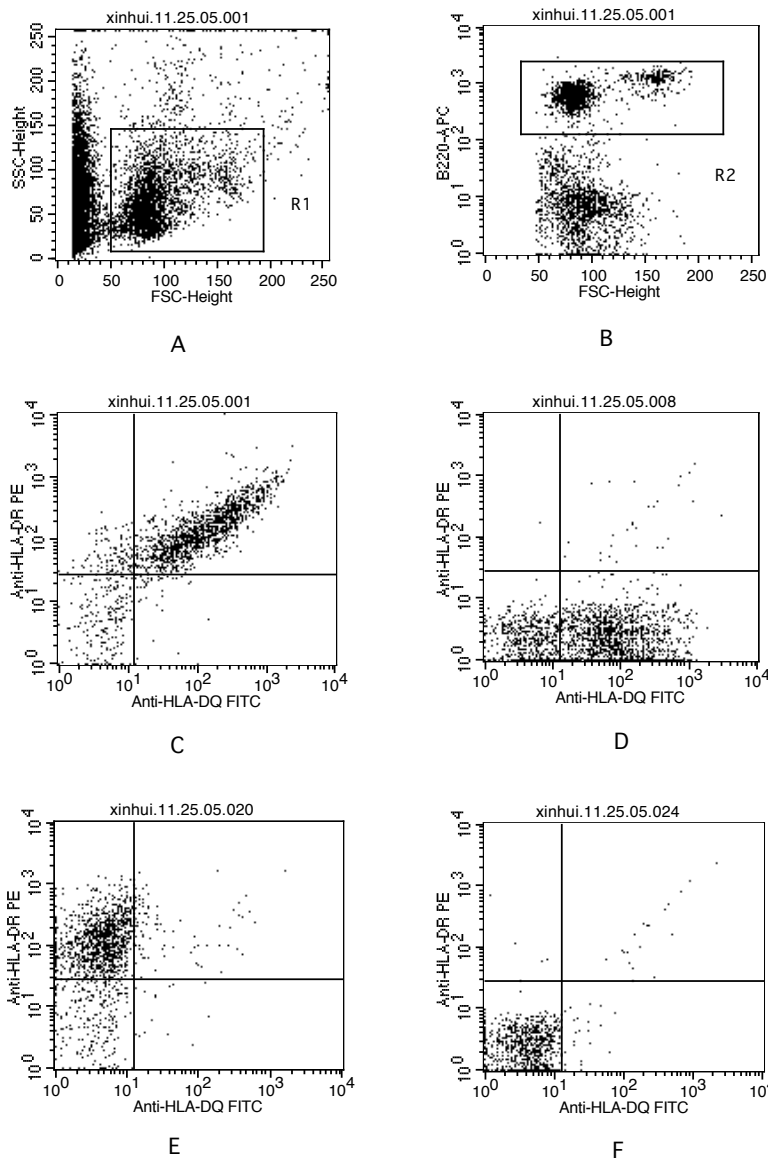
Figure 16. The genotype of an HLA transgenic mouse identified by flow cytometry analysis using fluorescence-conjugated anti-HLA-DQ and –DR monoclonal antibodies

Red blood lysis buffer pre-treated mouse peripheral blood sample was analyzed by flow cytometer. (**A**) The dot plot distinguished white blood cells from non-depleted red blood cells or dead cells by relative large size (indicated by the value of forward-scatter channel or FSC) and low granule intensity (indicated by the value of side-scatter channel or SSC). (**B**). Among gated white blood cell population, B lymphocytes subset was distinguished from others by the expression of surface marker B220 (CD45R), revealed by APC-conjugated anti-B220 mAb staining. (**C**), (**D**), (**E**) and (**F**) FITC-conjugated anti-HLA-DQ mAb and PE-conjugated anti-HLA-DR mAb staining patterns of B lymphocytes (gated from B220$^+$ cell populations) from different transgenic mice indicated the HLA genotypes were DQ8$^+$DR4$^+$ (**C**), DQ8$^+$DR4$^-$ (**D**), DQ8$^-$DR4$^+$ (**E**), and DQ8$^-$DR4$^-$ (**F**), respectively.
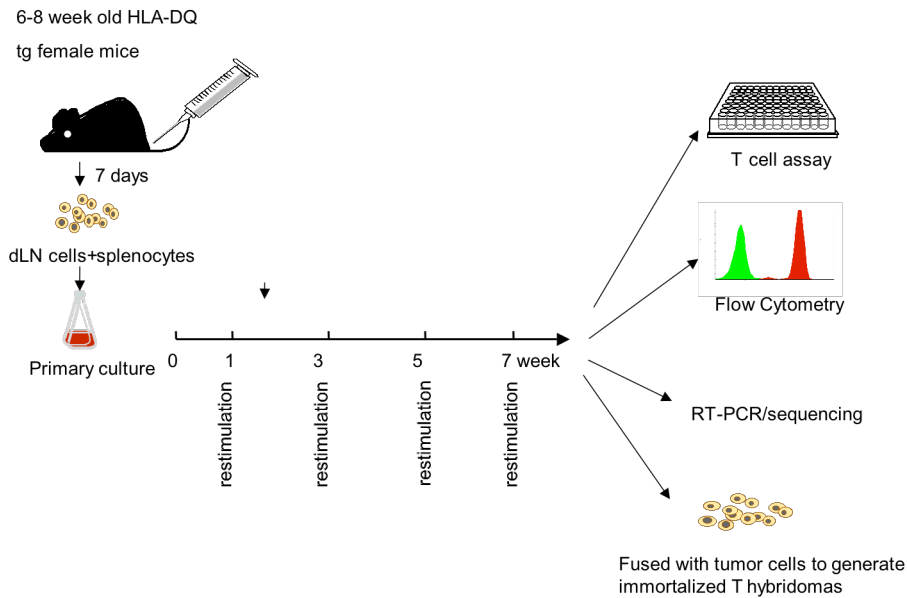
A
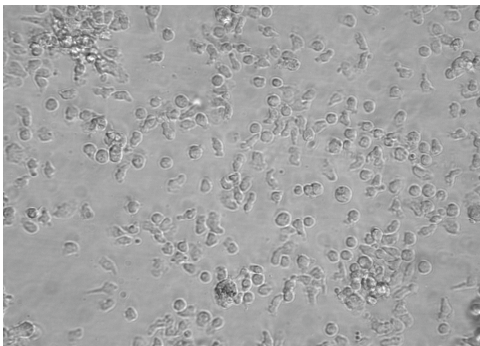
B
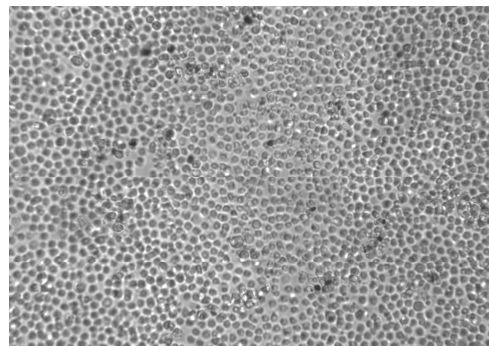
C

Figure 17. The generation of antigen-specific CD4 T cell lines from HLA-DQ8 transgenic mice

(A) A brief illustration of the protocol used for *in vitro* T cell line generation. A group (generally, 4 mice) of 6-8 week old female HLA-DQ8 transgenic mice were immunized by antigenic peptide subcutaneously. Primary culture was then established one week later from the spleen and draining lymph node cells. The culture was passaged every two weeks after a single one-week culturing. The culture was then characterized for antigen specificity and homogeneity by *in vitro* T cell restimulation assay and flow cytometry analysis or RT-PCR for TCR Vβ usage, respectively. Selected T cell lines were also fused with T lymphoma to generate T hybridomas. (B) In restimulation culture, activated antigen-specific CD4 T cells displayed enlarged size with episodic clustering under microscope (x400). (C) In contrast, non-antigen-specific (without activation) cells display homogeneously small size without clustering (x400).
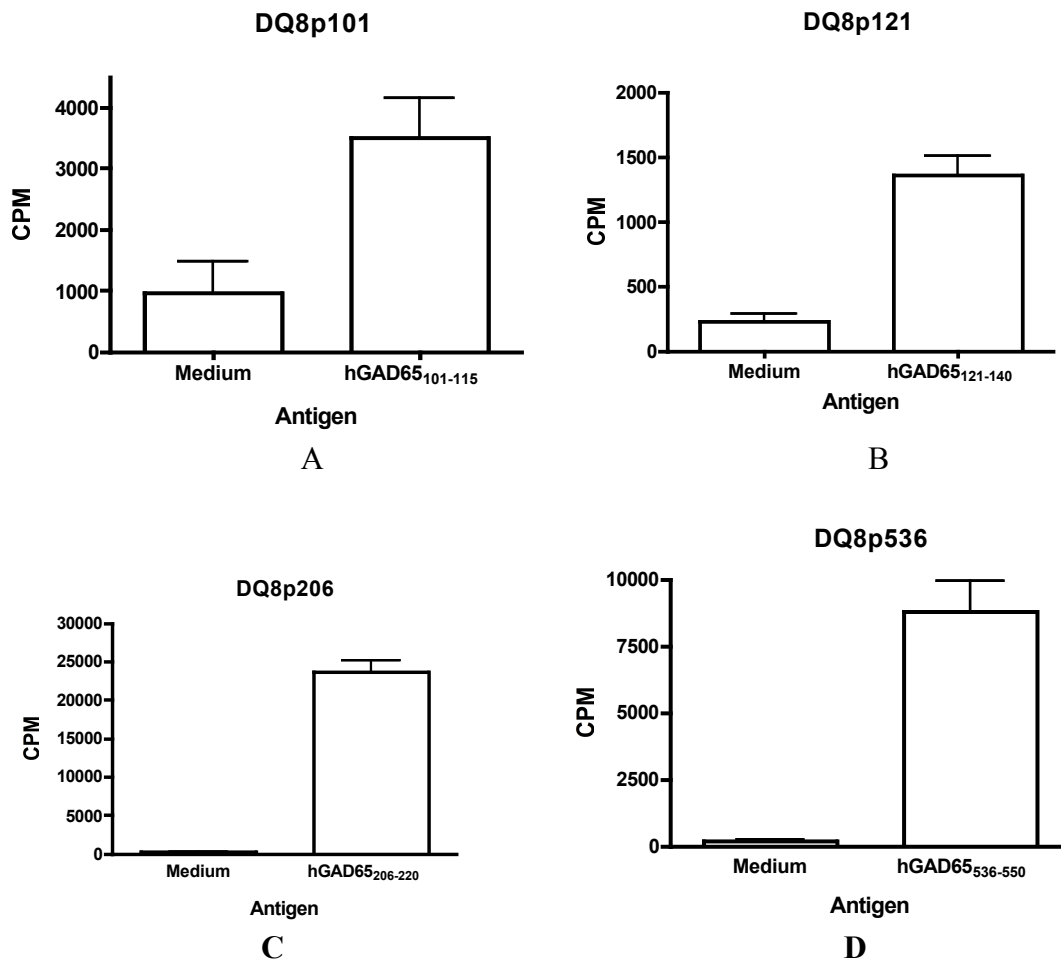
Figure 18. DQ8-restricted T cell lines specifically responded to cognate peptides

In vitro proliferation of CD4$^+$ T cell lines DQ8p101 (**A**), DQ8p121 (**B**), DQ8p206 (**C**), and DQ8p536 (**D**) co-cultured with irradiated syngenic DQ8$^+$ splenocytes in the presence of medium alone (as blank control) or 10 ug/ml of cognate peptide (hGAD65$_{101-115}$, hGAD65$_{121-140}$, hGAD65$_{206-220}$, and hGAD65$_{536-550}$, respectively).
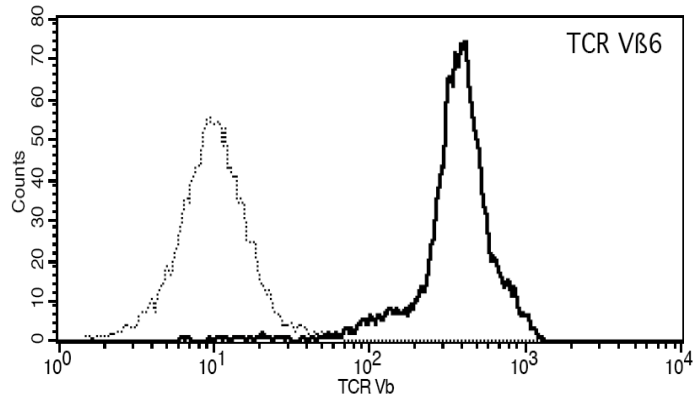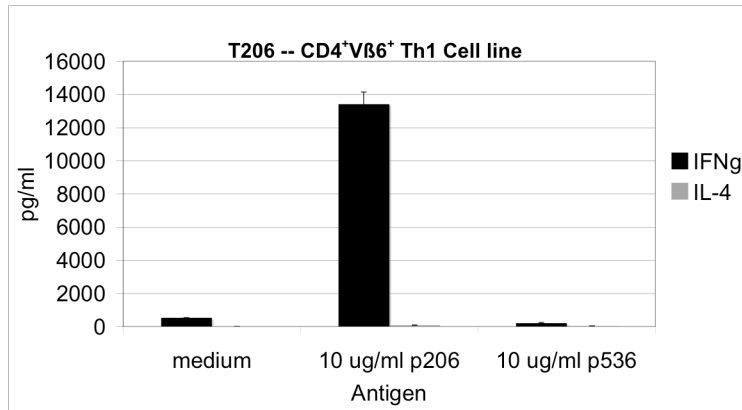
A

CTC ACT GTG ACA TCT GCC CAG AAG AAC GAG ATG GCC GTT TTT CTC TGT GCC AGC AGT AGG CAG GAT AAC
 L   T   V   T   S   A   Q   K   N   E   M   A   V   F   L   C   A   S   S   R   Q   D   N
TAT GCT GAG CAG TTC TTC GGA CCA GGG ACA CGA CTC ACC GTC CTA GAG GAT CTG AGA AAT GTG ACT CCA
 Y   A   E   Q   F   F   G   P   G   T   R   L   T   V   L   E   D   L   R   N   V   T   P
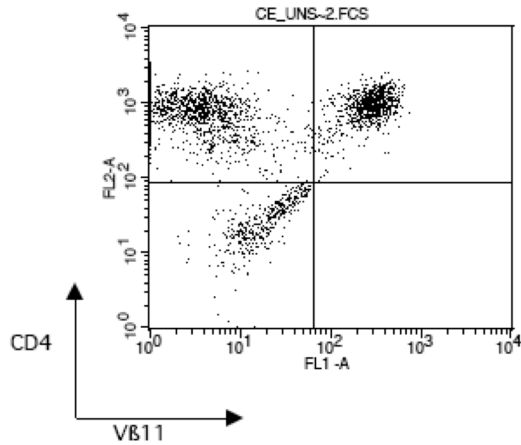CCC AAG
 P   K

B

C

Figure 19. Characterization of clonal T206 cell.

(**A**) CD4 T cell line T206 was stained by a panel of FITC-conjugated anti-TCR Vβ mAb for flow cytometry analysis. The histogram represents staining results of Vβ6-specific mAb (thick line) and isotype control antibody (thin line). (**B**) cDNA and amino acid sequence of T206 cell TCR β-chain VDJC joint. (**C**) IFN-γ and IL-4 produced by T206 cell as co-cultured with irradiated syngenic DQ8$^+$ splenocytes in the presence of medium (blank control), or 10 ug/ml cognate peptide hGAD65$_{206-220}$, or 10 ug/ml unrelated control peptide hGAD65$_{536-550}$.
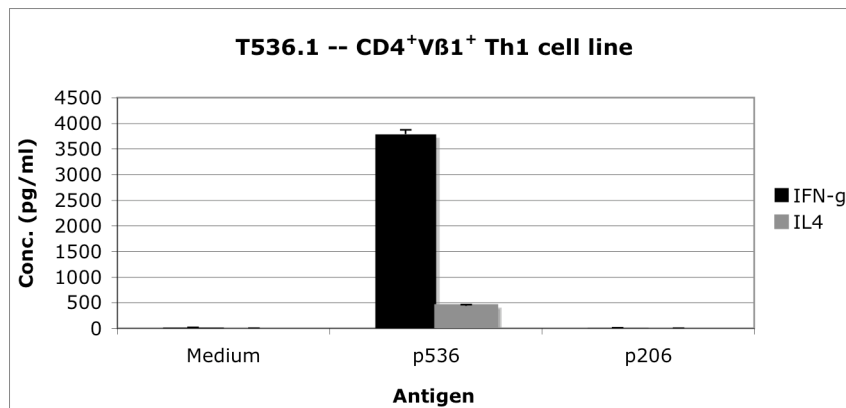
A

GAA TGC CCA GAC AGC TCC AAG CTA CTT TTA CAT ATA TCT GCC GTG GAT CCA GAA GAC TCA GCT GTC TAT
 E   C   P   D   S   S   K   L   L   L   H   I   S   A   V   D   P   E   D   S   A   V   Y
TTT TGT GCC AGC AGC CAA GAG GCA GGG TGG AGT CAA AAC ACC TTG TAC TTT GGT GCG GGC ACC CGA CTA
 F   C   A   S   S   Q   E   A   G   W   S   Q   N   T   L   Y   F   G   A   G   T   R   L
TCG GTG CTA GAG GAT CTG AGA AAT GTG ACT CCA CCC AAG
 S   V   L   E   D   L   R   N   V   T   P   P   K

B

C

Figure 20. Characterization of clonal T536.1 cell

(A) DQ8p536 cells consist of Vβ11⁻ and Vβ11⁺ subset, revealed by Flow cytometry analysis with PE-conjugated anti-CD4 mAb and FITC-conjugated anti-Vβ11 mAb double staining. Vβ11⁻ subset was separated from Vβ11⁺ subset by cell sorter and named T536.1. (**B**) cDNA and amino acid sequence of T536.1 cell TCR β-chain VDJC joint. (**C**). IFN-γ and IL-4 produced by T536.1 cell cultured with irradiated syngenic DQ8⁺ splenocytes in the presence of medium alone (blank control), or 10 ug/ml cognate peptide hGAD65$_{536-550}$ (p536), or 10 ug/ml unrelated control peptide hGAD65$_{206-220}$ (p206).
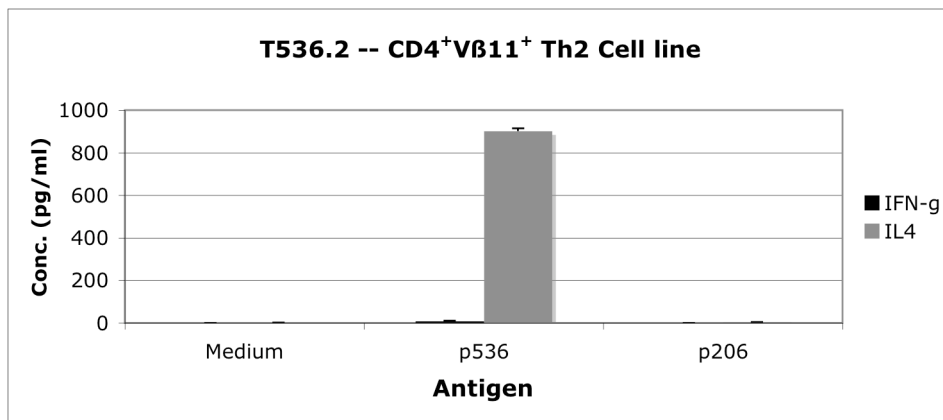
81
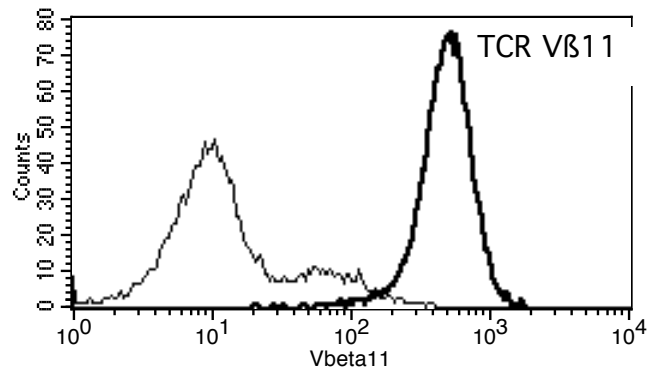
A

TTC AGA TTG CAC TCA ACT CTG AAG ATC CAG AGC ACG CAA CCC CAG GAC TCA GCG GTG TAT CTT TGT GCA
 F   R   L   H   S   T   L   K   I   Q   S   T   Q   P   Q   D   S   A   V   Y   L   C   A
AGC AGC TTA GGA CGG GAC TGG ACT AGT GCA GAA ACG CTG TAT TTT GGC TCA GGA ACC AGA CTG ACT GTT
 S   S   L   G   R   D   W   T   S   A   E   T   L   Y   F   G   S   G   T   R   L   T   V
CTC GAG GAT CTG AGA AAT GTG ACT CCA CCC AAG AAT CAC G
 L   E   D   L   R   N   V   T   P   P   K   N   H

B

C

Figure 21. Characterization of clonal T536.2 cell

(**A**) CD4 T cell line T536.2 (separated apart from T536.1 by cell sorter) was stained by a panel of FITC-conjugated anti-TCR Vβ mAb for flow cytometry analysis. The histogram represented staining results of Vβ11-specific mAb (thick line) and isotype control antibody (thin line). (**B**) cDNA and amino acid sequence of T536.2 cell TCR β-chain VDJC joint. (**C**) IFN-γ and IL-4 produced by T536.2 cell co-cultured with irradiated syngenic DQ8$^+$ splenocytes in the presence of medium alone (blank control), or 10 ug/ml cognate peptide hGAD65$_{536-550}$ (p536), or 10 ug/ml unrelated control peptide hGAD65$_{206-220}$ (p206).
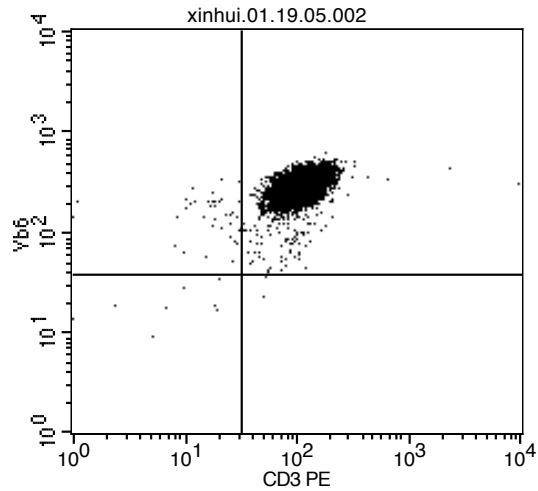
A
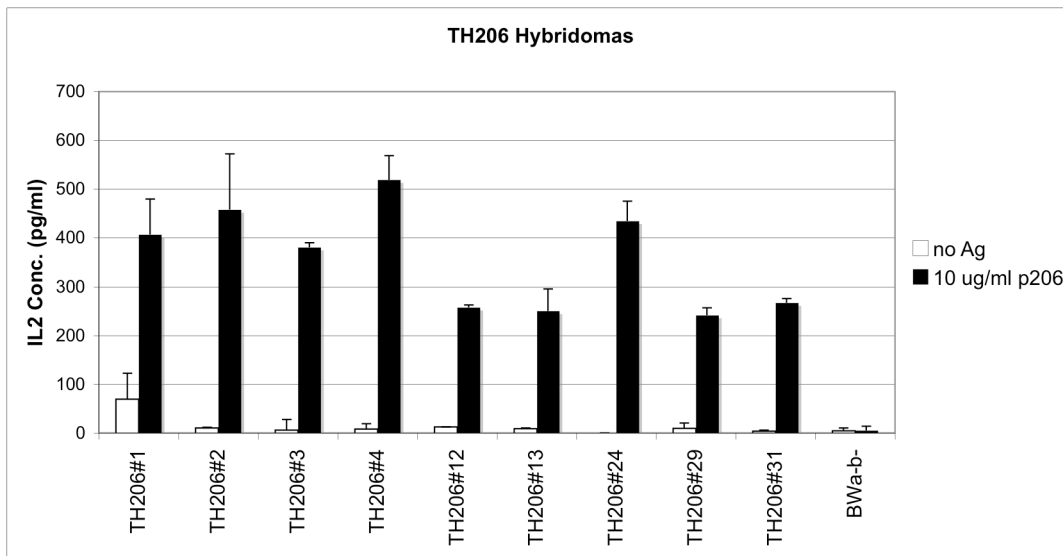
B

Figure 22. T206-derived T hybridomas – TH206.

(**A**) Hybridomas surviving HAT selection were screened for CD3 and TCR Vβ6 expression by flow cytometry analysis. Dot plot represented one of candidate T hybridomas expressing both CD3 and Vβ6 – the same TCR Vβ expressed by parental T206 cell. (**B**) IL-2 produced by a panel of $CD3^+Vβ6^+$ hybridomas co-cultured with irradiated $DQ8^+$ splenocytes in the presence of medium alone (no Ag: as blank control) or with 10 ug/ml cognate peptide $hGAD65_{206-220}$. Non-fused fusion partner $BWα^-β^-$ was also tested under the same assay condition as negative control.

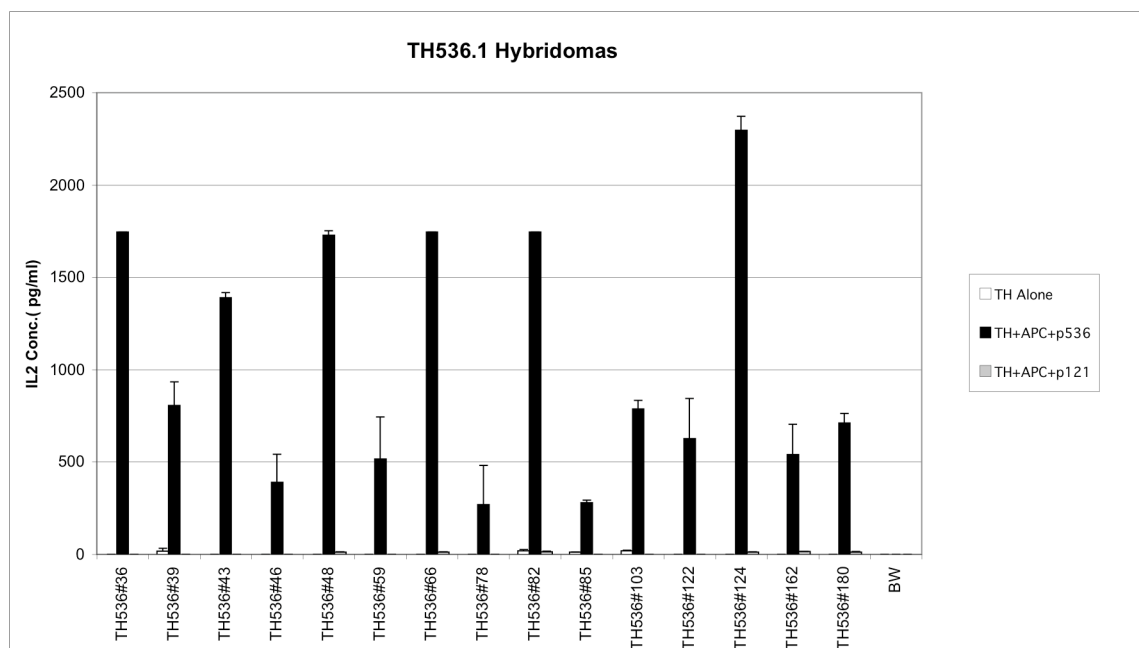**Figure 23. T536.1-derived T hybridomas – TH536.1**

IL-2 produced by a panel of hybridomas co-cultured with medium alone (as blank control), or 10 ug/ml cognate peptide hGAD65$_{536-550}$, or 10 ug/ml unrelated control peptide hGAD65$_{121-140}$ in the presence of irradiated DQ8^{+} splenocytes. Non-fused fusion partner BW$\alpha^{-}\beta^{-}$ was also tested under the same assay condition as negative control.
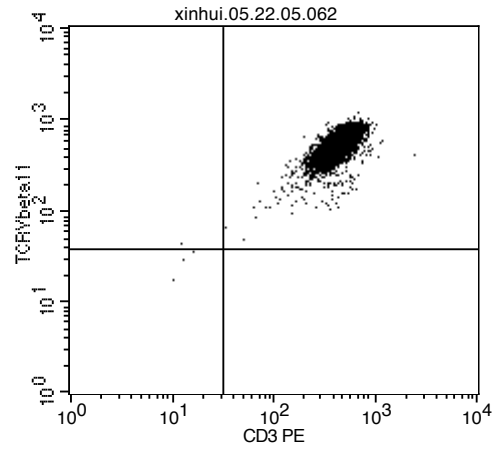
A
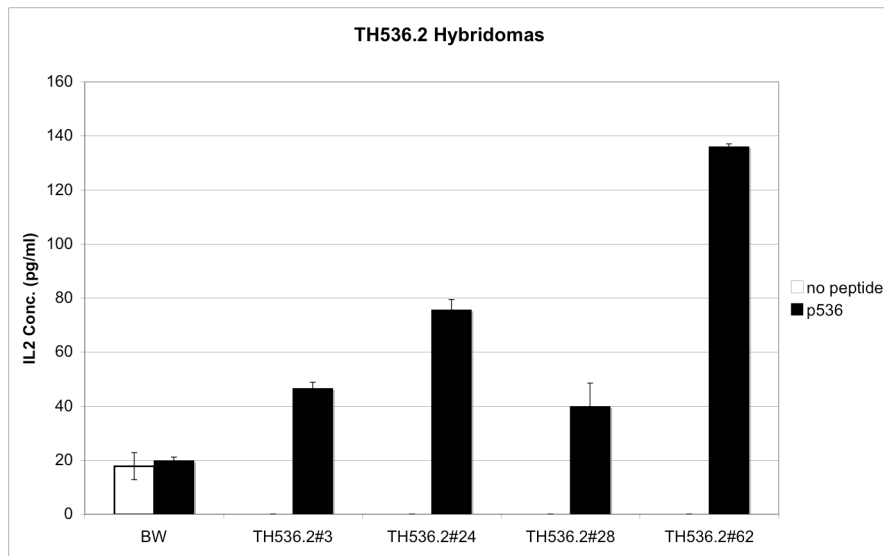
B

Figure 24. T536.2-derived T hybridomas – TH536.2

(**A**) Hybridomas surviving HAT selection were screened for CD3 and TCR Vβ11 expression by flow cytometry analysis. Dot plot represents one of candidate T hybridomas expressing both CD3 and Vβ11 – the same TCR Vβ expressed by parental T536.2 cell. (**B**) IL-2 produced by a panel of $CD3^+Vβ11^+$ hybridomas co-cultured with irradiated $DQ8^+$ splenocytes in the presence of medium alone (no peptide: as blank control) or 10 ug/ml cognate peptide $hGAD65_{536-550}$ (p536). Non-fused fusion partner $BWα^-β^-$ was also tested under the same assay condition as negative control.

Figure 25. *In vitro* **T cell response of DR4p206 cells**

IFN-γ produced by DR4p206 cell co-cultured with irradiated DQ8^{+} splenocytes, DR4^{+} splenocytes or DQ8^{+}DR4^{+} splenocytes in the presence of medium alone (as blank control), or 10ug/ml of cognate peptide hGAD65$_{206-220}$.

A
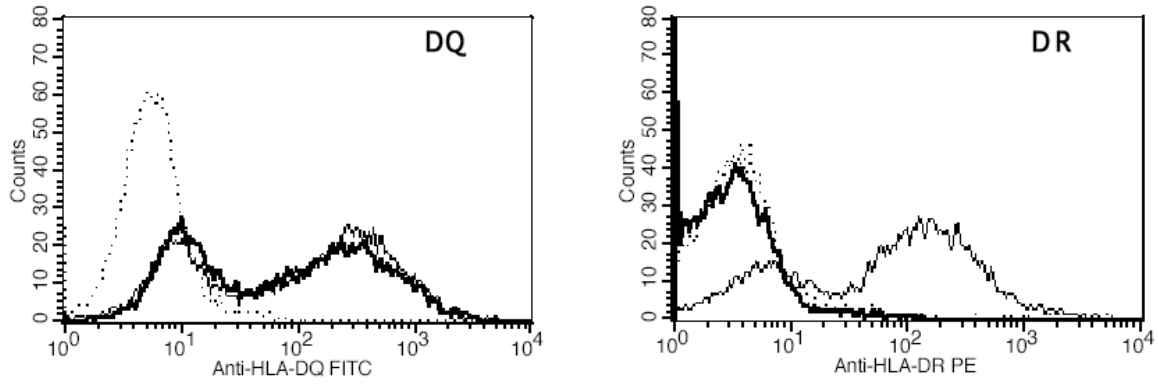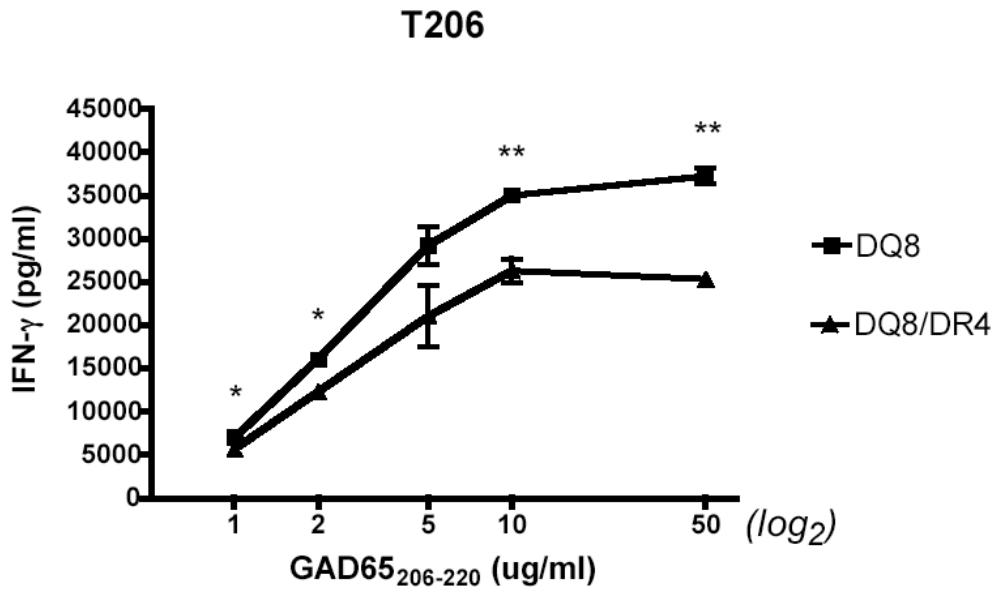
B

T536.1 response to DQ8 APC *vs.* DQ8/DR4 APC
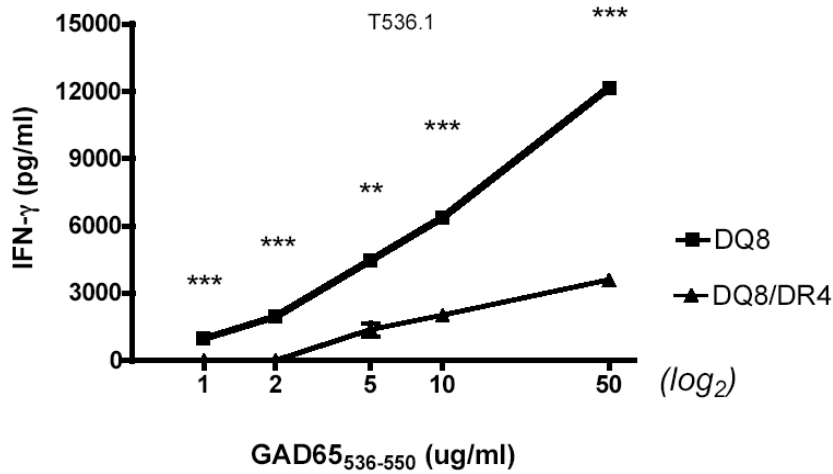
C

T536.2 response to DQ8 APC *vs.* DQ8/DR4 APC
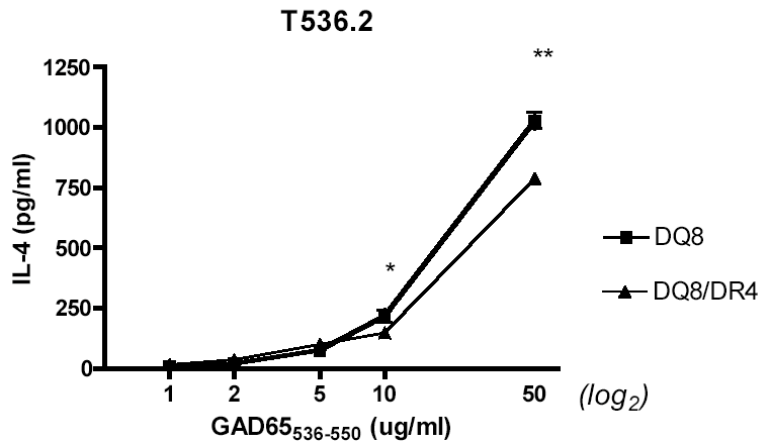
D

Figure 26. Influence of HLA-DR4 (0401) co-expression to antigen specific DQ8-restricted CD4 T cell responses.

(A) RBC-depleted splenocytes from DQ8 (thick lines) and DQ8/DR4 transgenic mice (thin lines) were stained with FITC-conjugated anti-HLA-DQ mAb (left panel), and PE-conjugated anti-HLA-DR mAb (right panel). Dotted line represents isotype control. Cytokine produced by T206 **(B)**, T536.1 **(C)**, and T536.2 **(D)** co-cultured with $DQ8^+$ splenocytes or $DQ8^+DR4^+$ splenocytes in the presence of indicated amount of cognate peptides.
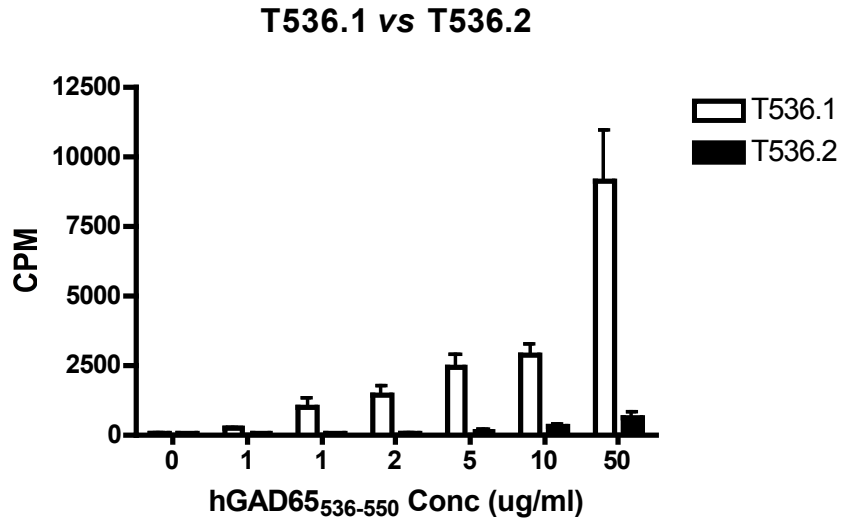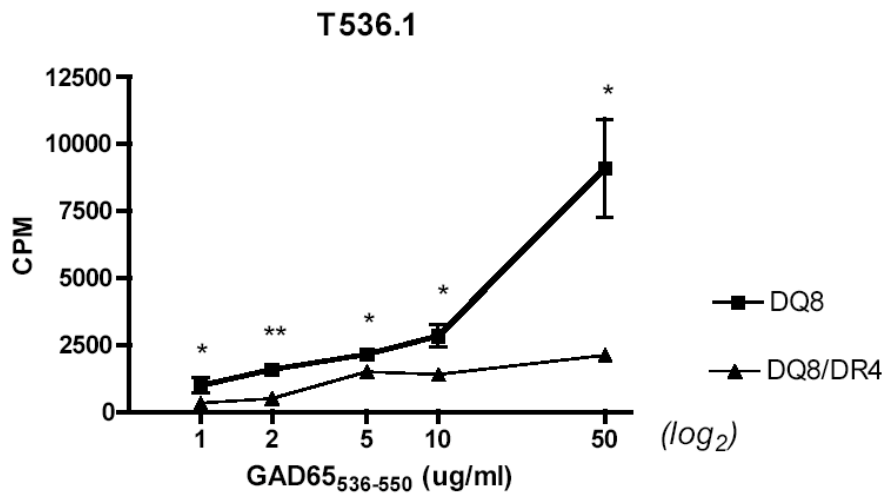
Figure 27. T536.2 cells expand poorly in comparison to T536.1 cells upon *in vitro* antigen restimulation.
(**A**) Proliferation of T536.1 and T536.2 cell co-cultured with irradiated syngenic DQ8^{+} splenocytes in the presence of indicated amount of cognate peptide hGAD65$_{536-550}$. (**B**) Proliferation of T536.1 cell co-cultured with irradiated DQ8^{+}, or DQ8^{+}DR4^{+} splenocytes in the presence of indicated amount of cognate peptide hGAD65$_{536-550}$.
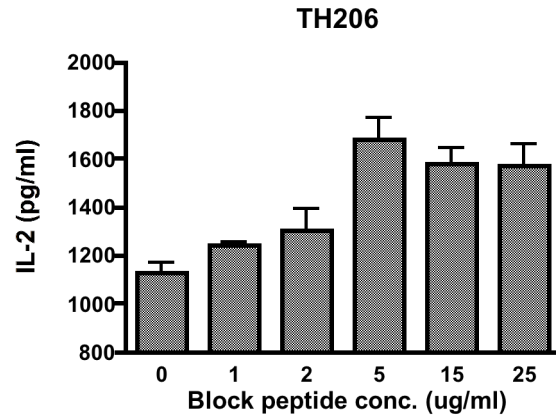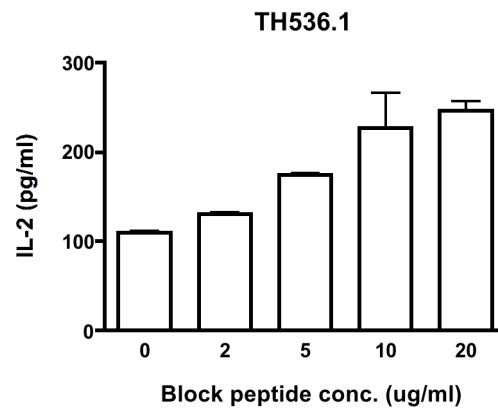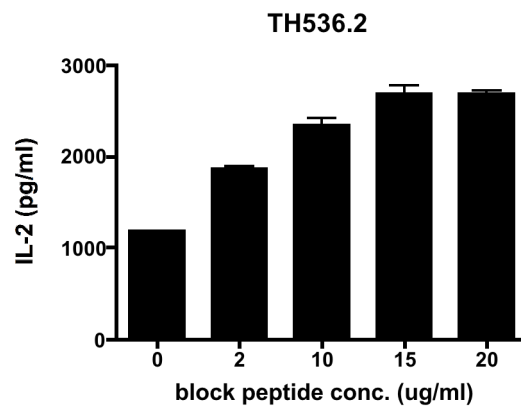
Figure 28. Blocking of DR4 binding site partially recovered DQ8-restricted T hybridoma responses

IL-2 produced by T hybridoma TH206 (**A**), TH536.1 (**B**) and TH536.2 (**C**) co-cultured with WT51 (human B cell line, $DQ8^+DR4^+$) in the presence of cognate peptides (10 ug/ml of $hGAD65_{209-217}$ for TH206, 2 ug/ml of $hGAD65_{536-550}$ for TH536.1 and TH536.2) and indicated amount of blocking peptide $hGAD65_{554-566}$, which bound only DR4 but not DQ8.
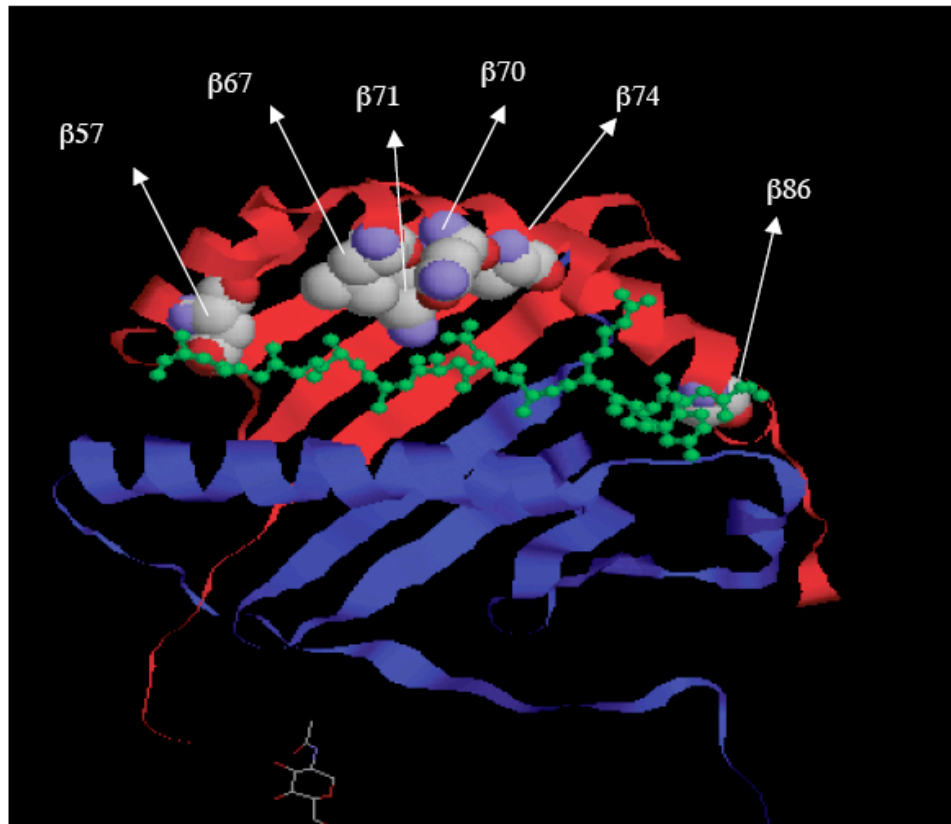
```
                    57               67  70 71  74           86
DRB1*0401  TELGRPDAEY WNSQKDLLEQ KRAAVDTYCR HNYGVGESFT
DRB1*0402  - - - - - - - - - -  - - - - - - - -I- - D E- - - - - - - - - -  - - - - - -V- - - - -
DRB1*0403  - - - - - - - - - -  - - - - - - - - - - -  R- - E- - - - - -  - - - - - -V- - - - -
DRB1*0404  - - - - - - - - - -  - - - - - - - - - - -  R- - - - - - - - - -  - - - - - -V- - - - -
DRB1*0405  - - - - - - -S- - -  - - - - - - - - - - -  R- - - - - - - - - -  - - - - - - - - - - -
DRB1*0406  - - - - - - - - - -  - - - - - - - - - - -  R- - E- - - - - - -  - - - - -V- - - - -
```

Figure 29. Alignment of selected DRB1*04 alleles

Peptide binding region amino acid sequences of DRB1*0402, 0403, 0404, 0405 and 0406 were aligned to DRB1*0401 (as reference). Short dashes represent the usage of identical amino acid residues. DRB1*0403 and DRB1*0406 share the identical sequence regarding peptide binding groove related fragment. The cartoon was adapted from 2SEB, a crystal structure file collected in Protein Database Bank (PDB), this ribbon and stick model summaries the association a peptide (ball-stick) from human Collagen II (1168-1179) with peptide binding groove of HLA-DR4 composed of DRA1*0101 (the ribbon at low position in dark color) and DRB1*0401 (the ribbon at up position in light color). Portions on β-chain highlighted as space-filled style represent amino acid residues differing DRB1*0401 from other DRB1*04 alleles according to the alignment. (adapted from reference 101 with slight modification)

91

TH206 responses to truncated peptide

(y-axis) truncated peptide

- p206/220* (15-mer)
- p212/220
- p211/219
- p210/218
- p209/217
- p208/216
- p207/215
- p206/214

(x-axis) IL-2 Conc. (pg/ml): 0, 100, 200, 300
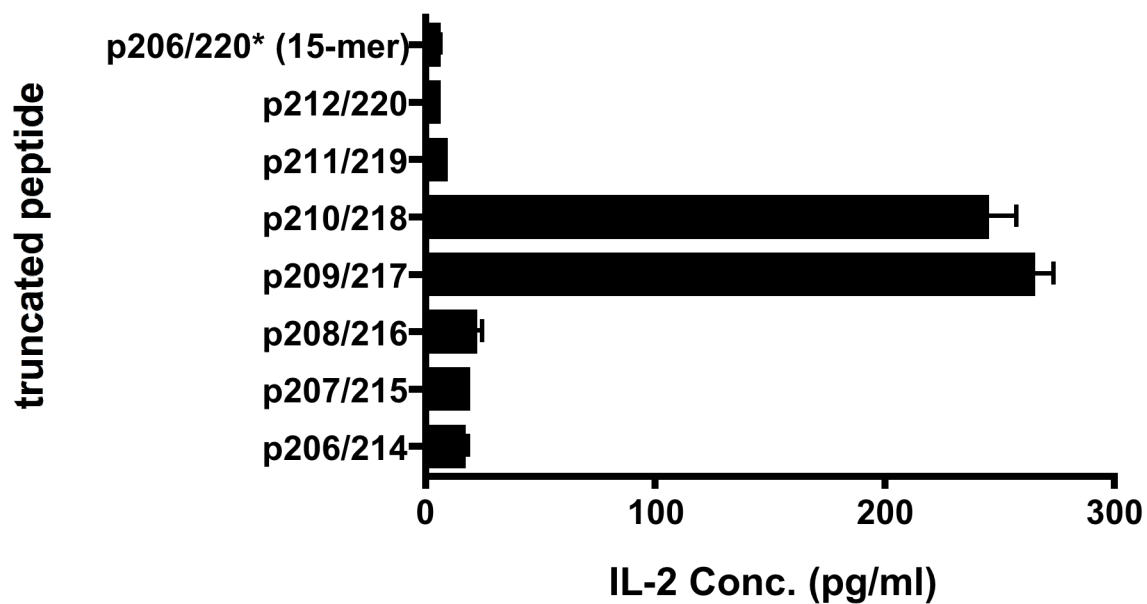
Figure 30. TH206 hybridoma responded to truncated 9-mers and a cognate 15-mer (hGAD65$_{206-220}$).
IL-2 produced by TH206 hybridoma co-cultured with Mitomycin C treated WT51 (a human B cell line expressing HLA-DQ8) in the presence a panel of partially overlapped peptide 9-mers, in comparison with hGAD65$_{206-220}$ 15-mer.

TH206

A

TH536.1

B

93
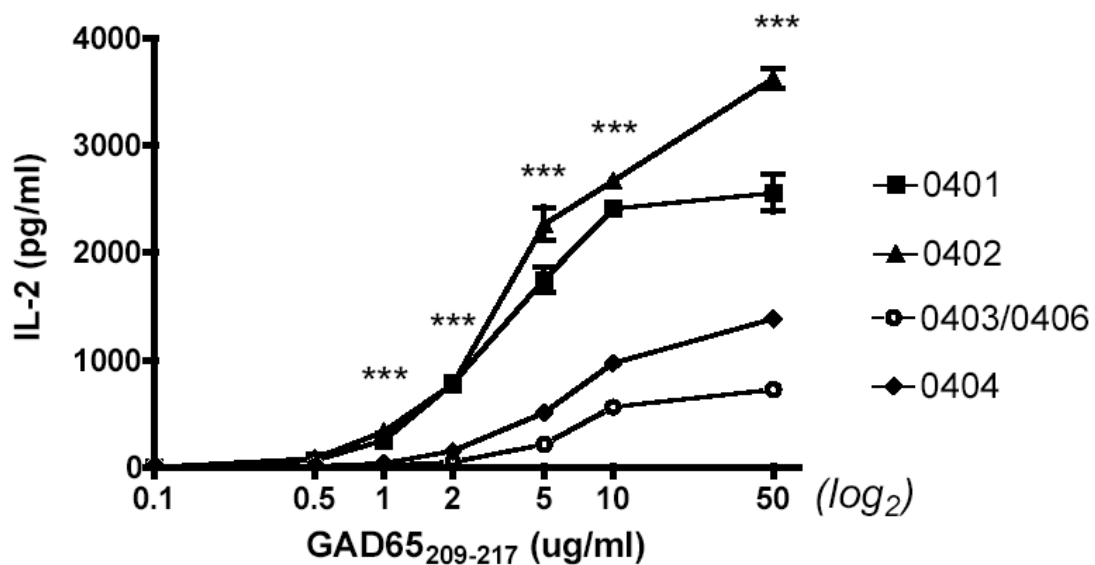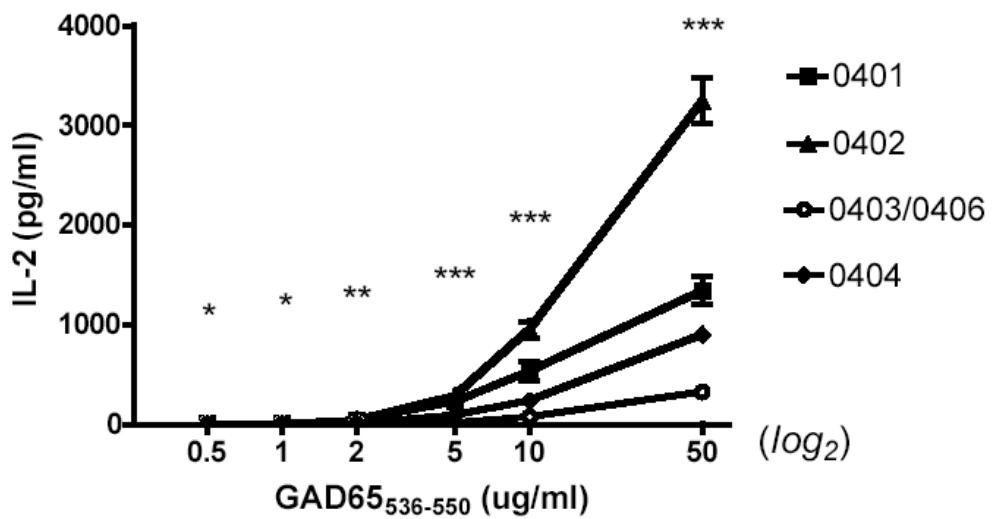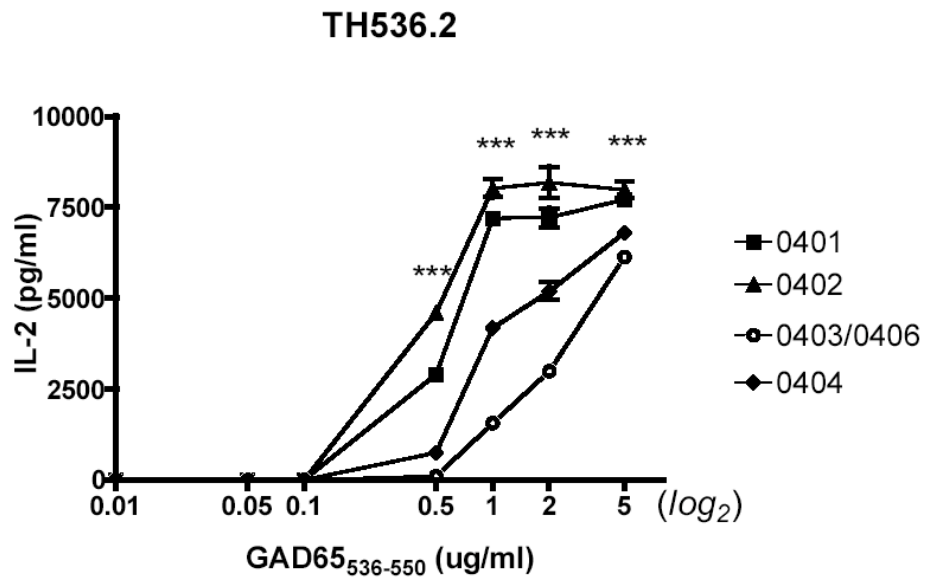
Figure 31. CD4^{+} T hybridoma responses to human B-LCLs expressing different DQ8-DRB1*04 haplotypes
IL-2 produced by hybridoma TH206 **(A)**, TH536.1 **(B)**, and TH536.2 **(C)** co-cultured with Mitomycin C treated human B-LCL WT51 (0401), FS (0402), KT17 (0403/0406), and BM92 (0404) in the presence of indicated amount of cognate peptides.
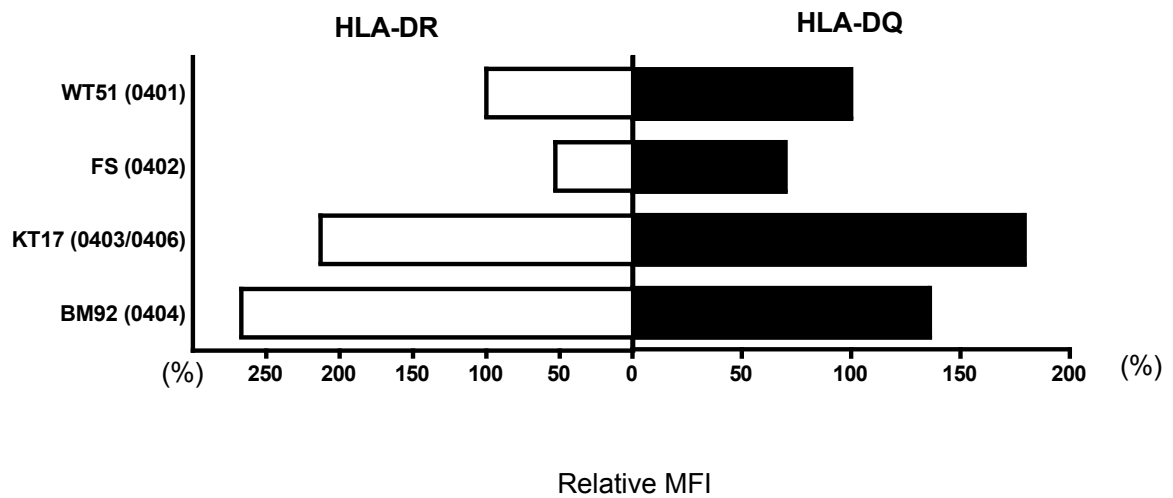
Figure 32. Relative abundance of HLA-DQ and HLA-DR expressed by B-LCLs.

Relative HLA-DQ (black filled bars) and HLA-DR (opened bars) expression level of human B cell lines. Mean fluorescence intensity of anti-HLA-DQ and anti-HLA-DR mAbs staining was normalized, with WT51 DQ and DR staining intensity as reference.
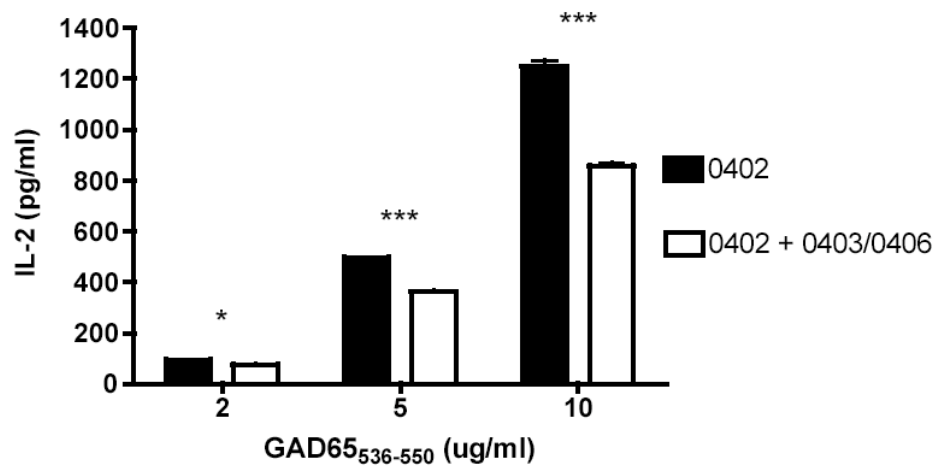
Figure 33. TH536.1 responses elicited by FS and FS/KT17 mixture

IL-2 produced by TH536 (20,000 cells/well) responding to DRB1*0402[+] FS (20,000 cells/well) was compared with the response to a "mixture" presenter -– DRB1*0402[+] FS (20,000 cells/well) plus extra DRB1*0403/0406[+] KT17 (10,000 cells/well).
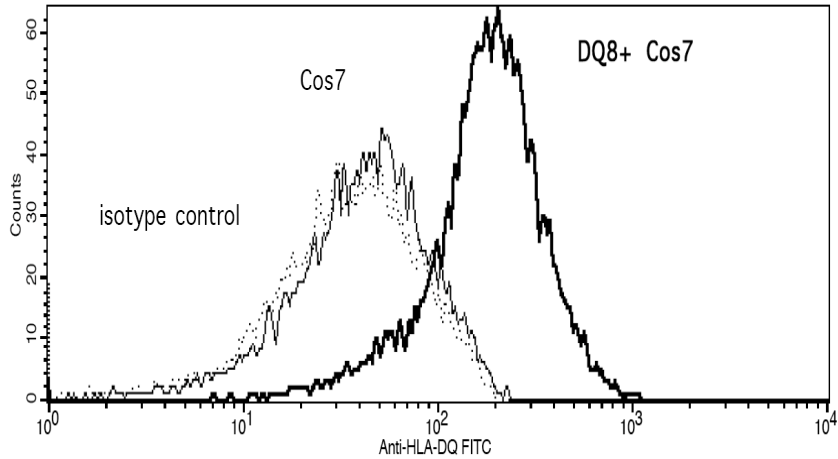
A
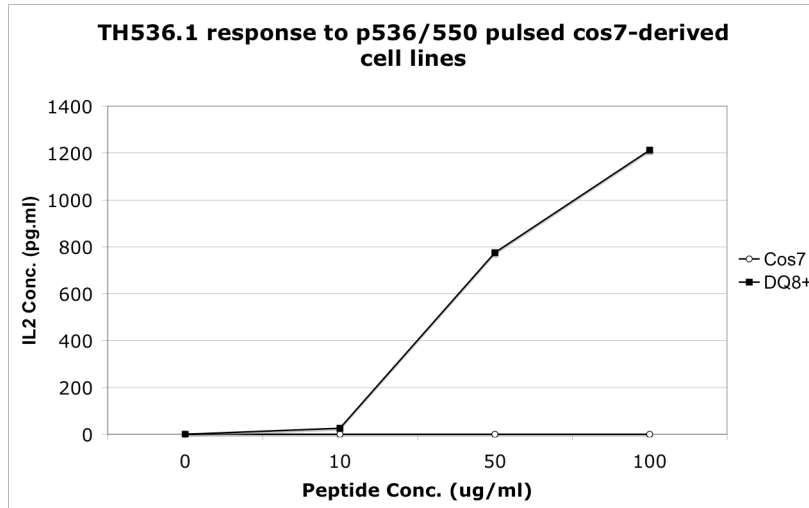
B

Figure 34. Expression and function of HLA-DQ8 in transfected COS7 cell line

(**A**) Histogram represents FITC-conjugated anti-HLA-DQ mAb staining results of HLA-DQ8-transfected COS7 clone -- DQ8#114 (thick line), and non-transfected COS7 (thin line). Dot line represents antibody isotype control. (**B**) IL-2 produced by TH536.1 hybridoma co-cultured with either DQ8#114 (DQ8$^+$) or COS7 cells in the presence of indicated amount of hGAD65$_{536-550}$, respectively.
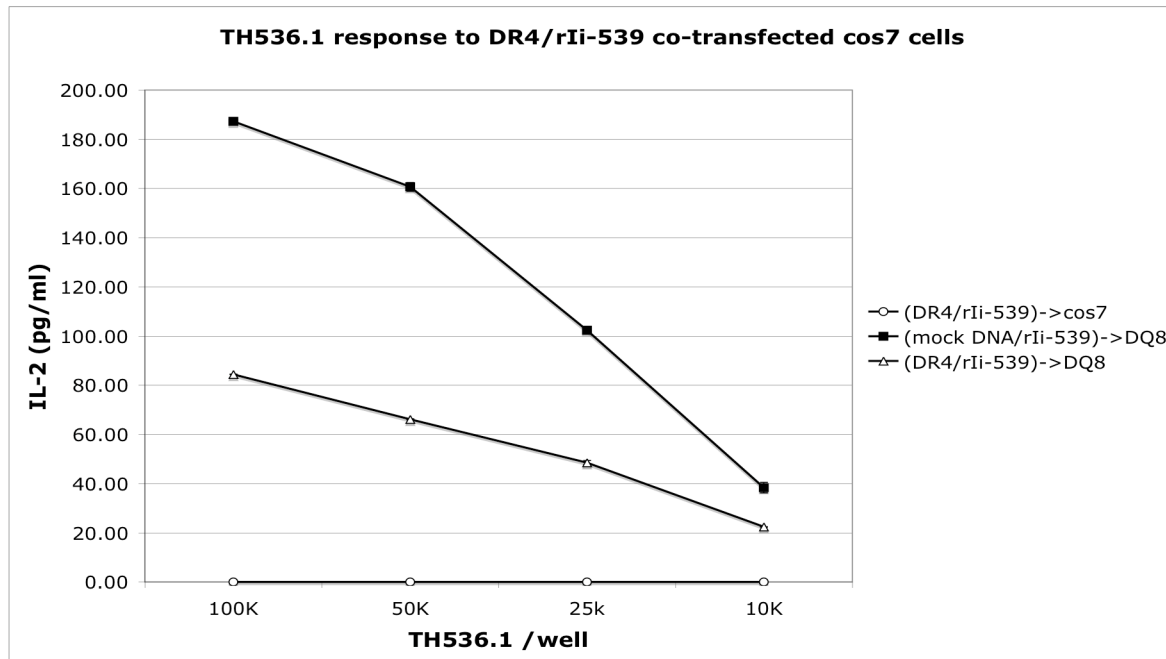
Figure 35. TH536.1 hybridoma responses elicited by endogenously synthesized peptide

IL-2 produced by indicated number of TH536.1 hybridoma in the presence of rIi-p539 transfected DQ8#114 (*(mock DNA/rIi-539)→DQ8*) or rIi-539/DR4 co-transfected DQ8#114 (*(DR4/rIi-539)→DQ8*). rIi-539 transfected DQ8⁻ COS7 (*(DR4/rIi-539)→COS7*) was applied as negative control.

5.0 DISCUSSION

This study addressed an important biological question, namely how certain HLA molecules modulate the disease risk conferred by other HLA molecules. HLA molecules under the investigation were HLA-DQ8 and HLA-DR4, the two most prevalent HLA Class II alleles found in Caucasian Type 1 Diabetes (T1D) patients.

The principle behind this study is that HLA molecules expressed from different alleles and/or loci compete with each other to bind peptides to form complexes driving T cell-mediated immune responses. Although Nepom proposed this model a decade ago (11), no experimental evidence has been shown since then to demonstrate the competition between DQ8 and DR4 molecules. One big obstacle was that the knowledge about DQ8-diabetogenic peptides was far from sufficient. Although autoantibodies against β-cell proteins such as insulin and GAD65 have been broadly used for many years to diagnose or predict the development of T1D, autoreactive T cell responses against β-cell antigens have not been clarified thoroughly, partially due to difficulties of obtaining replicable *in vitro* T cell assay results, partially due to the complexity of human HLA system (people differing from each other for their HLA haplotypes). In addition, distinct strategies (such as insect cell expression systems or bacterial expression systems) of recombinant protein (of candidate β-cell autoantigen pareparations) for *in vitro* T cell assays generates unexpectedly variability between different labs (162). Another obstacle was the co-expression of closely linked DQ and DR in human antigen presenting cells so that it was nearly impossible to dissect the role of DQ from DR. At the end, it was still not an easy task to have a reliable readout system that was sensitive enough to detect the peptide competition.

We thus decided to develop an experimental system to circumvent these barriers to test this hypothesis. The approach taken was to generate T cells as reagents. This was accomplished

by immunizing HLA-DQ8 transgenic mice *in vivo* with GAD65-derived peptides. As in this transgenic strain, human HLA-DQ8 was the only functional MHC Class II molecule, all CD4 T cell responses were restricted to DQ8. It hence allowed us to dissect the effect of DR4 from the effect of DQ8. GAD65-derived peptides used in this study were identified as DQ8-restricted T epitopes from a previous study, in which a similar HLA-DQ8 transgenic mouse system was used (154). Although there was no direct evidence to demonstrate that these peptides were diabetogenic, they were found to be the strongest binding peptides (to DQ8) derived from GAD65 – one of the most important autoantigens in human T1D. Having obtained a panel of CD4 T cell lines, we further confirmed that these T cell lines were not cross-reactive with DR4 molecules. Therefore, these T cell reagents were qualified as readout systems to evaluate cognate peptide occupancy of HLA-DQ8 on various antigen presenting cell surfaces including $DQ8^+DR4^-$ and $DQ8^+DR4^+$ APCs. When HLA-DR4 was co-expressed with DQ8, there was a reduction in T cell response, which indicated a reduction in peptide/DQ8 occupancy.

Unlike traditional approaches studying the dissociation rate of purified MHC molecules and labeled peptide, we didn't directly examine the affinity between the peptide and MHC molecules. However, we addressed the event of antigen presentation that occurred on the cell surface, a scenario being more similar to what happens in the immune system than in a "cell-free" system (binding between purified MHC and labeled peptide). In the "cell-free" system, purified protein is dissolved in the solution that not only contains special detergents allowing the protein to fold into a proper conformation, but also has a pH and ion strength environment preventing the protein from aggregation. However, these *in vitro* conditions are still very different from the condition on the cell surface and intracellular vesicles such as late endosome where peptides interacted with HLA/MHC Class II molecules. In the solution, either DQ8 or DR4 might fold into a conformation slightly different from their original conformation on the cell surface. Then is it unambiguous enough to compare the affinity of a peptide to DQ8 with the affinity of the same peptide to DR4? Actually, the relative affinity of a peptide binding to a MHC Class II molecule is characterized by the IC_{50} value, which represents the concentration of a tested peptide required to replace 50 % of labeled reference peptide occupancy. The IC_{50} value is thus heavily dependent on the affinity of reference peptide and tested MHC Class II. Apparently, reference peptides for DQ8 and DR4 are very different. It was thus not practical to normalize the

binding between DQ8 and a peptide to the binding between DR4 and the same peptide. Therefore, the cell-free peptide/MHC binding system does not serve our purpose very well.

Since the peptide competition theory is based on the premise that peptides are binding to HLA-DR4, it is essential to show that DR4 could bind the candidate peptides. Wicker et al previously reported that some GAD65 derived peptides, including GAD65$_{201-220}$ and GAD65$_{531-550}$, were able to bind both DQ8 and DR4 (DRB1*0401) using an MHC Class II binding assay (150). Interestingly, these two 20-mers overlap with the peptides we used in this study (GAD65$_{206-220}$ and GAD65$_{536-550}$). The data from their "cell-free" protein binding assay provides chemical evidence that DR4 is able to bind the peptides (hGAD65$_{206-220}$ and hGAD65$_{536-550}$) that we used to generate DQ8-restricted CD4 T cell lines. In this study, this issue was addressed in an alternative approach. Instead of performing peptide binding assay as previously described (150), we showed the restimulation assay results of two distinct CD4 T cell lines, DQ8p206 and DR4p206 (**Figure 18C** and **Figure 25**). DQ8p206 only responded to the cognate peptide hGAD65$_{206-220}$ when it was presented by DQ8, whereas DQ4p206 only responded to hGAD65$_{206-220}$ when it was presented by DR4. The evidence from DR4p206 unambiguously demonstrated that DR4 was able to bind the same peptide, which was bound DQ8. Therefore, DR4 had intrinsic potential to compete for hGAD65$_{206-220}$ with DQ8.

We also used recombinant hGAD65 whole protein as the antigen for *in vitro* T cell assays. All DQ8-restricted CD4 T cell lines were tested and able to respond to hGAD65 in a recall assay at early stage of the study. Lately, however, these T cell lines surprisingly lost their responses to the same batch of hGAD65 whole protein. It is possible that the recombinant protein became modified and lost its predominant epitopes due to a suboptimal storing condition and was thus unable to be processed and presented onto the cell surface properly. The recombinant hGAD65 used in this study was expressed in sf9 cell (an insect cell line) using baculovirus expressing system, and was purified by Ni-NTA affinity column that bound the 6xHis tag on the C-terminal of recombinant protein. After being dialyzed into imidozale-free sodium phosphate buffer, the protein was concentrated and stored in the buffer at 4 ºC. After a few months, we observed that the protein solution started to be more and more "cloudy" and finally white precipitant was formed. By using SDS-PAGE, we found out that the white precipitant was

actually the aggregation of pure hGAD65 protein. Therefore, the spontaneous aggregation of the protein under 4 ºC might account for the loss of antigenesis. In addition, the reference indicates that oxidation is another modification during a long-term storage (163-165). It occurs most readily at methionine and cysteine residues as well as those that possess aromatic side-chains such as phenylalanine, histidine, tyrosine and tryptophan. It has been widely acknowledged that side-chains of amino acids are involved in the interaction between the peptide and HLA/MHC molecules. The modification of the side-chain might cause improper interaction to HLA/MHC molecules. It is noteworthy that the hGAD65$_{206-220}$ possesses a phenylalanine within the core region that is required for the binding, and hGAD65$_{536-550}$ possesses two tyrosine residues and a methionine within its core region. Thus, it was very likely that the oxidation modified side-chains of important amino acids involved in interacting with DQ8, including those that located within hGAD65$_{206-220}$ region and hGAD65$_{536-550}$ region and caused the loss of antigenesis of the protein.

Although in total we obtained five DQ8-restricted CD4 T cell lines, we only chose three of them –T206, T536.1 and T536.2 as reagents for further study. The major consideration was that these three T cell lines had low background responses in the absence of cognate peptide, and more important, the composition of these three cell lines was homogeneous (revealed by analyzing the usage of TCR β-chain). In contrast, another two lines DQ8p101 and DQ8p121 didn't serve these two criteria so well. Many different strategies could still be tried to improve the purity of cell lines, but we decided not to do it for time considerations. By having three homogeneous cell lines, we had sufficient confidence to accomplish the experiment and draw the conclusion from it, especially we had direct evidence that one of peptides hGAD65$_{206-220}$ was able to bind both DQ8 and DR4.

The consequence of peptide competition, revealed in our study as reduced IFN-γ production and reduced Th1 cell clonal expansion (**Figure 26B, 26C and 27B**), may explain the moderate insulitis, and reduced diabetes incidence observed in DQ8^{+}DR4^{+} transgenic mice, in comparison with DQ8^{+}DR4^{-} transgenic mice (10). As IFN-γ is responsible for immunopathogenesis at different stages of β-cell destruction (56), the variation of IFN-γ production influences: 1) antigen processing/presenting by controlling MHC Class I/II and co-

stimulatory molecule expression, 2) recruitment of other islet-reactive leukocytes by regulating the expression of adhesive molecules, chemokines and their receptors on endothelia, 3) β-cell apoptosis. The impact of IFN-γ is further synergized by clonal expansion. Thus, the diminished IFN-γ production, together with reduced Th1 cell expansion is relevant to interpret the regulatory role of DR4 to autoimmune diabetes susceptibility conferred by DQ8.

Two issues were raised when we designed the experiment to compare T cell responses elicited by $DQ8^+$ splenocytes *vs*. $DQ8^+DR4^+$ splenocytes. One issue concerned the expression level of DQ8 on the surface of antigen presenting cells from different sources. The copy number of the DQ8 transgene in experimental animals might have dose effect and determine DQ8 expression level. Therefore, it would be meaningless if we intended to test the hypothesis that the peptide occupancy of DQ8 was reduced in the presence of DR4 by using $DQ8^+DR4^+$ APCs with intrinsically lower DQ8 expression on the surface than $DQ8^+$ APCs. This issue was realized and circumvented by quantitatively examining a group of pups for both DQ8 and DR4 expression. Flow cytometry analysis revealed not only the frequency but also the (anti-HLA mAb staining) intensity of $DQ8^+$ cells. Accordingly, we could easily choose mice with similar DQ8 expression patterns as sources of APCs. A second issue concerned the presence of non-antigen presenting cells within splenocyte population. It was suspected that the number of $CD4^+CD25^+$ T cells – T_{reg} cells was different in splenocytes from different mice. We repeated the experiment using T cell-depleted splenocytes as APCs so that all possible T_{reg} cells, non-specific CD4, CD8 T cells (dead or alive) interference were removed from the system. Results were similar to what we presented in this thesis (**Figure 26B, 26C** and **26D**). Actually, the effect of T_{reg} cell was beyond the scope of the dissertation. The Treg cells were still mysterious with respects to how they were selected in the thymus, what their antigen specificity was about, how they obtained activation and how they suppressed other T cells. In addition, the experiment in this study used irradiated splenocytes as antigen presenting cells. Irradiation should disable T_{reg} cell activity (if there was any). Therefore, there was no strong reason that T_{reg} cells would confound our results.

Further evidence for peptide competition would be that the competition should be inhibited by DR4 blockade. An anti-HLA-DR monoclonal antibody was originally considered to serve this purpose. However, it was not clear whether antibody binding would affect peptides to

access the DR4 peptide binding site. In other words, anti-DR antibody would not necessary inhibit DR4 peptide binding. In addition, antibody only bound to DR4 molecules on the surface but not DR4 molecules located within intracellular vesicles Therefore, antibody blockade was not able to serve this purpose perfectly. Another choice was a peptide that had been demonstrated to bind only DR4 but not DQ8. As this blocking peptide shared similar molecular weight (9 to 15 amino acid residues) and conformation (linear conformation, without complicated secondary structure) with cognate peptide, they could access DR4 peptide binding sites as readily as cognate peptide. The outcome of peptide blockade was very clear (**Figure 28A, 28B**, and **28C**). By using as low as 2 ug/ml of blocking peptide, we observed the recovery of all three DQ8-restricted CD4 T cell responses. It implicated that this blocking peptide bound DR4 with higher priority than DQ8 cognate peptide. It also strongly supported our conclusion that the co-expression of DR4 competed for peptides with DQ8 and consequently diminished DQ8-restrcited T cell responses. Actually, the decision of choosing this particular peptide – hGAD65$_{554-566}$ as a blockade was based on binding affinity of DR4 with the peptide from a previous study (150). According to the same information from that study, we also chose another peptide – hGAD65$_{274-286}$ only binding to DR4 but not DQ8 to serve the blockade purpose. The result however was less supportive than blocking peptide hGAD65$_{554-566}$. We could only observe the recovery of DQ8-restricted T cell responses when high dose (>10 ug/ml) of hGAD65$_{274-286}$ blockade was applied. We then realized this second blocking peptide bound DR4 with lower affinity than the first blocking peptide. Increasing amount of blocking peptide was thus required to occupy DR4 binding groove effectively.

A surprising fact from previous studies trying to clone CD4 T cells from peripheral blood of T1D patients was that all T cells were restricted to DR4 instead of DQ8 (6). There were two issues related to the techniques for *in vitro* human T cell culturing that possibly generated this outcome. 1) Within the peripheral blood lymphocytes (PBL)—the primary source for *in vitro* T cell cloning, the frequency of DR4-restricted T cells was much higher than the frequency of DQ8-restricted T cells. 2) The protocol of cloning human T cells required autologus APCs that are normally obtained from the PBL of the same human subject where T cells came from. The APCs (mainly B cells) thus express DQ, DR and other HLA molecules. Therefore, both DR4-restricted T cells and DQ8-restricted T cells would have a chance to be activated and expand

upon antigen restimulation. At this point, the peptide competition demonstrated by our results might serve as another explanation of unsuccessful cloning of DQ8-restrcited T cells from human PBL. Under the competition of DR4, DQ8-restricted T cells would be in a disadvantage regarding the antigen sources required for their expansion. On the other hand, DR4-restricted T cells, with high starting frequencies, have many growth advantages over DQ8-restricted T cells. Accordingly, the peptide competition should be paid more attention in the efforts aimed to clone human DQ8-restricted T cells from human peripheral blood lymphocyte. For an instance, perhaps the addition of DR4 blockade peptide to block DR4 peptide binding site might increase the odds to obtain a DQ8-restricted T cell line.

Since we demonstrated that DR4 (0401) competed with DQ8 for the peptide, we further pursued the competition potential of other individual DR4 alleles. We believed that it extended our understanding to some subtle aspects of HLA genetics in T1D, saying the different T1D association of distinct DR4 subtypes (0401, 0402, 0403, 0404, 0405, and 0406) that also closely linked with DQ8 susceptible genes. DQ8-DR4 haplotypes with DRB1*0405, 0402, 0401, 0404, 0403 and 0406 were all associated with T1D but with decreased relative risk, in the order of 0405>0402>0401>0404>0403, 0406. The 0405, 0402 and 0401 haplotypes were still disease susceptible, while the 0404 haplotype was neutral and the 0403/0406 haplotype were disease resistant. A straightforward interpretation was that these DRB1*04 alleles had a variable affinity for same diabetogenic peptides that bound DQ8 in T1D. However, relative affinities for peptide binding were in the order of 0405<0402<0401<0404<0403, 0406. In this way, DRB1*0403 or 0406 manifested the strongest competition capacity with DQ8 for diabetogenic peptides and was able to maximally diminish DQ8-restricted autoreactive T cell responses. Therefore, the DQ8-DRB1*0403/0406 haplotype were disease resistant, in comparison with other DQ8-DRB1*04 haplotypes. On the other hand, DRB1*0401 only manifested an intermediate level of competition potential and was still able to diminish DQ8-restricted autoreactive T cell responses, but the effect was weaker than that of DRB1*0403/0406 alleles. As for the DRB1*0405 and 0402, these two alleles probably had the weakest competition capacity for diabetogenic peptides and were not able to affect DQ8-restricted autoreactive T cell responses at all. Therefore, DQ8-DRB1*0405 and DQ8-DRB1*0402 haplotypes were associated with T1D with the highest risk. Our results didn't show relative affinities of this panel of DR4 subtypes to peptide hGAD65$_{209-217}$

or hGAD65$_{536-550}$ because we didn't have the intention to express/purify all these HLA-DR4 molecules in a great amount and make them re-fold into an appropriate conformation so that the direct peptide binding assay could be applied. However, we addressed this question in a simple alternative way – showing effects of this panel of DRB1*04 alleles to DQ8-restricted T cell responses. Results were quite consistent with what was assumed under the hypothesis of the peptide competition model (**Figure 31A, 31B,** and **31C**). All three T hybridoma responses elicited by a panel of B cells carrying different DQ8-DRB1*04 haplotypes were in the order of 0402 >0401>0404>0403/0406. For the KT17—the B cell expressing DRB1*0403/0406, it always needed as much as 5 to 10-fold more peptide to induce a T cell response equivalent to that induced by another B cell line – FS that expressed DRB1*0402. It indirectly suggested that 0403/0406 was much more capable of competing for peptides than 0402 allele. It has been widely discussed by many previous reports about the association between polymorphisms within the peptide binding groove and relative risk to T1D. Variable degrees of protection conferred by distinct DRB1*04 alleles were primarily determined by amino acid sequences within peptide binding grooves. According to the sequence alignment shown in (**Figure 29**), it was clear that amino acid differences among distinct DRB1*04 alleles rendered each individual allele a distinct peptide binding capability that could be correlated with their different peptide competition potentials. It gave the explanation at the level of molecular structures to support what we observed in our T hybridoma assay.

Unable to obtain a B cell line homozygously expressing DQ8-DRB1*0405 haplotype made our study a little bit less ideal. As all B cell lines used in this study and many other antigen presenting studies were obtained from EBV-transformed human PBL B cell, the availability of a B cell line expressing a desirable haplotype was depending on the availability of such a haplotype in general population. DRB1*0405 was actually a rare allele and was only relatively enriched in *Sardinia, Italy*. We contacted investigators in *Sardinia* who most possibly had DRB1*0405$^+$ patient blood samples. Unfortunately, a DQ8-DRB*0405 homozygous sample was still not available.

It is noteworthy that our results were obtained from *in vitro* T cell assays using activated/effector T cells to evaluate peptide occupancy. The decreased T cell responses caused

by peptide competition implied more profound biological significance under in vivo situations, where the autoantigen resource was limited, the frequency of autoreactive T cell was low, and most T cells expressed naïve phenotypes. Mature/effector T cells and naïve/immature T cells have been known to be different regarding the requirements for activation. For the naïve T cells, the quantity of TCR:peptide:DQ8 engagement had to reach a threshold (~8,000 TCR/cell) to obtain activation, otherwise, these autoreactive T cells are "silenced" or anergic (124, 166). Although co-stimulation lowers the requirement to one fifth as great, the number of available self-peptide:DQ8 complex on the APCs is still a crucial parameter to direct naïve autoreactive T cells to differentiate into harmful effector Th1 cells, or become nonresponsive. It was more critical for the cells that naturally have lower TCR numbers. They might require an unattainably high concentration of antigen to engage enough TCRs for a "successful" activation. Indeed, T cells that escaped thymic selection with potentially autoreactive TCRs often intrinsically had a lower TCR density on their surface (167).

There was no doubt that the expression of DR4 MHC Class II directed positive selection of TCRs with novel specificities, and some of those might potentially recognized islet antigen derived peptides. Whether those DR4-restricted CD4 T cells regulated DQ8-restricted autoreactive T cells *via* secreting "protective" Th2 cytokines such as IL4/IL-10, or whether some of those DR4-restricted T cells developed into T_{reg} cells, was not addressed in this experimental model.

Our observations provided *in vitro* evidence for peptide competition as an explanation of the modulatory role of DR4 in the T cell response to diabetes related autoantigens. Our T cell response data was consistent to the hierarchical association of different DQ8-DRB1*04 haplotypes with T1D susceptibility by bridging protein structure studies with genetic analysis. In addition, the TCR information we obtained from re-cloned hybridomas might help us develop an *in vivo* model to investigate the regulatory role of the DR4 to DQ8 restricted T cell response. Considering the DQ8-DR4 was the most prevalent haplotype in the Caucasian T1D population, the efforts to increase the regulatory effect, particularly in the prediabetic or earlier stages might provide novel therapeutic strategies to interfere with autoimmune progression.

6.0   CONCLUSION

1. **HLA-DQ8 and HLA-DR4 are able to bind the same peptides, including peptides derived from putative autoantigens of T1D such as GAD65**

2. **The presence of HLA-DR4 reduces DQ8-peptide occupancy.**

3. **The outcome of the peptide competition diminishes Th1 cell responses regarding both cytokine production and proliferation, whereas it has less effect to Th2 responses.**

4. **The polymorphisms within peptide binding sites of different DR4 alleles are associated to variable peptide competition capacities.**

5. **DR4 also competes with DQ8 for peptides within the intracellular compartment.**

BIBLIOGRAPHY

1. DeFranco A, Howard J, Janeway CA, Littman D, Marrack P, Mitchison NA, Neuberger M, Paul WE, Rajewsky K, S. R, and T. P. 2002. The Adaptive Immune System. In *Molecular Biology of the Cell*, Vol. chapter 24. J. A. Alberts B, Lewis J, Raff M, Roberts K, Walter P, ed. Garland Publishing, New York.

2. Bach, J. F. 1994. Insulin-dependent diabetes mellitus as an autoimmune disease. *Endocr Rev 15:516*.

3. Castano, L., and G. S. Eisenbarth. 1990. Type-I diabetes: a chronic autoimmune disease of human, mouse, and rat. *Annu Rev Immunol 8:647*.

4. Todd, J. A., J. I. Bell, and H. O. McDevitt. 1987. HLA-DQ beta gene contributes to susceptibility and resistance to insulin-dependent diabetes mellitus. *Nature 329:599*.

5. Morel, P. A., J. S. Dorman, J. A. Todd, H. O. McDevitt, and M. Trucco. 1988. Aspartic acid at position 57 of the HLA-DQ beta chain protects against type I diabetes: a family study. *Proc Natl Acad Sci U S A 85:8111*.

6. Sonderstrup, G., and H. O. McDevitt. 2001. DR, DQ, and you: MHC alleles and autoimmunity. *J Clin Invest 107:795*.

7. Trucco, M. 1992. To be or not to be Asp 57, that is the question. *Diabetes Care 15:705*.

8. Undlien, D. E., T. Friede, H. G. Rammensee, G. Joner, K. Dahl-Jorgensen, O. Sovik, H. E. Akselsen, I. Knutsen, K. S. Ronningen, and E. Thorsby. 1997. HLA-encoded genetic predisposition in IDDM: DR4 subtypes may be associated with different degrees of protection. *Diabetes 46:143*.

9. Cucca, F., R. Lampis, F. Frau, D. Macis, E. Angius, P. Masile, M. Chessa, P. Frongia, M. Silvetti, A. Cao, and et al. 1995. The distribution of DR4 haplotypes in Sardinia suggests a primary association of type I diabetes with DRB1 and DQB1 loci. *Hum Immunol 43:301*.

10. Wen, L., N. Y. Chen, J. Tang, R. Sherwin, and F. S. Wong. 2001. The regulatory role of DR4 in a spontaneous diabetes DQ8 transgenic model. *J Clin Invest 107:871*.

11. Nepom, G. T. 1990. A unified hypothesis for the complex genetics of HLA associations with IDDM. *Diabetes 39:1153*.

12. Sakamoto, K., Brownlee, M. 2003. Biochemistry and Molecular Biology of Diabetes Complications. In *Type 1 Diabetes: Etiology and Treatment*. M. Sperling, ed. Human Press, Inc., Totowa, p. 375.

13. Ruderman, N. B., J. R. Williamson, and M. Brownlee. 1992. Glucose and diabetic vascular disease. *Faseb J 6:2905*.

14. Skyler, J. 1996. Diabetic complications: the importance of glucose control. In *Endocrinol Metab Clin North Am*, Vol. 25. K. G. Brownlee MB, ed. WB Saunders, Philadelphia, p. 243.

15. Lampeter, E. F., M. Homberg, K. Quabeck, P. Werner, F. A. Gries, and H. Kolb. 1993. [Accidental transmission of type-1 diabetes mellitus with HLA-identical bone marrow]. *Med Klin (Munich) 88:272*.

16. Lampeter, E. F., M. Homberg, K. Quabeck, U. W. Schaefer, P. Wernet, J. Bertrams, H. Grosse-Wilde, F. A. Gries, and H. Kolb. 1993. Transfer of insulin-dependent diabetes between HLA-identical siblings by bone marrow transplantation. *Lancet 341:1243*.

17. Mathews, C. E. 2005. Utility of murine models for the study of spontaneous autoimmune type 1 diabetes. *Pediatr Diabetes 6:165*.

18. Makino, S., K. Kunimoto, Y. Muraoka, Y. Mizushima, K. Katagiri, and Y. Tochino. 1980. Breeding of a non-obese, diabetic strain of mice. *Jikken Dobutsu 29:1*.

19. Jarpe, A. J., M. R. Hickman, J. T. Anderson, W. E. Winter, and A. B. Peck. 1990. Flow cytometric enumeration of mononuclear cell populations infiltrating the islets of Langerhans in prediabetic NOD mice: development of a model of autoimmune insulitis for type I diabetes. *Reg Immunol 3:305*.

20. Miyazaki, A., T. Hanafusa, K. Yamada, J. Miyagawa, H. Fujino-Kurihara, H. Nakajima, K. Nonaka, and S. Tarui. 1985. Predominance of T lymphocytes in pancreatic islets and spleen of pre-diabetic non-obese diabetic (NOD) mice: a longitudinal study. *Clin Exp Immunol 60:622*.

21. Faveeuw, C., M. C. Gagnerault, and F. Lepault. 1995. Isolation of leukocytes infiltrating the islets of Langerhans of diabetes-prone mice for flow cytometric analysis. *J Immunol Methods 187:163*.

22. Christianson, S. W., L. D. Shultz, and E. H. Leiter. 1993. Adoptive transfer of diabetes into immunodeficient NOD-scid/scid mice. Relative contributions of CD4+ and CD8+ T-cells from diabetic versus prediabetic NOD.NON-Thy-1a donors. *Diabetes 42:44*.

23. Matsumoto, M., H. Yagi, K. Kunimoto, J. Kawaguchi, S. Makino, and M. Harada. 1993. Transfer of autoimmune diabetes from diabetic NOD mice to NOD athymic nude mice: the roles of T cell subsets in the pathogenesis. *Cell Immunol 148:189*.

24. Miller, B. J., M. C. Appel, J. J. O'Neil, and L. S. Wicker. 1988. Both the Lyt-2+ and L3T4+ T cell subsets are required for the transfer of diabetes in nonobese diabetic mice. *J Immunol 140:52*.

25. Serreze, D. V., H. D. Chapman, D. S. Varnum, I. Gerling, E. H. Leiter, and L. D. Shultz. 1997. Initiation of autoimmune diabetes in NOD/Lt mice is MHC class I-dependent. *J Immunol 158:3978*.

26. Falcone, M., J. Lee, G. Patstone, B. Yeung, and N. Sarvetnick. 1998. B lymphocytes are crucial antigen-presenting cells in the pathogenic autoimmune response to GAD65 antigen in nonobese diabetic mice. *J Immunol 161:1163*.

27. Noorchashm, H., Y. K. Lieu, N. Noorchashm, S. Y. Rostami, S. A. Greeley, A. Schlachterman, H. K. Song, L. E. Noto, A. M. Jevnikar, C. F. Barker, and A. Naji. 1999. I-Ag7-mediated antigen presentation by B lymphocytes is critical in overcoming a checkpoint in T cell tolerance to islet beta cells of nonobese diabetic mice. *J Immunol 163:743*.

28. Feutren, G., L. Papoz, R. Assan, B. Vialettes, G. Karsenty, P. Vexiau, H. Du Rostu, M. Rodier, J. Sirmai, A. Lallemand, and et al. 1986. Cyclosporin increases the rate and

length of remissions in insulin-dependent diabetes of recent onset. Results of a multicentre double-blind trial. *Lancet 2:119*.

29. The Canadian-European Randomized Control Trial Group. 1988. Cyclosporin-induced remission of IDDM after early intervention. Association of 1 yr of cyclosporin treatment with enhanced insulin secretion. *Diabetes 37:1574*.

30. Carroll, P. B., A. G. Tzakis, C. Ricordi, H. R. Rilo, K. Abu-Elmagd, N. Murase, Y. J. Zeng, R. Alejandro, D. Mintz, and T. E. Starzl. 1991. The use of FK 506 in new-onset type I diabetes in man. *Transplant Proc 23:3351*.

31. Secchi, A., M. R. Pastore, A. Sergi, A. E. Pontiroli, and G. Pozza. 1990. Prednisone administration in recent onset type I diabetes. *J Autoimmun 3:593*.

32. Cook, J. J., I. Hudson, L. C. Harrison, B. Dean, P. G. Colman, G. A. Werther, G. L. Warne, and J. M. Court. 1989. Double-blind controlled trial of azathioprine in children with newly diagnosed type I diabetes. *Diabetes 38:779*.

33. Herold, K. C., W. Hagopian, J. A. Auger, E. Poumian-Ruiz, L. Taylor, D. Donaldson, S. E. Gitelman, D. M. Harlan, D. Xu, R. A. Zivin, and J. A. Bluestone. 2002. Anti-CD3 monoclonal antibody in new-onset type 1 diabetes mellitus. *N Engl J Med 346:1692*.

34. Bottazzo, G. F., A. Florin-Christensen, and D. Doniach. 1974. Islet-cell antibodies in diabetes mellitus with autoimmune polyendocrine deficiencies. *Lancet 2:1279*.

35. Baekkeskov, S., H. J. Aanstoot, S. Christgau, A. Reetz, M. Solimena, M. Cascalho, F. Folli, H. Richter-Olesen, and P. De Camilli. 1990. Identification of the 64K autoantigen in insulin-dependent diabetes as the GABA-synthesizing enzyme glutamic acid decarboxylase. *Nature 347:151*.

36. Atkinson, M. A., D. L. Kaufman, L. Campbell, K. A. Gibbs, S. C. Shah, D. F. Bu, M. G. Erlander, A. J. Tobin, and N. K. Maclaren. 1992. Response of peripheral-blood mononuclear cells to glutamate decarboxylase in insulin-dependent diabetes. *Lancet 339:458*.

37. Honeyman, M. C., D. S. Cram, and L. C. Harrison. 1993. Glutamic acid decarboxylase 67-reactive T cells: a marker of insulin-dependent diabetes. *J Exp Med 177:535*.

38. Rudy, G., N. Stone, L. C. Harrison, P. G. Colman, P. McNair, V. Brusic, M. B. French, M. C. Honeyman, B. Tait, and A. M. Lew. 1995. Similar peptides from two beta cell autoantigens, proinsulin and glutamic acid decarboxylase, stimulate T cells of individuals at risk for insulin-dependent diabetes. *Mol Med 1:625*.

39. Alleva, D. G., P. D. Crowe, L. Jin, W. W. Kwok, N. Ling, M. Gottschalk, P. J. Conlon, P. A. Gottlieb, A. L. Putnam, and A. Gaur. 2001. A disease-associated cellular immune response in type 1 diabetics to an immunodominant epitope of insulin. *J Clin Invest 107:173*.

40. Congia, M., S. Patel, A. P. Cope, S. De Virgiliis, and G. Sonderstrup. 1998. T cell epitopes of insulin defined in HLA-DR4 transgenic mice are derived from preproinsulin and proinsulin. *Proc Natl Acad Sci U S A 95:3833*.

41. Kaufman, D. L., M. Clare-Salzler, J. Tian, T. Forsthuber, G. S. Ting, P. Robinson, M. A. Atkinson, E. E. Sercarz, A. J. Tobin, and P. V. Lehmann. 1993. Spontaneous loss of T-cell tolerance to glutamic acid decarboxylase in murine insulin-dependent diabetes. *Nature 366:69*.

42. Tisch, R., X. D. Yang, S. M. Singer, R. S. Liblau, L. Fugger, and H. O. McDevitt. 1993. Immune response to glutamic acid decarboxylase correlates with insulitis in non-obese diabetic mice. *Nature 366:72*.

43. Lieberman, S. M., and T. P. DiLorenzo. 2003. A comprehensive guide to antibody and T-cell responses in type 1 diabetes. *Tissue Antigens 62:359*.

44. Trudeau, J. D., J. P. Dutz, E. Arany, D. J. Hill, W. E. Fieldus, and D. T. Finegood. 2000. Neonatal beta-cell apoptosis: a trigger for autoimmune diabetes? *Diabetes 49:1*.

45. Finegood, D. T., L. Scaglia, and S. Bonner-Weir. 1995. Dynamics of beta-cell mass in the growing rat pancreas. Estimation with a simple mathematical model. *Diabetes 44:249*.

46. Scaglia, L., C. J. Cahill, D. T. Finegood, and S. Bonner-Weir. 1997. Apoptosis participates in the remodeling of the endocrine pancreas in the neonatal rat. *Endocrinology 138:1736*.

47. Petrik, J., E. Arany, T. J. McDonald, and D. J. Hill. 1998. Apoptosis in the pancreatic islet cells of the neonatal rat is associated with a reduced expression of insulin-like growth factor II that may act as a survival factor. *Endocrinology 139:2994*.

48. Meier, P., A. Finch, and G. Evan. 2000. Apoptosis in development. *Nature 407:796*.

49. Mayor, F., and J. M. Cuezva. 1985. Hormonal and metabolic changes in the perinatal period. *Biol Neonate 48:185*.

50. Tisch, R., and H. McDevitt. 1996. Insulin-dependent diabetes mellitus. *Cell 85:291*.

51. Bach, J. F., and D. Mathis. 1997. The NOD mouse. *Res Immunol 148:285*.

52. Amrani, A., J. Verdaguer, B. Anderson, T. Utsugi, S. Bou, and P. Santamaria. 1999. Perforin-independent beta-cell destruction by diabetogenic CD8(+) T lymphocytes in transgenic nonobese diabetic mice. *J Clin Invest 103:1201*.

53. Chervonsky, A. V., Y. Wang, F. S. Wong, I. Visintin, R. A. Flavell, C. A. Janeway, Jr., and L. A. Matis. 1997. The role of Fas in autoimmune diabetes. *Cell 89:17*.

54. Kagi, D., B. Odermatt, P. Seiler, R. M. Zinkernagel, T. W. Mak, and H. Hengartner. 1997. Reduced incidence and delayed onset of diabetes in perforin-deficient nonobese diabetic mice. *J Exp Med 186:989*.

55. Kagi, D., B. Odermatt, P. S. Ohashi, R. M. Zinkernagel, and H. Hengartner. 1996. Development of insulitis without diabetes in transgenic mice lacking perforin-dependent cytotoxicity. *J Exp Med 183:2143*.

56. Boehm, U., T. Klamp, M. Groot, and J. C. Howard. 1997. Cellular responses to interferon-gamma. *Annu Rev Immunol 15:749*.

57. Dorman JS, L. R., Songer TJ. 2003. Epidemiology of Type 1 Diabetes. In *Type 1 Diabetes: Etiology and Treatment*. M. Sperling, ed. Human Press, Inc., Totowa, p. 3.

58. Warram, J. H., A. S. Krolewski, M. S. Gottlieb, and C. R. Kahn. 1984. Differences in risk of insulin-dependent diabetes in offspring of diabetic mothers and diabetic fathers. *N Engl J Med 311:149*.

59. Wagener, D. K., J. M. Sacks, R. E. LaPorte, and J. M. Macgregor. 1982. The Pittsburgh study of insulin-dependent diabetes mellitus. Risk for diabetes among relatives of IDDM. *Diabetes 31:136*.

60. Bleich, D., M. Polak, G. S. Eisenbarth, and R. A. Jackson. 1993. Decreased risk of type I diabetes in offspring of mothers who acquire diabetes during adrenarchy. *Diabetes 42:1433*.

61. Warram, J. H., A. S. Krolewski, and C. R. Kahn. 1988. Determinants of IDDM and perinatal mortality in children of diabetic mothers. *Diabetes 37:1328*.

62. WHO Multinational Project for Childhood Diabetes Group. Familial insulin-dependent diabetes mellitus (IDDM) epidemiology: standardization of data for the DIAMOND project. WHO Bull 1991. *69:767.*

63. The Eurodiab Ace Study Group and The Eurodiab Ace Substudy 2 Study Group. 1998.Familial risk of type I diabetes in European children. *Diabetologia 41:1151.*

64. Redondo, M. J., M. Rewers, L. Yu, S. Garg, C. C. Pilcher, R. B. Elliott, and G. S. Eisenbarth. 1999. Genetic determination of islet cell autoimmunity in monozygotic twin, dizygotic twin, and non-twin siblings of patients with type 1 diabetes: prospective twin study. *Bmj 318:698.*

65. Smink, L. J., E. M. Helton, B. C. Healy, C. C. Cavnor, A. C. Lam, D. Flamez, O. S. Burren, Y. Wang, G. E. Dolman, D. B. Burdick, V. H. Everett, G. Glusman, D. Laneri, L. Rowen, H. Schuilenburg, N. M. Walker, J. Mychaleckyj, L. S. Wicker, D. L. Eizirik, J. A. Todd, and N. Goodman. 2005. T1DBase, a community web-based resource for type 1 diabetes research. *Nucleic Acids Res 33:D544.*

66. Concannon, P., H. A. Erlich, C. Julier, G. Morahan, J. Nerup, F. Pociot, J. A. Todd, and S. S. Rich. 2005. Type 1 diabetes: evidence for susceptibility loci from four genome-wide linkage scans in 1,435 multiplex families. *Diabetes 54:2995.*

67. Rich, S. S. 1990. Mapping genes in diabetes. Genetic epidemiological perspective. *Diabetes 39:1315.*

68. Arnheim, N., C. Strange, and H. Erlich. 1985. Use of pooled DNA samples to detect linkage disequilibrium of polymorphic restriction fragments and human disease: studies of the HLA class II loci. *Proc Natl Acad Sci U S A 82:6970.*

69. Nerup, J., P. Platz, O. O. Andersen, M. Christy, J. Lyngsoe, J. E. Poulsen, L. P. Ryder, L. S. Nielsen, M. Thomsen, and A. Svejgaard. 1974. HLA antigens and diabetes mellitus. *Lancet 2:864.*

70. Cudworth, A. G., and J. C. Woodrow. 1976. Genetic susceptibility in diabetic identical twins. *Lancet 1:518.*

71. Platz, P., B. K. Jakobsen, N. Morling, L. P. Ryder, A. Svejgaard, M. Thomsen, M. Christy, H. Kromann, J. Benn, J. Nerup, A. Green, and M. Hauge. 1981. HLA-D and -DR antigens in genetic analysis of insulin dependent diabetes mellitus. *Diabetologia 21:108.*

72. Barbosa, J., M. M. Chern, N. Reinsmoen, H. Noreen, R. Ramsey, and L. Greenberg. 1979. HLA-Dw antigens in unrelated juvenile, insulin-dependent diabetics. *Tissue Antigens 14:426.*

73. Sachs, J. A., A. G. Cudworth, D. Jaraquemada, A. N. Gorsuch, and H. Festenstein. 1980. Type 1 diabetes and the HLA-D locus. *Diabetologia 18:41.*

74. Khalil, I., L. d'Auriol, M. Gobet, L. Morin, V. Lepage, I. Deschamps, M. S. Park, L. Degos, F. Galibert, and J. Hors. 1990. A combination of HLA-DQ beta Asp57-negative and HLA DQ alpha Arg52 confers susceptibility to insulin-dependent diabetes mellitus. *J Clin Invest 85:1315.*

75. Acha-Orbea, H., and H. O. McDevitt. 1987. The first external domain of the nonobese diabetic mouse class II I-A beta chain is unique. *Proc Natl Acad Sci U S A 84:2435.*

76. Kanagawa, O., B. A. Vaupel, G. Xu, E. R. Unanue, and J. D. Katz. 1998. Thymic positive selection and peripheral activation of islet antigen-specific T cells: separation of two diabetogenic steps by an I-A(g7) class II MHC beta-chain mutant. *J Immunol 161:4489.*

77. Endl, J., H. Otto, G. Jung, B. Dreisbusch, F. Donie, P. Stahl, R. Elbracht, G. Schmitz, E. Meinl, M. Hummel, A. G. Ziegler, R. Wank, and D. J. Schendel. 1997. Identification of naturally processed T cell epitopes from glutamic acid decarboxylase presented in the context of HLA-DR alleles by T lymphocytes of recent onset IDDM patients. *J Clin Invest 99:2405*.

78. Molvig, J., G. Sonderstrup McDevitt, M. Thomsen, B. Bosmann, C. Blangero, C. de Preval, L. Baek, and J. Nerup. 1989. Characterization of PPD-specific T-cell lines generated in type I (insulin-dependent) diabetic and healthy individuals. *Scand J Immunol 30:615*.

79. Kent, S. C., Y. Chen, L. Bregoli, S. M. Clemmings, N. S. Kenyon, C. Ricordi, B. J. Hering, and D. A. Hafler. 2005. Expanded T cells from pancreatic lymph nodes of type 1 diabetic subjects recognize an insulin epitope. *Nature 435:224*.

80. Hattori, M., J. B. Buse, R. A. Jackson, L. Glimcher, M. E. Dorf, M. Minami, S. Makino, K. Moriwaki, H. Kuzuya, H. Imura, and et al. 1986. The NOD mouse: recessive diabetogenic gene in the major histocompatibility complex. *Science 231:733*.

81. Hanson, M. S., M. Cetkovic-Cvrlje, V. K. Ramiya, M. A. Atkinson, N. K. Maclaren, B. Singh, J. F. Elliott, D. V. Serreze, and E. H. Leiter. 1996. Quantitative thresholds of MHC class II I-E expressed on hemopoietically derived antigen-presenting cells in transgenic NOD/Lt mice determine level of diabetes resistance and indicate mechanism of protection. *J Immunol 157:1279*.

82. Bell, G. I., J. H. Karam, and W. J. Rutter. 1981. Polymorphic DNA region adjacent to the 5' end of the human insulin gene. *Proc Natl Acad Sci U S A 78:5759*.

83. Owerbach, D., and J. Nerup. 1982. Restriction fragment length polymorphism of the insulin gene in diabetes mellitus. *Diabetes 31:275*.

84. Vafiadis, P., S. T. Bennett, J. A. Todd, J. Nadeau, R. Grabs, C. G. Goodyer, S. Wickramasinghe, E. Colle, and C. Polychronakos. 1997. Insulin expression in human thymus is modulated by INS VNTR alleles at the IDDM2 locus. *Nat Genet 15:289*.

85. Pugliese, A., M. Zeller, A. Fernandez, Jr., L. J. Zalcberg, R. J. Bartlett, C. Ricordi, M. Pietropaolo, G. S. Eisenbarth, S. T. Bennett, and D. D. Patel. 1997. The insulin gene is transcribed in the human thymus and transcription levels correlated with allelic variation at the INS VNTR-IDDM2 susceptibility locus for type 1 diabetes. *Nat Genet 15:293*.

86. Diabetes Epidemiology Research International Group. 1988. Geographic patterns of childhood insulin-dependent diabetes mellitus. *Diabetes 37:1113*.

87. Patrick, S. L., C. S. Moy, and R. E. LaPorte. 1989. The world of insulin-dependent diabetes mellitus: what international epidemiologic studies reveal about the etiology and natural history of IDDM. *Diabetes Metab Rev 5:571*.

88. Menser, M. A., J. M. Forrest, and R. D. Bransby. 1978. Rubella infection and diabetes mellitus. *Lancet 1:57*.

89. Yoon, J. W. 1991. Role of viruses in the pathogenesis of IDDM. *Ann Med 23:437*.

90. Yoon, J. W., M. Austin, T. Onodera, and A. L. Notkins. 1979. Isolation of a virus from the pancreas of a child with diabetic ketoacidosis. *N Engl J Med 300:1173*.

91. King, M. L., D. Bidwell, A. Voller, J. Bryant, and J. E. Banatvala. 1983. Role of Coxsackie B viruses in insulin-dependent diabetes mellitus. *Lancet 2:915*.

92. King, M. L., A. Shaikh, D. Bidwell, A. Voller, and J. E. Banatvala. 1983. Coxsackie-B-virus-specific IgM responses in children with insulin-dependent (juvenile-onset; type I) diabetes mellitus. *Lancet 1:1397*.

93. Conrad, B., E. Weidmann, G. Trucco, W. A. Rudert, R. Behboo, C. Ricordi, H. Rodriquez-Rilo, D. Finegold, and M. Trucco. 1994. Evidence for superantigen involvement in insulin-dependent diabetes mellitus aetiology. *Nature 371:351.*

94. Karjalainen, J., J. M. Martin, M. Knip, J. Ilonen, B. H. Robinson, E. Savilahti, H. K. Akerblom, and H. M. Dosch. 1992. A bovine albumin peptide as a possible trigger of insulin-dependent diabetes mellitus. *N Engl J Med 327:302.*

95. Atkinson, M. A., M. A. Bowman, K. J. Kao, L. Campbell, P. J. Dush, S. C. Shah, O. Simell, and N. K. Maclaren. 1993. Lack of immune responsiveness to bovine serum albumin in insulin-dependent diabetes. *N Engl J Med 329:1853.*

96. Gale, E. A. 2002. A missing link in the hygiene hypothesis? *Diabetologia 45:588.*

97. Feillet, H., and J. F. Bach. 2004. On the mechanisms of the protective effect of infections on type 1 diabetes. *Clin Dev Immunol 11:191.*

98. Ceman, S., S. Wu, T. S. Jardetzky, and A. J. Sant. 1998. Alteration of a single hydrogen bond between class II molecules and peptide results in rapid degradation of class II molecules after invariant chain removal. *J Exp Med 188:2139.*

99. Stern, L. J., J. H. Brown, T. S. Jardetzky, J. C. Gorga, R. G. Urban, J. L. Strominger, and D. C. Wiley. 1994. Crystal structure of the human class II MHC protein HLA-DR1 complexed with an influenza virus peptide. *Nature 368:215.*

100. Dessen, A., C. M. Lawrence, S. Cupo, D. M. Zaller, and D. C. Wiley. 1997. X-ray crystal structure of HLA-DR4 (DRA*0101, DRB1*0401) complexed with a peptide from human collagen II. *Immunity 7:473.*

101. Jardetzky, T. S., W. S. Lane, R. A. Robinson, D. R. Madden, and D. C. Wiley. 1991. Identification of self peptides bound to purified HLA-B27. *Nature 353:326.*

102. Falk, K., O. Rotzschke, S. Stevanovic, G. Jung, and H. G. Rammensee. 1991. Allele-specific motifs revealed by sequencing of self-peptides eluted from MHC molecules. *Nature 351:290.*

103. Hunt, D. F., R. A. Henderson, J. Shabanowitz, K. Sakaguchi, H. Michel, N. Sevilir, A. L. Cox, E. Appella, and V. H. Engelhard. 1992. Characterization of peptides bound to the class I MHC molecule HLA-A2.1 by mass spectrometry. *Science 255:1261.*

104. Buus, S., S. Colon, C. Smith, J. H. Freed, C. Miles, and H. M. Grey. 1986. Interaction between a "processed" ovalbumin peptide and Ia molecules. *Proc Natl Acad Sci U S A 83:3968.*

105. Swain, S. L. 1981. Significance of Lyt phenotypes: Lyt2 antibodies block activities of T cells that recognize class 1 major histocompatibility complex antigens regardless of their function. *Proc Natl Acad Sci U S A 78:7101.*

106. Greenstein, J. L., J. Kappler, P. Marrack, and S. J. Burakoff. 1984. The role of L3T4 in recognition of Ia by a cytotoxic, H-2Dd-specific T cell hybridoma. *J Exp Med 159:1213.*

107. Bank, I., and L. Chess. 1985. Perturbation of the T4 molecule transmits a negative signal to T cells. *J Exp Med 162:1294.*

108. Bekoff, M., T. Kakiuchi, and H. M. Grey. 1985. Accessory cell function in the Con A response: role of Ia-positive and Ia-negative accessory cells. *J Immunol 134:1337.*

109. Wilson IA, C. P., Davis MM, Allen PM, Trowsdale J. 2001. The Generation of Lymphocyte Antinge Receptors. In *Immunology.* T. P. Janeway CA, Walport M, Shlomchik M, ed. Garland Publishing, new York.

110. Malissen, M., J. Trucy, E. Jouvin-Marche, P. A. Cazenave, R. Scollay, and B. Malissen. 1992. Regulation of TCR alpha and beta gene allelic exclusion during T-cell development. *Immunol Today 13:315*.

111. Uematsu, Y., S. Ryser, Z. Dembic, P. Borgulya, P. Krimpenfort, A. Berns, H. von Boehmer, and M. Steinmetz. 1988. In transgenic mice the introduced functional T cell receptor beta gene prevents expression of endogenous beta genes. *Cell 52:831*.

112. Malissen, M., J. Trucy, F. Letourneur, N. Rebai, D. E. Dunn, F. W. Fitch, L. Hood, and B. Malissen. 1988. A T cell clone expresses two T cell receptor alpha genes but uses one alpha beta heterodimer for allorecognition and self MHC-restricted antigen recognition. *Cell 55:49*.

113. Heath, W. R., and J. F. Miller. 1993. Expression of two alpha chains on the surface of T cells in T cell receptor transgenic mice. *J Exp Med 178:1807*.

114. Sprent, J., D. Lo, E. K. Gao, and Y. Ron. 1988. T cell selection in the thymus. *Immunol Rev 101:173*.

115. Anderson, M. S., E. S. Venanzi, L. Klein, Z. Chen, S. P. Berzins, S. J. Turley, H. von Boehmer, R. Bronson, A. Dierich, C. Benoist, and D. Mathis. 2002. Projection of an immunological self shadow within the thymus by the aire protein. *Science 298:1395*.

116. Derbinski, J., J. Gabler, B. Brors, S. Tierling, S. Jonnakuty, M. Hergenhahn, L. Peltonen, J. Walter, and B. Kyewski. 2005. Promiscuous gene expression in thymic epithelial cells is regulated at multiple levels. *J Exp Med 202:33*.

117. Ramsey, C., O. Winqvist, L. Puhakka, M. Halonen, A. Moro, O. Kampe, P. Eskelin, M. Pelto-Huikko, and L. Peltonen. 2002. Aire deficient mice develop multiple features of APECED phenotype and show altered immune response. *Hum Mol Genet 11:397*.

118. Anderson, M. S., E. S. Venanzi, Z. Chen, S. P. Berzins, C. Benoist, and D. Mathis. 2005. The cellular mechanism of Aire control of T cell tolerance. *Immunity 23:227*.

119. Lee, K. H., K. W. Wucherpfennig, and D. C. Wiley. 2001. Structure of a human insulin peptide-HLA-DQ8 complex and susceptibility to type 1 diabetes. *Nat Immunol 2:501*.

120. Stratmann, T., V. Apostolopoulos, V. Mallet-Designe, A. L. Corper, C. A. Scott, I. A. Wilson, A. S. Kang, and L. Teyton. 2000. The I-Ag7 MHC class II molecule linked to murine diabetes is a promiscuous peptide binder. *J Immunol 165:3214*.

121. Quartey-Papafio, R., T. Lund, P. Chandler, J. Picard, P. Ozegbe, S. Day, P. R. Hutchings, L. O'Reilly, D. Kioussis, E. Simpson, and et al. 1995. Aspartate at position 57 of nonobese diabetic I-Ag7 beta-chain diminishes the spontaneous incidence of insulin-dependent diabetes mellitus. *J Immunol 154:5567*.

122. Wen, L., F. S. Wong, J. Tang, N. Y. Chen, M. Altieri, C. David, R. Flavell, and R. Sherwin. 2000. In vivo evidence for the contribution of human histocompatibility leukocyte antigen (HLA)-DQ molecules to the development of diabetes. *J Exp Med 191:97*.

123. Shaw, A. S., and M. L. Dustin. 1997. Making the T cell receptor go the distance: a topological view of T cell activation. *Immunity 6:361*.

124. Viola, A., and A. Lanzavecchia. 1996. T cell activation determined by T cell receptor number and tunable thresholds. *Science 273:104*.

125. Burns, J., A. Rosenzweig, B. Zweiman, and R. P. Lisak. 1983. Isolation of myelin basic protein-reactive T-cell lines from normal human blood. *Cell Immunol 81:435*.

126. Yan, T., H. Burkhardt, T. Ritter, B. Broker, K. H. Mann, W. M. Bertling, K. von der Mark, and F. Emmrich. 1992. Specificity and T cell receptor beta chain usage of a human

collagen type II-reactive T cell clone derived from a healthy individual. *Eur J Immunol 22:51.*

127. Ohashi, P. S., S. Oehen, K. Buerki, H. Pircher, C. T. Ohashi, B. Odermatt, B. Malissen, R. M. Zinkernagel, and H. Hengartner. 1991. Ablation of "tolerance" and induction of diabetes by virus infection in viral antigen transgenic mice. *Cell 65:305.*

128. Oehen, S., P. S. Ohashi, P. Aichele, K. Burki, H. Hengartner, and R. M. Zinkernagel. 1992. Vaccination or tolerance to prevent diabetes. *Eur J Immunol 22:3149.*

129. Guerder, S., J. Meyerhoff, and R. Flavell. 1994. The role of the T cell costimulator B7-1 in autoimmunity and the induction and maintenance of tolerance to peripheral antigen. *Immunity 1:155.*

130. Sakaguchi, S., N. Sakaguchi, M. Asano, M. Itoh, and M. Toda. 1995. Immunologic self-tolerance maintained by activated T cells expressing IL-2 receptor alpha-chains (CD25). Breakdown of a single mechanism of self-tolerance causes various autoimmune diseases. *J Immunol 155:1151.*

131. Kronenberg, M., and A. Rudensky. 2005. Regulation of immunity by self-reactive T cells. *Nature 435:598.*

132. Sakaguchi, S. 2004. Naturally arising CD4+ regulatory t cells for immunologic self-tolerance and negative control of immune responses. *Annu Rev Immunol 22:531.*

133. Hsieh, C. S., Y. Liang, A. J. Tyznik, S. G. Self, D. Liggitt, and A. Y. Rudensky. 2004. Recognition of the peripheral self by naturally arising CD25+ CD4+ T cell receptors. *Immunity 21:267.*

134. Bennett, C. L., J. Christie, F. Ramsdell, M. E. Brunkow, P. J. Ferguson, L. Whitesell, T. E. Kelly, F. T. Saulsbury, P. F. Chance, and H. D. Ochs. 2001. The immune dysregulation, polyendocrinopathy, enteropathy, X-linked syndrome (IPEX) is caused by mutations of FOXP3. *Nat Genet 27:20.*

135. Wildin, R. S., F. Ramsdell, J. Peake, F. Faravelli, J. L. Casanova, N. Buist, E. Levy-Lahad, M. Mazzella, O. Goulet, L. Perroni, F. D. Bricarelli, G. Byrne, M. McEuen, S. Proll, M. Appleby, and M. E. Brunkow. 2001. X-linked neonatal diabetes mellitus, enteropathy and endocrinopathy syndrome is the human equivalent of mouse scurfy. *Nat Genet 27:18.*

136. Brunkow, M. E., E. W. Jeffery, K. A. Hjerrild, B. Paeper, L. B. Clark, S. A. Yasayko, J. E. Wilkinson, D. Galas, S. F. Ziegler, and F. Ramsdell. 2001. Disruption of a new forkhead/winged-helix protein, scurfin, results in the fatal lymphoproliferative disorder of the scurfy mouse. *Nat Genet 27:68.*

137. Hori, S., T. Nomura, and S. Sakaguchi. 2003. Control of regulatory T cell development by the transcription factor Foxp3. *Science 299:1057.*

138. Fontenot, J. D., M. A. Gavin, and A. Y. Rudensky. 2003. Foxp3 programs the development and function of CD4+CD25+ regulatory T cells. *Nat Immunol 4:330.*

139. Asseman, C., S. Mauze, M. W. Leach, R. L. Coffman, and F. Powrie. 1999. An essential role for interleukin 10 in the function of regulatory T cells that inhibit intestinal inflammation. *J Exp Med 190:995.*

140. Powrie, F., J. Carlino, M. W. Leach, S. Mauze, and R. L. Coffman. 1996. A critical role for transforming growth factor-beta but not interleukin 4 in the suppression of T helper type 1-mediated colitis by CD45RB(low) CD4+ T cells. *J Exp Med 183:2669.*

141. Paust, S., L. Lu, N. McCarty, and H. Cantor. 2004. Engagement of B7 on effector T cells by regulatory T cells prevents autoimmune disease. *Proc Natl Acad Sci U S A 101:10398.*

142. Fallarino, F., U. Grohmann, K. W. Hwang, C. Orabona, C. Vacca, R. Bianchi, M. L. Belladonna, M. C. Fioretti, M. L. Alegre, and P. Puccetti. 2003. Modulation of tryptophan catabolism by regulatory T cells. *Nat Immunol 4:1206*.
143. Thornton, A. M., E. E. Donovan, C. A. Piccirillo, and E. M. Shevach. 2004. Cutting edge: IL-2 is critically required for the in vitro activation of CD4+CD25+ T cell suppressor function. *J Immunol 172:6519*.
144. Barthlott, T., G. Kassiotis, and B. Stockinger. 2003. T cell regulation as a side effect of homeostasis and competition. *J Exp Med 197:451*.
145. Barthlott, T., H. Moncrieffe, M. Veldhoen, C. J. Atkins, J. Christensen, A. O'Garra, and B. Stockinger. 2005. CD25+ CD4+ T cells compete with naive CD4+ T cells for IL-2 and exploit it for the induction of IL-10 production. *Int Immunol 17:279*.
146. Cucca, F., R. Lampis, M. Congia, E. Angius, S. Nutland, S. C. Bain, A. H. Barnett, and J. A. Todd. 2001. A correlation between the relative predisposition of MHC class II alleles to type 1 diabetes and the structure of their proteins. *Hum Mol Genet 10:2025*.
147. Steimle, V., C. A. Siegrist, A. Mottet, B. Lisowska-Grospierre, and B. Mach. 1994. Regulation of MHC class II expression by interferon-gamma mediated by the transactivator gene CIITA. *Science 265:106*.
148. Cresswell, P. 1996. Invariant chain structure and MHC class II function. *Cell 84:505*.
149. Shams, H., P. Klucar, S. E. Weis, A. Lalvani, P. K. Moonan, H. Safi, B. Wizel, K. Ewer, G. T. Nepom, D. M. Lewinsohn, P. Andersen, and P. F. Barnes. 2004. Characterization of a Mycobacterium tuberculosis peptide that is recognized by human CD4+ and CD8+ T cells in the context of multiple HLA alleles. *J Immunol 173:1966*.
150. Wicker, L. S., S. L. Chen, G. T. Nepom, J. F. Elliott, D. C. Freed, A. Bansal, S. Zheng, A. Herman, A. Lernmark, D. M. Zaller, L. B. Peterson, J. B. Rothbard, R. Cummings, and P. J. Whiteley. 1996. Naturally processed T cell epitopes from human glutamic acid decarboxylase identified using mice transgenic for the type 1 diabetes-associated human MHC class II allele, DRB1*0401. *J Clin Invest 98:2597*.
151. Valitutti, S., S. Muller, M. Cella, E. Padovan, and A. Lanzavecchia. 1995. Serial triggering of many T-cell receptors by a few peptide-MHC complexes. *Nature 375:148*.
152. Donovan, J., Brown, P. 1995. Blood Collection. In *Current Protocols in Immunology*, Vol. 1. K. A. Coligan JE, Margulies DM, Shevach EM, Strober W, ed. John Wiley & Sons, Inc., New York, p. 1.7.1.
153. Wen, L., F. S. Wong, L. Burkly, M. Altieri, C. Mamalaki, D. Kioussis, R. A. Flavell, and R. S. Sherwin. 1998. Induction of insulitis by glutamic acid decarboxylase peptide-specific and HLA-DQ8-restricted CD4(+) T cells from human DQ transgenic mice. *J Clin Invest 102:947*.
154. Herman, A. E., R. M. Tisch, S. D. Patel, S. L. Parry, J. Olson, J. A. Noble, A. P. Cope, B. Cox, M. Congia, and H. O. McDevitt. 1999. Determination of glutamic acid decarboxylase 65 peptides presented by the type I diabetes-associated HLA-DQ8 class II molecule identifies an immunogenic peptide motif. *J Immunol 163:6275*.
155. Milton, M. J., M. Poulin, C. Mathews, and J. D. Piganelli. 2004. Generation, maintenance, and adoptive transfer of diabetogenic T-cell lines/clones from the nonobese diabetic mouse. *Methods Mol Med 102:213*.
156. Pannetier, C., M. Cochet, S. Darche, A. Casrouge, M. Zoller, and P. Kourilsky. 1993. The sizes of the CDR3 hypervariable regions of the murine T-cell receptor beta chains vary as a function of the recombined germ-line segments. *Proc Natl Acad Sci U S A 90:4319*.

157. Kappler, J. W., B. Skidmore, J. White, and P. Marrack. 1981. Antigen-inducible, H-2-restricted, interleukin-2-producing T cell hybridomas. Lack of independent antigen and H-2 recognition. *J Exp Med 153:1198*.

158. Schwartz, R. H. 1990. A cell culture model for T lymphocyte clonal anergy. *Science 248:1349*.

159. White, J., M. Blackman, J. Bill, J. Kappler, P. Marrack, D. P. Gold, and W. Born. 1989. Two better cell lines for making hybridomas expressing specific T cell receptors. *J Immunol 143:1822*.

160. Fujii, S., S. Senju, Y. Z. Chen, M. Ando, S. Matsushita, and Y. Nishimura. 1998. The CLIP-substituted invariant chain efficiently targets an antigenic peptide to HLA class II pathway in L cells. *Hum Immunol 59:607*.

161. Malcherek, G., C. Wirblich, N. Willcox, H. G. Rammensee, J. Trowsdale, and A. Melms. 1998. MHC class II-associated invariant chain peptide replacement by T cell epitopes: engineered invariant chain as a vehicle for directed and enhanced MHC class II antigen processing and presentation. *Eur J Immunol 28:1524*.

162. Peakman, M., T. I. Tree, J. Endl, P. van Endert, M. A. Atkinson, and B. O. Roep. 2001. Characterization of preparations of GAD65, proinsulin, and the islet tyrosine phosphatase IA-2 for use in detection of autoreactive T-cells in type 1 diabetes: report of phase II of the Second International Immunology of Diabetes Society Workshop for Standardization of T-cell assays in type 1 diabetes. *Diabetes 50:1749*.

163. Jaenicke, R. 2000. Stability and stabilization of globular proteins in solution. *J Biotechnol 79:193*.

164. Volkin, D. B., H. Mach, and C. R. Middaugh. 1997. Degradative covalent reactions important to protein stability. *Mol Biotechnol 8:105*.

165. Manning, M. C., K. Patel, and R. T. Borchardt. 1989. Stability of protein pharmaceuticals. *Pharm Res 6:903*.

166. Grakoui, A., S. K. Bromley, C. Sumen, M. M. Davis, A. S. Shaw, P. M. Allen, and M. L. Dustin. 1999. The immunological synapse: a molecular machine controlling T cell activation. *Science 285:221*.

167. Miller, J. F., and R. A. Flavell. 1994. T-cell tolerance and autoimmunity in transgenic models of central and peripheral tolerance. *Curr Opin Immunol 6:892*.